

THE EFFECT OF OCULAR AXIAL LENGTH ON PHOTORECEPTORS

A thesis presented to the graduate faculty of New England College of Optometry in partial fulfillment of
the requirements for the degree of Master of Science

Srinivasa R. Srirangam

May 2025

© Srinivasa R Srirangam

All rights reserved

The author hereby grants New England College of Optometry permission to reproduce and to publicly distribute this
paper and electronic copies of the thesis document in whole or in part.

THE EFFECT OF OCULAR AXL ON PHOTORECEPTORS

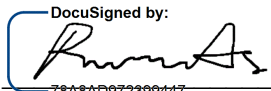
Srinivasa R. Srirangam

This manuscript has been read and accepted by the Thesis Committee in satisfaction of the thesis requirement for the degree of Master of Science

5/11/2025

Date

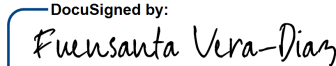
DocuSigned by:



78A8AD972399447...

Thanasis Panorgias, MS, PhD
Graduate Faculty Advisor

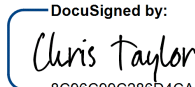
DocuSigned by:



1502BB240B7D484...

Fuensanta A. Vera-Diaz, OD, PhD, FAAO, FARVO
Thesis Committee Member

DocuSigned by:



8C96C99C286B4CA...

Christopher Patrick Taylor, PhD
Thesis Committee Member

DocuSigned by:



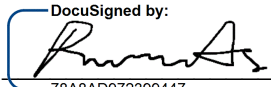
3E92398B601647F...

Peter J. Bex, PhD
Thesis Committee Member

5/11/2025

Date

DocuSigned by:



78A8AD972399447...

Thanasis Panorgias, MS, PhD
Director of Graduate Studies

ABSTRACT

The effect of ocular axial length on photoreceptors

Srinivasa R. Srirangam

New England College of Optometry, 2025

PURPOSE: The purpose of this study is to determine the relationship between ocular axial length (AXL) and the retinal photoreceptor layer functioning through electrophysiology and psychophysics. The study was part of a larger project that involved the assessment of photoreceptors, bipolar cells, horizontal cells, amacrine cells, and ganglion cells.

METHODS: Subjects were recruited from the NECO population for four visits that were each one week apart. During the course of the visits, various ERGs and psychophysics experiments were performed to assess the retinal layers. For this study, the following experiments were performed: (1) Single flash ERGs to determine the maximum saturating amplitude R_{max} , and sensitivity S of rods and cones in scotopic and photopic conditions respectively, (2) Paired flash ERGs to determine the rate of phototransduction of cones and rate of recovery in cones and rods, and (3) psychophysics experiment to determine the total contrast sensitivity (CS) recovery, maximum CS recovery, and growth rate of CS recovery in cones. We did a correlation analysis between the AXL and each of these characteristics of the photoreceptors and performed a split median analysis to determine the significance in subjects with shorter versus longer AXL.

RESULTS: A total of 36 subjects were recruited and completed all four of the visits of the study. Due to the evolving nature of the protocols in some of the experiments, not all 36 subjects were

included in the final analysis of the experiments. For the 34 subjects included in the electrophysiology analyses, there was a positive correlation between AXL and the rod Rmax ($p = 0.033$). A variance analysis of the data also showed that there was a significant difference in the distribution of the rod rate of recovery in subjects with shorter AXLs ($p < 0.001$) in the rod-paired flash methods. For the 24 subjects included in the psychophysical analyses, there were no significant correlations in the psychophysical data. For the 34 subjects included in both the electrophysiology and psychophysical analyses, linear mixed effect modeling showed significant differences in measuring cone maximum contrast sensitivity recovery with psychophysics compared to paired flash ERGs ($p = 0.005$).

CONCLUSIONS: This study showed significant findings on the effects of AXL on the rod Rmax, as subjects with longer AXL displayed lower Rmax amplitudes. There was also a significant variance in the rod rate of recovery between subjects with longer AXL and those with shorter AXL. Both findings can be attributed to the stretched receptor hypothesis, which postulates that a longer AXL can lead to increased spacing and decreased density of the photoreceptors in a non-uniform, varied manner. This study also showed how the method used to assess the function of photoreceptors can influence the data. There was a larger amount of cone recovery that was observed psychophysically compared to that from the electrophysiological experiments. This difference in cone recovery is likely due to the nature of both methods, as ERGs highlight the biochemical processes in photoreceptors while psychophysics incorporate post-cortical processes. The small sample size limits the findings as much of the study was underpowered and further work can be done by future researchers to analyze rod function through psychophysics.

ACKNOWLEDGEMENTS

I would first like to thank my advisor, Dr. Thanasis Panorgias for his mentorship. From showing me how to hook up my very first electrode to staying after class to troubleshoot protocols to providing extensive feedback on my thesis, Dr. Panorgias has been with me at every step of my research experience at NECO. His patience and knowledge has been invaluable to me and I've become a better researcher, clinician, and person under his guidance.

I would also like to thank my thesis committee, Dr. Fuensanta A. Vera-Diaz, Dr. Christopher Taylor, and Dr. Peter J. Bex for all their expertise in developing this project. Special thanks as well to my fellow masters candidates Rachel Harmon, Raviv Katz, and Simon Wong for working alongside me in this project. It was an absolute privilege to be in a team with such brilliant individuals and learn as much as I have from each of them.

The past four years of optometry school have been transformational for me both in my personal and professional life. I could not have gotten through optometry school without the support of my classmates, teachers, and family. Words will never be enough to convey my eternal gratitude and love for them.

TABLE OF CONTENTS

ABSTRACT.....	iii
ACKNOWLEDGEMENTS.....	v
LIST OF FIGURES, TABLES, AND EQUATIONS.....	viii
1. Background and General Problem.....	1
1.1. Myopia Overview.....	1
1.2. Myopia and Photoreceptors.....	1
1.3. Electroretinograms (ERGs) and The Phototransduction Cascade.....	3
1.4 Myopia and ERGs.....	4
1.5 Psychophysics and The Visual Cascade.....	6
2. Rationale, Specific Aims and Hypotheses.....	7
2.1. Rationale for the Study.....	7
2.2. Specific Aims.....	7
3. Design and Methods.....	8
3.1. Setting and Recruitment.....	8
3.2. Visits.....	8
3.2.1 - Order of Visits.....	8
3.2.2 - Visit #1.....	9
3.2.3 - Visit #2.....	10
3.2.4 - Visit #3.....	10
3.2.5 - Visit #4.....	11
3.3 - Electroretinography.....	11
3.3.1 - ERG Set-Up.....	11
3.3.2 - Single Flash ERGs for cones and rods.....	12
3.3.3 - Paired-Flash ERGs for cones and rods.....	14
3.3.4 - Paired-flash Rod ERGs Parameters.....	16

3.3.5 - Rod-Isolating ERGs Parameters.....	17
3.3.6 - Paired-flash Cone ERGs Parameters.....	18
3.4 - Cone Psychophysics.....	19
3.5. Apparatus.....	20
3.6. Statistical analysis.....	20
4. Results.....	21
4.1. Subjects.....	21
4.2. Electrophysiology: Rod Isolating ERGs.....	21
4.3. Electrophysiology: Cone ERGs.....	25
4.4. Electrophysiology: Rod Paired Flash ERGs.....	28
4.5. Electrophysiology: Cone Paired Flash.....	30
4.6. Psychophysics: Cones.....	33
5. Discussion.....	38
5.1. Summary.....	38
5.2. Electrophysiology.....	40
5.3. Cones and Psychophysics.....	41
5.4. Variance Analysis.....	41
5.5. Linear Mixed Effect Modeling.....	43
5.6. Limitations and Future Directions.....	45
6. Conclusions.....	48
7. Bibliography.....	49
8. Appendix.....	55

LIST OF FIGURES, TABLES, AND EQUATIONS

FIGURES

Figure 3.1 - Classic Full-Field Electroretinogram.....	12
Figure 3.2 - Rod-Isolating ERG recording.....	13
Figure 3.3 - Paired-Flash Method Diagram.....	15
Figure 4.1 - Correlation between Axial Length and Refractive Error.....	21
Figure 4.2 - RL001 - Rod-Isolating ERG.....	22
Figure 4.3 - Correlation between Axial Length and Rod Rmax.....	23
Figure 4.4 - Correlation between Axial Length and Rod Sensitivity.....	23
Figure 4.5 - Boxplot of Rod Rmax by Median Split of Axial Length.....	24
Figure 4.6 - Boxplot of Rod Sensitivity by Median Split of Axial Length.....	24
Figure 4.7 - RL002 - Cone ERG.....	25
Figure 4.8 - Correlation between Axial Length and Cone Rmax.....	26
Figure 4.9 - Correlation between Axial Length and Cone Sensitivity.....	26
Figure 4.10 - Boxplot of Cone Rmax by Median Split of Axial Length.....	27
Figure 4.11 - Boxplot of Cone Sensitivity by Median Split of Axial Length.....	28
Figure 4.12 - RL013 - Rod-Paired Flash ERG.....	29
Figure 4.13 - Correlation between Axial Length and Rod Rate of Recovery.....	29
Figure 4.14 - Boxplot of Rod Rate of Recovery by Median Split of Axial Length.....	30
Figure 4.15 - RL010 - Cone-Paired Flash ERG.....	31
Figure 4.16 - Correlation between Axial Length and Cone Rate of Phototransduction.....	31
Figure 4.17 - Correlation between Axial Length and Cone Rate of Recovery.....	32
Figure 4.18 - Boxplot of Cone Rate of Phototransduction by Median Split of Axial Length.....	32
Figure 4.19 - Boxplot of Cone Rate of Recovery by Median Split of Axial Length.....	33
Figure 4.20 - RL007 - Total Cone CS Recovery.....	34
Figure 4.21 - Correlation between Axial Length and Total Cone CS Recovery.....	35

Figure 4.22 - Correlation between Axial Length and Maximum Cone CS Recovery.....	35
Figure 4.23 - Correlation between Axial Length and Maximum Cone Growth Rate.....	35
Figure 4.24 - Boxplot of Total Cone CS Recovery by Median Split of Axial Length	36
Figure 4.25 - Boxplot of Maximum Cone CS Recovery by Median Split of Axial Length	37
Figure 4.26 - Boxplot of Cone Growth Rate by Median Split of Axial Length	37

TABLES

Table 3.1 - Rod Paired-flash ERG Time Course.....	17
Table 3.2 - Rod Isolating ERG Time Course.....	18
Table 3.3 - Cone Paired-flash ERG Time Course.....	19
Table 5.1 - Summary of Correlation and Split Median Analyses.....	39
Table 5.2 - Summary of Variance Analyses.....	42
Table 5.3 - Summary of Linear Mixed-Effect Modeling Analyses	44
Table 5.4 - Summary of Post-Hoc Power Analysis.....	46

EQUATIONS

Equation 1 - Photoreceptor Modeling Equation.....	4
Equation 2 - Time Course of Test Flash Equation (Photoreceptor Paired-Flash ERGs).....	16
Equation 3 - Negative Exponential Growth Model (Cone Psychophysics).....	34
Equation 4 - Linear Mixed Effect Modeling Equation.....	43

1. Background and General Problem

1.1. Myopia Overview

Myopia is a condition that involves an increase in the ocular axial length (AXL) and the subsequent elongation of the eye relative to its refractive power. Optically, this manifests with light rays focusing in front of the retina (Flitcroft et al., 2019) and clinically, a myopic patient will show signs and symptoms of impaired distance vision, eyestrains, squinting, and headaches (Saw et al., 1996). The prevalence of myopia has continued to rise in recent decades (Dolgin, 2015) and it is predicted that more than half the global population will develop myopia by 2050 (Holden et al., 2016). Moreover, myopia is associated with a number of ocular pathologies such as glaucoma, myopic maculopathy, and retinal detachment (Cho et al., 2016), making it a major public health concern.

1.2. Myopia and Photoreceptors

Physiologically, the elongation of the eye in myopia affects many ocular structures including the choroid, optic nerve, and the retina (Gupta et al., 2021). The retina is of particular interest as it is a multilayered structure composed of photoreceptors, horizontal cells, bipolar cells, amacrine cells, and ganglion cells. The intricate arrangement of these cells allows photons to be detected, electrical signals to be converted to chemical signals, and for information to be transmitted to the brain (Hunter et al., 2019). Photoreceptors are the first cells involved in the visual pathway.

Photoreceptors are located in the outer layer of the retina and they consist of rods and cones. Both contain an outer and inner segment that are joined by a connecting cilium. The outer segment captures the light and initiates the phototransduction cascade while the inner segment contains the organelles for the cell's metabolic processes. The photoreceptor axons terminate at

the synaptic region where the neurotransmitter is released and any changes in its concentration are sensed by horizontal and bipolar cells (Molday & Moritz, 2015). The main distinction between rods and cones lies in their outer segments. Both of their outer segments are embedded in the apical processes of the retinal pigment epithelium (RPE). However, rods have a longer outer segment consisting of distinct, unconnected discs (Mustafi et al., 2009) whereas cones contain a shorter outer segment with a lamella that is continuously connected to the cilium (Eckmiller, 1997). This, in turn, affects the rate at which rods and cones are renewed by the RPE. Prior radiolabeling research showed that the rods produce 80-90 discs per day and that their entire outer segment is renewed every 9-13 days (Young, 1971) as opposed to cones which have a longer, unidentified period of renewal for their outer segments (Eckmiller, 1997), even though AO-OCT imaging studies estimate it to be in the range of 10-12 days (Jonnal et al., 2007).

The distribution of the two photoreceptors also differs, as there are approximately 120 million rods and six million cones in the human retina (Molday & Moritz, 2015). While there is a greater density of rods than cones throughout the retina, this distribution changes drastically in the fovea, a region in the central retina with a diameter of 0.35 mm that is densely packed with photoreceptors (50 cone cells per 100 mm²) in a hexagonal pattern (Rehman et al., 2023). Rods function optimally under dim, scotopic lighting conditions and cones function best in bright, photopic lighting conditions (Molday & Moritz, 2015).

The axial elongation of the eye in myopia is thought to disrupt the packing of the photoreceptors and lead to fewer rods and cones per unit of area throughout the retina (Chen et al., 1992), hence disrupting the photon capture ability of the photoreceptors. In an elongated eye, rods and cones need to spread out to cover a larger surface area on the retina and this subsequently leads to a reduced density of the photoreceptors in that region (Wang et al., 2019).

Additionally, increased ocular elongation is shown to affect the choroid as well. This physical change has been demonstrated in chicken models with form deprivation myopia as the stretched eye resulted in thicker inner and outer segments in rods and cones (Liang et al., 1995). The tips of these outer segments would indent and exert pressure on the RPE nuclei and might contribute to a reduction in choroidal thickness that is frequently seen in myopia, an increased separation between the photoreceptors and the choroid, and a collapse of the choroidal vasculature (Liang et al., 1995).

1.3. Electroretinograms (ERGs) and The Phototransduction Cascade

The electroretinogram (ERG) is a specific type of electrophysiological test that is utilized to measure retinal function. In order for light to be perceived, biopotentials need to be generated by the retinal cells in the different stages of the visual pathway. During ERG testing, flashes of light illuminate the retina to generate biopotentials that can be recorded with high temporal resolution (Gupta et al., 2021). A standard ERG recording consists of a biphasic waveform of a negative a-wave followed by a positive b-wave.

The a-wave consists of the electrical activity of photoreceptors and it signals the initiation of the phototransduction cascade. In this process, a photon gets absorbed by the photopigment molecules in the outer segments of the photoreceptors. This causes the photoisomerization of 11-cis-retinal, the sensitive form of the chromophore found in photoreceptors, to its all-trans-retinal form. At this point, the respective opsin in rods and cones is activated, subsequently activating the G-protein transducin. Transducin goes on to activate phosphodiesterase (PDE) by binding to the gamma subunits of PDE, which normally inhibit the enzyme. PDE begins to hydrolyze cGMP and the decreased concentration of cGMP causes the

cGMP-gated ionic channels of the outer segment to close. This blocks the influx of sodium and calcium ions into the cell and hyperpolarizes the membrane, resulting in the reduction of glutamate release from the photoreceptors and the negative deflection of the a-wave (Lamb, 2022).

Moreover, the a-waves of rods and cones can be fitted with the following mathematical model in order to assess the saturation point and sensitivity of the photoreceptors. Based on the Lamb and Pugh model (Pugh & Lamb, 1993), Equation 1 expresses the photoreceptor a-waves where I is the intensity of the flash stimulus, S is the sensitivity of the respective photoreceptors, R is the saturated maximum amplitude of the respective photoreceptors, and t_d is a brief delay related to the recording equipment.

$$(1) R(i, t) = [1 - \exp\{-0.5 I S(t-t_d)^2\}] * R$$

ERGs can be performed by using the standard ISCEV protocol to assess the a-waves of rods and cones in scotopic and photopic conditions respectively. In these experiments, the background illumination, the intensity of the flash, and the light or dark-adapted state of the eye can be manipulated to measure the responses of the retinal cells (Robson et al., 2018). Moreover, these electrophysiological tests can help investigate changes in the retina that arise from ocular conditions such as retinitis pigmentosa (Hood & Birch, 1994), retinopathy of prematurity (Harris et al., 2011), and myopia (Gupta et al., 2021).

1.4 Myopia and ERGs

Numerous studies have been conducted to assess the effects of myopia on retinal function using

ERGs. The amplitude of the a-wave has frequently been shown to be decreased in a myopic eye in both scotopic and photopic conditions (Ishikawa et al., 1990; Kader, 2012; Wang et al., 2013). Other studies have also highlighted the effects of AXL on the a-wave such as showcasing a reduced a-wave amplitude in dark-adapted condition with every millimeter increase in AXL (Sachidanandam et al., 2017) or a correlation between the degree of myopia and a decreased scotopic a-wave amplitude (Westall et al., 2001). Regarding the impact of myopia on the photopic, cone-driven a-wave response, full-field ERG and focal macular ERG experiments have shown reduced a-wave findings in myopic eyes (Blach et al., 1966; Ishikawa et al., 1990). ERGs also provide information on the implicit time, the time from the onset of the stimulus to the maximum amplitude of the respective waveform, and the latency period, the time from the onset of the stimulus to the onset of the response (Asanad & Karanjia, 2023). Studies have shown normal implicit times and delayed latency periods in myopic patients, which could suggest reductions in the photoreceptor density (Ishikawa et al., 1990).

Various theories have been hypothesized as to how the elongation of the myopic eye affects the ERG responses. The stretched receptor hypothesis postulated that the photoreceptors would exhibit reduced sensitivity but a normal saturated amplitude due to the spacing between the receptors in the myopic eye (Chen et al., 1992). Thereby, higher intensities of light would be needed to generate a threshold response, while the maximum, saturated response remains constant (Chen et al., 1992). However, later research appears to support the alternative hypothesis in which the photoreceptor sensitivity is the same but the saturated amplitude is reduced (Westall et al., 2001). According to this theory, since the saturated amplitude represents the response of the photoreceptors, it's the photoreceptor function that is affected by the elongation of the eye as opposed to their structure and spacing. Additionally, the elongated eye

not only affects the spacing of the photoreceptors but also the shape of posterior segment, the pupil size, and the optics of an eye (Nusinowitz, 2006). Therefore, more research is needed to better understand the low retinal response in myopic patients.

1.5 Psychophysics and The Visual Cascade

Psychophysical techniques can also be used to assess photoreceptor function. While ERGs allow for an objective measure of photoreceptor function, psychophysics take into account the perceptual processes involved in a subject's response to a stimulus. For photoreceptor function, psychophysical tests commonly involve bleaching the retina with intense bright flashes and assessing the recovery of cones and rods during dark adaptation (Shapley & Enroth-Cugell, 1984). After its photoisomerization, the inactive form of the chromophore, all-trans-retinal, gets released from the photoreceptor opsin, converted to all-trans-retinol, and transferred to the RPE. There, it gets converted back to its sensitive 11-cis-retinal state and returns to the outer segment and combines with the opsin (Jiang & Mahroo, 2022). Psychophysical tests can be utilized to analyze this visual cycle and the regeneration of photopigment (Jiang & Mahroo, 2022).

Along with the recovery, psychophysical tests can also provide insight into the visual system's ability to detect, discriminate, recognize, and quickly respond to a stimulus. They have been utilized in researching ocular diseases such as glaucoma (Anderson, 2006), retinitis pigmentosa (Brouzas, 1995), and diabetic retinopathy (Chen & Gardner, 2021). Moreover, a variety of psychophysical experiments have been conducted to show the various effects of myopia may or may not have on peripheral spatial resolution (Chui et al., 2005), contrast sensitivity (Thorn et al., 1986), critical flicker frequency (Chen et al., 2000), dark adaptation (Mäntyjärvi & Tuppurainen, 1995), and spatial summation (Jaworski et al., 2006).

2. Rationale, Specific Aims and Hypotheses

2.1. Rationale for the Study

This study is unique in how it combines both elements of electrophysiology and psychophysics. The former would provide an objective assessment of the effects of the AXL on the function of photoreceptors while the latter assesses the effects of myopia on photoreceptors and visual function subjectively. Data from both of these components of the study will allow for a better understanding of the effects of axial elongation on the photoreceptors.

2.2. Specific Aims

Specific Aim 1. The first aim of this study is to investigate the relationship between AXL and photoreceptor function in the human retina as measured objectively with electrophysiological methods.

We hypothesize that the function of both rods and cones will be reduced as a function of AXL.

Specific Aim 2. The second aim of this study is to investigate the relationship between AXL and cone recovery as measured psychophysically.

We hypothesize that the rate of cone recovery will be reduced as a function of AXL.

3. Design and Methods

3.1. Setting and Recruitment

The study was conducted at the New England College of Optometry (NECO) as part of a larger project with classmates and Master candidates Rachel Harmon, Raviv Katz, and Simon Wong. This large project involved the assessment of photoreceptors, bipolar cells, horizontal cells, amacrine cells, and ganglion cells using electrophysiology and psychophysics. Subjects were recruited from the NECO population and were scheduled for four visits that were spaced between 7-10 days. The procedures were self-paced and subjects were permitted to take breaks during the testing as needed. Subjects were informed that they are under no obligation to complete the study and may discontinue participation at any time without penalty. Subjects were also informed that their participation may be terminated if the investigators or the Institutional Review Board (IRB) believe it to be in their best interest.

Subjects were eligible based on the following inclusion criteria: 1) within 18 and 30 years of age, 2) best corrected logMAR VA=0.00 (20/20 Snellen equivalent) or better in each eye, 3) refractive error with a spherical equivalent between +5.00D to -6.00D and cylinder within 2.50D, 4) no history of ocular surgery or disease that may have resulted in visual consequences, 5) not using ocular or systemic drugs that may affect their vision, 6) no history of seizures or diagnosis of epilepsy, 7) able to provide verbal or written informed assent, 8) not pregnant or nursing, 9) no strabismus or near vision binocular abnormalities, and 10) no history of allergy to any eye drop.

3.2. Visits

3.2.1 - Order of Visits

Given the complex nature of this study, the four visits could not be conducted in order. Visit #1

was always the first visit because it consisted of an explanation of the purpose of the study, an overview of the Informed Consent Form that the subject would sign if agreed to participate, and completion of a de-identifier form that assigned a number to the subject with no identifiable information. The experimental procedures performed in Visit #2, Visit #3, and Visit #4 were performed on a date that was best for the subject, the master's student conducting the visit, and availability of the lab space. The forms for each visit can be found in the Appendix.

3.2.2 - Visit #1

At the first visit, subjects were informed of the study's procedures and the experimenters answered any questions the subjects might have. After explaining all the procedures and answering all the questions, the subjects signed an informed consent form, approved by the NECO IRB. Visit #1 also consisted of a vision screening performed to determine the subject's eligibility and refractive group inclusion with the following procedures: comprehensive case history, lensometry of habitual glasses, habitual distance and near visual acuity OD/OS/OU using a computerized logMAR chart, habitual estimated cover test for distance and near, near point of convergence (NPC) using an accommodative target, counting fingers confrontation fields (CFF), extraocular muscle (EOMs) testing, pupil evaluation, monocular estimation method (MEM) to measure the accommodative accuracy, objective refraction with static retinoscopy as well as a WAM open-field autorefractor, subjective refraction with binocular balance (if necessary), anterior ocular health evaluation, and IOP check with an iCare ic100.

After the vision screening, Visit #1 would conclude with a psychophysics procedure to assess the contrast sensitivity of ON Bipolar cells (results are available in Raviv Katz' thesis). An optical biometer (Lenstar 900, Haag-Streit, Germany) was used to obtain: AXL, anterior

chamber depth, lens thickness and keratometry. Five readings were taken for each eye before and after the psychophysical session for bipolar cells.

3.2.3 - Visit #2

Before the start of the remaining visits, visual acuities and anterior segment slit lamp examination tasks were performed to confirm that there were no changes in ocular health since the previous visit.

Visit #2 consisted of two psychophysical tasks and three electrophysiological procedures. The psychophysical tasks involved determining the contrast sensitivity function and center-surround contrast threshold in the fovea and peripheral retina. With these tasks, the lateral interactions of amacrine and horizontal cells were assessed (results are available in Rachel Harmon's thesis). Following the psychophysical tasks, the subject was dilated with two drops of 0.5% tropicamide. Afterwards, three ERG experiments were performed to determine the recovery rate of rods, the rod-contributing signal of the a-wave, and the recovery rate of cones. These ERG procedures and results are presented in this thesis and explained below in greater detail.

3.2.4 - Visit #3

Visit #3 consisted of a psychophysical task to assess contrast sensitivity of ganglion cells (results presented in Simon Wong's thesis), an OCT measurement, three ERGs, and one visually evoked potential (VEP). Following the contrast sensitivity psychophysical task, the subject was dilated with one drop of 0.5% tropicamide and a wide-field (55 degrees) optical coherence tomography instrument (Spectralis, Heidelberg, Germany) was used to obtain two custom radial scans. The

subject would then undergo multifocal ERG testing and ERG/VEP recordings to ON- and OFF-ramp flash stimuli.

3.2.5 - Visit #4

Visit #4 consisted of two psychophysical tasks. The first involved assessing the rate of cone contrast sensitivity recovery for each subject in photopic conditions. The second psychophysics task involved measuring the contrast sensitivity of OFF Bipolar cells. The optical biometer (Lenstar 900) was used again before and after the psychophysical measures, as described for Visit #3. The psychophysical data of the photoreceptor portion of this visit are presented in this thesis and explained below in greater detail.

3.3 - Electretinography

3.3.1 - ERG Set-Up

The ERG experiments were all performed during visit #2 in the following order: paired-flash rod ERGs, rod-isolating ERGs, and paired-flash cone ERGs. At the start of the ERG portion of the visit, subjects were dark-adapted for 30 minutes. During dark adaptation, the subjects were dilated with 2 drops of 0.5% tropicamide with a five-minute interval between drops. Next, the skin on their forehead and right fornix were exfoliated and ground (3M Dot, forehead) and reference electrodes (Natusdisposable skin electrode, ipsilateral temple) were placed. Afterwards, the DTL active electrode (Diagnosys) was placed along the inferior bulbar conjunctiva of the subject and the impedance of the electrodes were measured to ensure that it was below 5 k Ω . A red light head mount lamp was utilized to set up the electrodes in these scotopic conditions. After set-up, the subjects were seated in the Diagnosys Ganzfeld

ColorDome using a chin rest to begin the experiment.

3.3.2 - Single Flash ERGs for cones and rods

A traditional flash electroretinogram represents the changes in the electrical current of the retina due to a single flash of light. This response primarily consists of a negative a-wave, which represents the photoreceptor activity with some OFF-bipolar cell contribution, and a positive b-wave, which represents the ON-bipolar cell activity (Bhatt et al., 2023).

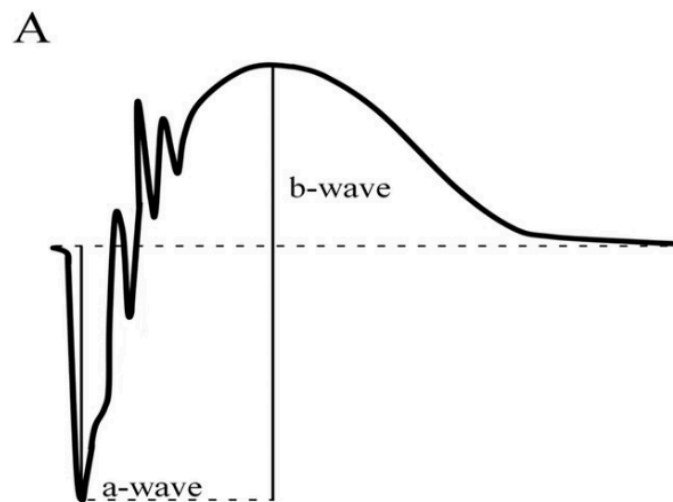


Figure 3.1 - a-wave and b-wave component of a full field electroretinogram from Bhatt et al. 2023 (pg 2).

Under photopic conditions, this technique measures the activity of the cone photoreceptors and the photopic system. The rod response can be diminished by recording the ERGs under a saturating, short-wavelength background to saturate rod activity and isolate cone activity (Robson et al., 2018).

Similarly, the rod photoreceptor activity can be measured under dark-adapted, scotopic conditions but, interestingly, cones are shown to also play a non-negligible role in the electrical

response in the scotopic ERGs (Brigell et al. 2020). Thereby, in order to isolate the rod electrical activity, two separate flashes must be presented: a scotopic flash under dark-adapted conditions to obtain the mixed rod and cone electrical activity and a photometrically matched flash in photopic conditions to obtain the cone electrical activity. Afterwards, the photopic recording would be subtracted from the scotopic recording to obtain the rod-driven response of the scotopic ERG. Figure 3.2 displays the process, with the black curve representing the mixed rod-cone response and the red curve representing the cone response (Brigell et al. 2020). The blue curve represents the rod-isolated response after subtracting the cone response from the rod-cone mixed response. This methodology was utilized to obtain the cone ERGs and the rod-isolated ERGs in this thesis.

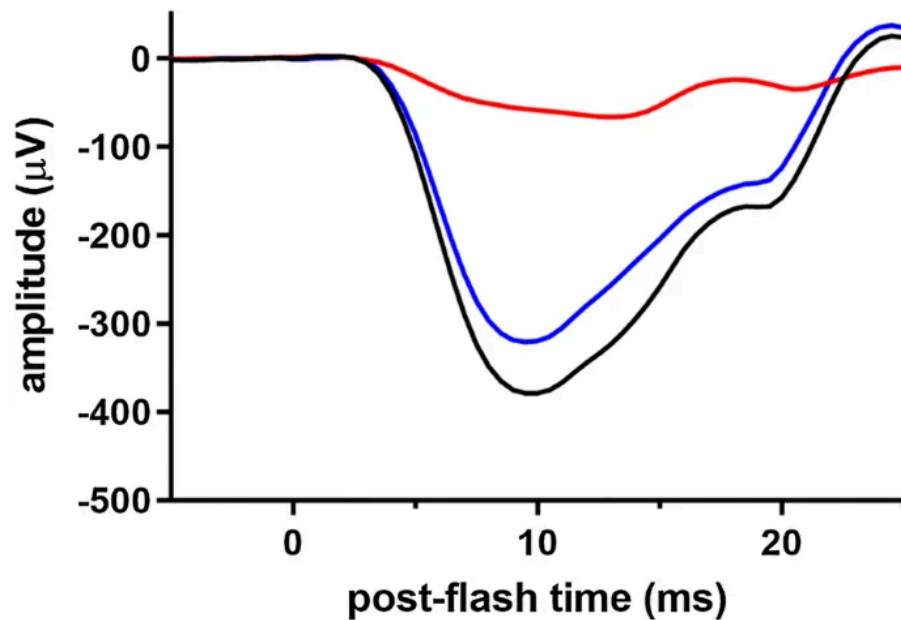


Figure 3.2 - ERG recordings from identical flashes (30 cd s/m²) that were presented in dark-adapted (black, DA) and light-adapted (red, LA) conditions. The rod-isolated recording was obtained by subtracting the LA signal from the DA signal, from Brigell et al. 2020 (pg 5).

3.3.3 - Paired-Flash ERGs for cones and rods

Even though the phototransduction process of rods and cones can be visualized with single flash ERGs through the a-wave, the remainder of the photoreceptor activity is masked by the proceeding b-wave. Thereby, the full time course of the photoreceptor activity cannot be analyzed. In order to bypass this constraint, the paired flash methodology was developed. As evidenced by its name, this method involves two successive flashes: a weak, low-intensity flash (test) that is followed by a bright, high-intensity flash (probe) at varying inter-stimulus intervals. The purpose of the probe flash is to essentially saturate the remaining circulating current from the b-wave and allow for the full-time course of the photoreceptor to be reconstructed.

Figure 3.3 visualizes this concept (Pepperberg et al., 2000). The top half displays a hypothetical paired flash ERG response. A test flash is presented at $t=0$, the a-wave, b-wave and oscillatory potentials develop soon after, and then a bright probe flash is presented after a certain interval of time to create a second ERG response with a rapidly developed a-wave. If the probe flash was closer to the test flash at a shorter interflash interval, the secondary a-wave would be generated earlier and essentially mask the a-wave of the test flash. Similarly, if the interflash interval was longer, then the secondary a-wave from the probe flash would mask the pre-existing electrical current from the b-wave of the initial test flash.

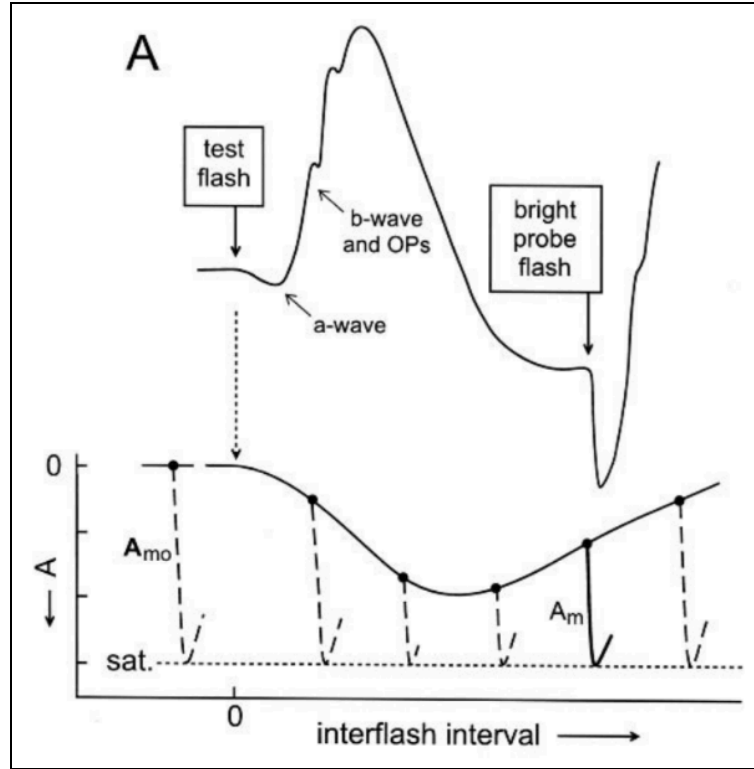


Figure 3.3 - Diagram of the paired-flash method from Pepperberg et al., 2000 (pg 206). (A) Hypothetical paired flash ERG response with a test-flash presented at $t=0$ followed by an a-wave, b-wave, and oscillatory potentials. The bright probe flash is presented after a certain interflash interval to elicit a second a-wave. (B) Reconstruction of test a-wave time course with equation two. A_{mo} is the dashed hook to the left of $t=0$ that represents the full, probe-alone stimulus. The proceeding dash hooks after $t=0$ represent the amplitude of the a-wave when the probe flash is presented at different interstimulus intervals after the test flash.

In Figure 3.3, this concept is used to construct a hypothetical a-wave time course. A_{mo} , the dashed hook to the left of $t=0$, represents the amplitude of the a-wave due to the probe-alone flash (i.e., the probe flash does not follow a test flash). The proceeding dashed hooks A_m after $t=0$ represent the amplitude of the a-wave due to a probe flash that is presented at different interstimulus intervals after the test flash. With these conditions, the a-wave amplitude of the test flash can be determined using equation two where $A(t)$ represents the a-wave amplitude of the test flash at a specific interflash interval t and A_m presents the a-wave amplitude of the probe flash at t .

$$(2) A(t) = A_{mo} - A_m(t)$$

Using equation 2, the bottom half of Figure 3.3 is constructed to depict the time course of the test flash a-wave. During shorter interflash intervals, the test flash will have a weaker amplitude because the probe flash is largely contributing to the a-wave of the electroretinogram. With longer interflash intervals, the photoreceptors from the initial test flash are able to recover and thereby, the probe flash will produce a higher amplitude a-wave. Plotting the amplitude over varying interflash intervals allows one to construct the time course of photoreceptors and analyze their rate of phototransduction and rate of recovery. In this study, the fractional response of the probe flash (A_{mo}/A_m) was measured at 6ms on the paired-flash ERG for cones and 10ms on the paired-flash ERG for rods and was plotted against the interstimulus interval to obtain the same time course of the photoreceptors. The amplitude of the a-wave in a paired flash paradigm is not measured at the trough of the a-wave, but rather a few ms earlier, to avoid any post-receptoral contribution in the measured amplitude.

Similar to the single-flash ERGs, the paired-flash ERGs can be performed in photopic and scotopic conditions. Likewise, the cone contribution to the scotopic signal must be subtracted with a photometrically matched long-wavelength flash.

3.3.4 - Paired-flash Rod ERGs Parameters

This method was largely adapted from the paired flash ERG protocol from Pepperberg et al., 1997. Two different colored probe flashes were used in order to subtract the cone contribution from the mixed rod-cone response. This protocol consists of a blue, short-wavelength test flash, a blue short-wavelength probe flash, and a red long-wavelength probe flash. The first three steps of

the ERG protocol involved individual blue test, red probe, and blue probe flashes alone. The remainder of the steps involved paired flashes of the blue test and the blue probe at specific interstimulus intervals (ISI). Three sweeps were recorded in each step and between each sweep, there was a one-minute dark-adaptation recovery period. Table 3.1 provides an overview of the stimulus timing and parameters which were all controlled with a custom script in the Diagnosys Ganzfeld ColorDome.

Table 3.1 - The rod paired-flash ERG time course. Steps 1, 2 and 3 consist of blue test, red probe, and blue probe flashes that were presented alone. Steps 3-9 consist of the blue test and blue probe paired flashes with 100, 175, 250, 325, 400, and 500ms interstimulus intervals (ISI) between the two flashes.

Step	Blue Test	Red Probe	Blue Probe	ISI (ms)
#1	5 cd/m ²	-	-	none
#2	-	507 cd/m ²	-	none
#3	-	-	507 cd/m ²	none
#4	5 cd/m ²	-	507 cd/m ²	100
#5	5 cd/m ²	-	507 cd/m ²	175
#6	5 cd/m ²	-	507 cd/m ²	250
#7	5 cd/m ²	-	507 cd/m ²	325
#8	5 cd/m ²	-	507 cd/m ²	400
#9	5 cd/m ²	-	507 cd/m ²	500

3.3.5 - Rod-Isolating ERGs Parameters

This method is largely adapted from the rod-isolating ERG protocol from Brigell et al., 2020. This experiment was performed after the paired-flash rod ERGs. Under the same dark-adapted conditions from the previous ERGs, the subject would receive a white flash to measure the rod-driven response. Afterward, subjects will be light-adapted for 10 minutes and will be

presented with a white flash to measure the cone-driven response. Five sweeps were recorded in each step. The cone response was then subtracted from the rod response in order to obtain the rod-isolating ERG. Under dark adaptation, there was a one minute recovery period for each sweep and under light adaptation, there was a thirty second recovery period for each sweep.

Table 3.2 provides an overview of the stimulus timing and parameters

Table 3.2 - The rod isolating-flash ERG time course. Step 1 consists of a single flash in scotopic conditions. After Step 1, subjects would remain in the ganzfeld apparatus for 10 minutes to light adapted with the appropriate background luminance. Step 2 would then proceed with a single flash in photopic conditions.

Step	Flash	Background luminance
#1	75 scotopic cd.s /m ²	-
10 minute light adaptation		
#3	30 photopic cd.s /m ²	30 cd /m ²

3.3.6 - Paired-flash Cone ERGs Parameters

This method is largely adapted from the paired flash ERG protocol from Friedburg et al., 2004. This protocol consisted of a white test flash and a white probe flash in photopic conditions with a blue background for rod saturation. The first two steps of the ERG protocol involved the test and probe flashes individually. The remainder of the steps involved paired flashes of the test and the probe at specific interstimulus intervals (ISI). Ten sweeps were recorded in each step and between each sweep, there was a two second recovery period. Table 3.3 provides an overview of the stimulus timing and parameters.

Table 3.3 - The cone paired-flash ERG time course. Steps 1 and 2 consist of a test and probe flashes that were presented alone. Steps 4-14 consist of the test and probe paired flashes with 2, 6, 10, 14, 18, 20, 22, 24, 26, and 30ms interstimulus intervals (ISI) between the two flashes.

Step	Test	Probe	Background (blue)	ISI (ms)
#1	150 cd/m ²	-	-	none
#2	-	20,000 cd.s /m ²	-	none
#4	150 cd/m ²	20,000 cd.s /m ²	3 cd/m ²	2
#5	150 cd/m ²	20,000 cd.s /m ²	3 cd/m ²	6
#6	150 cd/m ²	20,000 cd.s /m ²	3 cd/m ²	10
#7	150 cd/m ²	20,000 cd.s /m ²	3 cd/m ²	14
#8	150 cd/m ²	20,000 cd.s /m ²	3 cd/m ²	18
#9	150 cd/m ²	20,000 cd.s /m ²	3 cd/m ²	20
#11	150 cd/m ²	20,000 cd.s /m ²	3 cd/m ²	22
#12	150 cd/m ²	20,000 cd.s /m ²	3 cd/m ²	24
#13	150 cd/m ²	20,000 cd.s /m ²	3 cd/m ²	26
#14	150 cd/m ²	20,000 cd.s /m ²	3 cd/m ²	30

3.4 - Cone Psychophysics

The purpose of the psychophysical experiment was to examine the recovery of contrast sensitivity in cone photoreceptors. The psychophysical task was developed by Dr. Peter Bex. The stimuli were created and displayed using MatLab (Mathworks) and the psychophysics toolbox.. During the experiment, subjects would sit in front of a screen that presents flashes, for bleaching the retina, with a fixed duration of 500 ms. The interval between two consecutive flashes was varied between 33, 66, 133, 267, 533, 1067, 3201, and 5335 ms. The photoreceptor recovery from the flash is measured at varying points post bleaching. Subjects were presented with an eight-alternative forced-choice identification task where subjects identified the gap of a Landolt

C that varied in contrast. This task was a continuous error measure, with error as a function of contrast fit with a cumulative Gaussian function. Threshold and 95% confidence intervals are estimated from the midpoint of the Gaussian. In shorter interflash intervals, the photoreceptor recovery time is shorter resulting in higher thresholds, and lower contrast sensitivity. At longer interflash intervals, the cones would have more time to recover from bleaching so subjects would have a lower threshold and higher contrast sensitivity.

3.5. Apparatus

The full field ERG stimuli were recorded monocularly on subjects using ColorDome (Diagnosys LLC, Lowell, MA). For the psychophysical experiments, a 48" LG OLED monitor (48GQ900-B 4K UHD, 3840x2160, 120 Hz) was used on a linux PC running MATLAB (Mathworks, MA) and Psychtoolbox (Brainard 1997).

3.6. Statistical analysis

A Levenberg-Marquardt nonlinear least squares algorithm was utilized with R studio to fit the photoreceptor mathematical model (Equation 1) in order to determine the sensitivity and maximum saturation of the photoreceptors. MATLAB software was performed to determine the area under the curve in the psychophysical tasks and linear regressions will be performed on R studio to analyze the correlations between the AXL and photoreceptor function as measured electrophysiologically and psychophysically.

4. Results

4.1. Subjects

A total of 36 subjects were recruited and completed all four visits of this study. These subjects' average age was 25.00 ± 2.22 years (mean \pm sd), with a range of 22 to 32 years, and the average refractive error (spherical equivalent, M) was -3.11 ± 2.30 D, with an average AXL of 24.97 ± 1.17 mm. Figure 4.1 displays the correlation between the refractive error (spherical equivalent, M) and AXL of these 36 subjects. Electrophysiological and psychophysical data were collected from the right eye only.

Due to the evolving nature of the protocols for some of the experiments, all 36 subjects were not included in the final analysis of each of the various electrophysiological and psychophysical experiments.

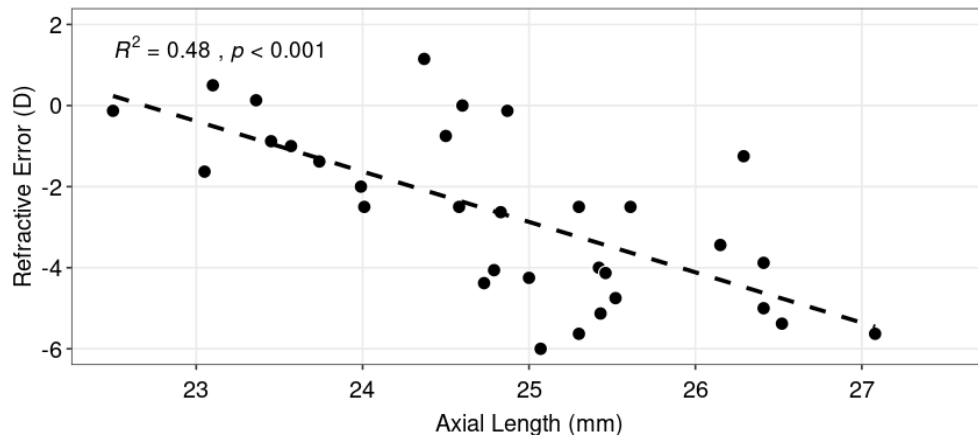


Figure 4.1 - Scatter plot of ocular axial length (AXL, in mm) and refractive error (spherical equivalent, M, in D) of the 36 subjects that were recruited for this study.

4.2. Electrophysiology: Rod Isolating ERGs

Data from 34 subjects were analyzed for the rod-isolating ERGs. The mean age for these subjects was 24.85 ± 2.20 years (mean \pm sd), and the average AXL 24.90 ± 1.14 mm. Figure 4.2 provides

an example of the data, with the solid black line representing the mixed rod and cone response in dark adaptation, the dotted black line representing the cone driven response in light adaptation, the dash black line representing the rod-isolating response (which is the solid black line minus the dotted black line), and the dashed grey line representing the mathematical model (Equation 1) that was fitted on the leading edge of the a-wave of the photoreceptor response.

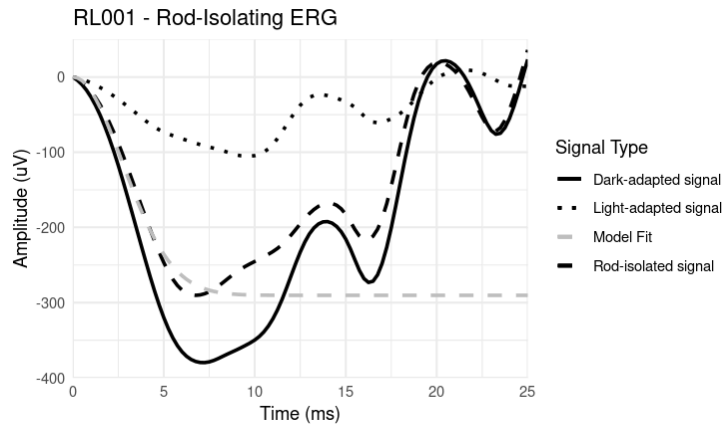


Figure 4.2 - Rod-Isolating ERG from subject RL001. Similar to Figure 3.2 from Brigell et al. 2020, a dark-adapted response (solid black line, DA) and light-adapted response (dotted black line, LA) were obtained and the rod-isolating response (dashed black line) was obtained by subtracting the LA response from the DA response. The Rmax and Sensitivity values were determined by fitting equation 1 to the rod-isolating response (dashed grey line).

The model fits the kinetics of the phototransduction of the photoreceptors (Pugh & Lamb, 1993) and can be utilized to extrapolate the sensitivity (S) and saturated maximum amplitude (Rmax) from the rods. Individual results for each of the 34 subjects can be found in the Appendix. The average Rmax was -218.979 ± 49.169 uV with a range of -307.988 to -135.266 uV and the average S was 18.068 ± 4.298 sec⁻² (td sec)⁻¹ with a range of 6.860 to 27.240 sec⁻² (td sec)⁻¹. Figures 4.3 and 4.4 show the correlation between the rod Rmax and S and AXL.

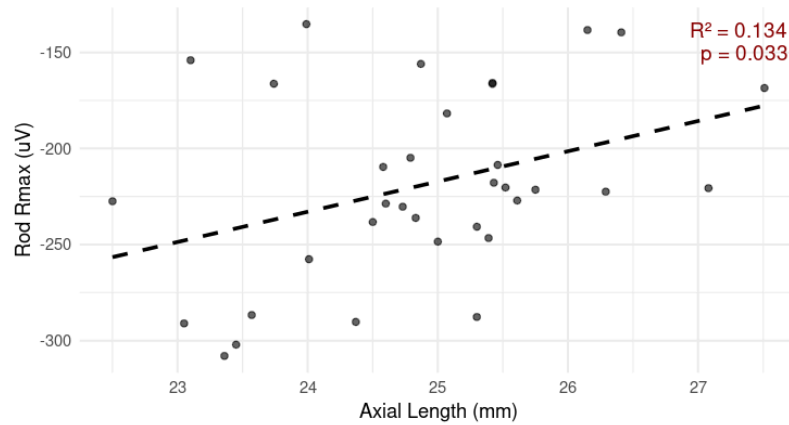


Figure 4.3 - Scatter plot between axial length (AXL, mm) and rod Rmax (saturating amplitude, uV) of the 34 subjects from the rod-isolating ERG experiments with a line of best fit (dashed black line).

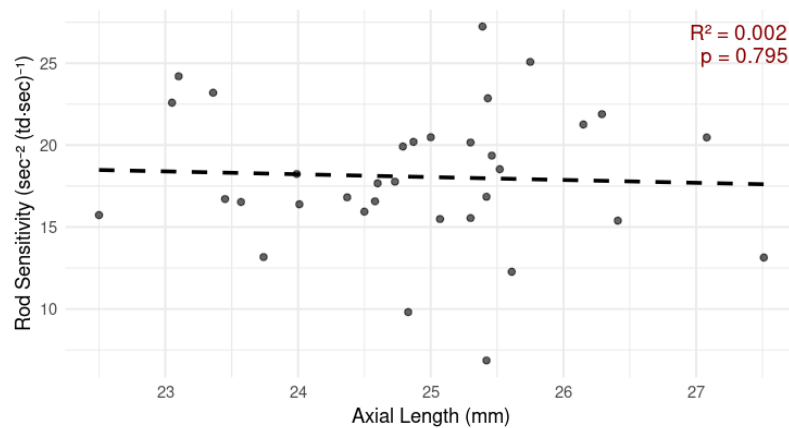


Figure 4.4 - Scatter plot between axial length (AXL, mm) and rod sensitivity ($\text{sec}^{-2} (\text{td sec})^{-1}$) of the 34 subjects from the rod-isolating ERG experiments with a line of best fit (dashed black line).

A Welch Two Sample t-test was performed to determine the median split for the AXL to categorize subjects into short (below the median split) or long AXL (above the median split). The purpose of the split median analysis is to determine if there was any significant difference in the Rmax values between the two groups. The median AXL was 24.935 mm, with the mean Rmax in the longer AXL group being -207.201 uV, and the mean Rmax in the shorter AXL group being -230.757 uV. The p-value for the difference was 0.167.

The same split median analysis was performed relating to the subject's AXL and rod sensitivity S. The mean S in the longer AXL group was $18.405 \text{ sec}^{-2}(\text{td sec})^{-1}$ and the mean S in the shorter AXL group was $17.732 \text{ sec}^{-2}(\text{td sec})^{-1}$, with a difference p-value of 0.656.

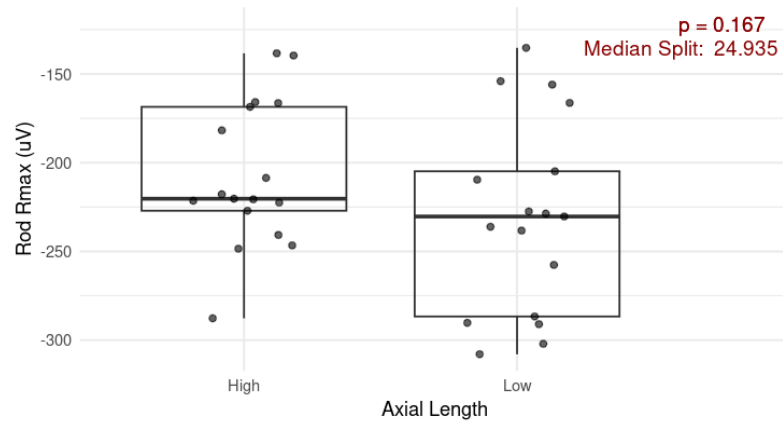


Figure 4.5 - Boxplot of rod Rmax in subjects with longer axial length (AXL) ($\geq 24.935\text{mm}$), and those with shorter AXL ($< 24.935\text{mm}$), based on the split median analysis.

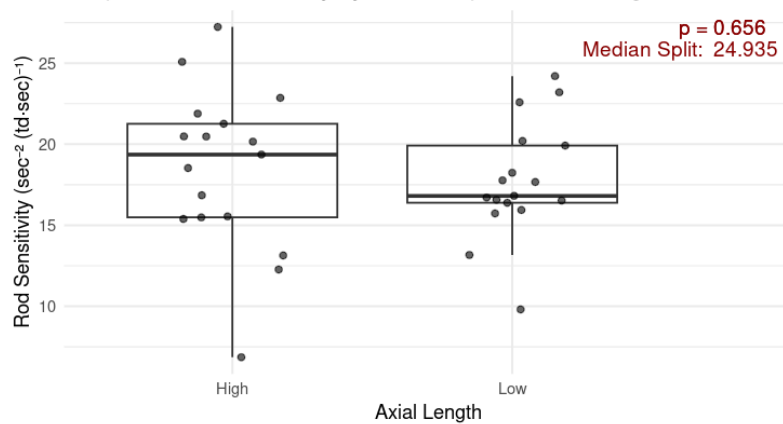


Figure 4.6 - Boxplot of rod sensitivity in subjects with longer axial length (AXL) ($\geq 24.935\text{mm}$), and those with shorter AXL ($< 24.935\text{mm}$), based on the split median analysis.

4.3. Electrophysiology: Cone ERGs

Data from 29 subjects were analyzed for the cone ERGs. Their mean age was 24.68 ± 1.81 years (mean \pm sd) and the average AXL of the subjects was 24.88 ± 1.22 mm. Figure 4.7 provides an example of the data, with the black line representing the cone driven response in light adaptation and the dashed grey line representing the mathematical model (Equation 1) that was fitted on the leading edge of the a-wave of the cone photoreceptor response. The model was then used to extrapolate the sensitivity and saturated maximum amplitude (Rmax) from the cones. Individual results for each of the 29 subjects can be found in the Appendix.

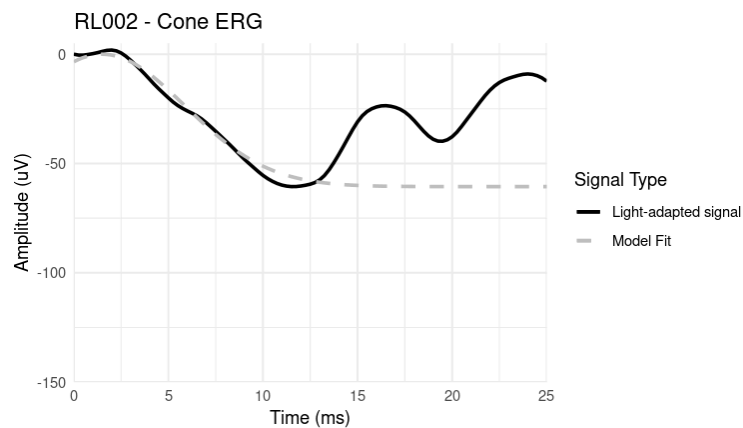


Figure 4.7 - Cone ERG from subject RL002. Light-adapted response (black solid line) was obtained and equation 1 was fitted to the response (dashed grey line). The Rmax and Sensitivity values were determined by fitting equation 1 to the cone, light-adapted response.

The average Rmax was -49.104 ± 18.102 uV, with a range of -94.487 to -23.985 uV, and the average sensitivity was 10.992 ± 4.599 sec⁻²(td sec)⁻¹, with a range of 4.890 to 23.539 sec⁻²(td sec)⁻¹. Figures 4.8 and 4.9 show the correlation between AXL and Rmax of cones as well as AXL and sensitivity of cones.

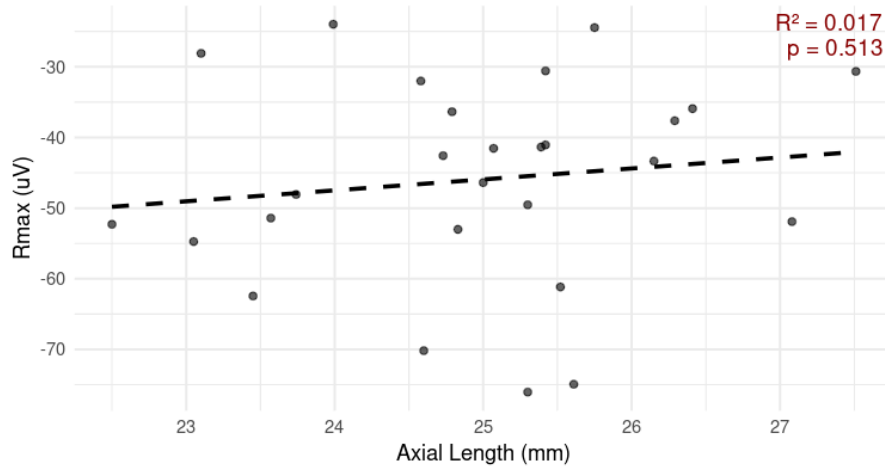


Figure 4.8 - Scatter plot between axial length (AXL, mm) and cone Rmax (saturating amplitude, uV) of the 29 subjects from the cone ERG experiments with a line of best fit (dashed black line).

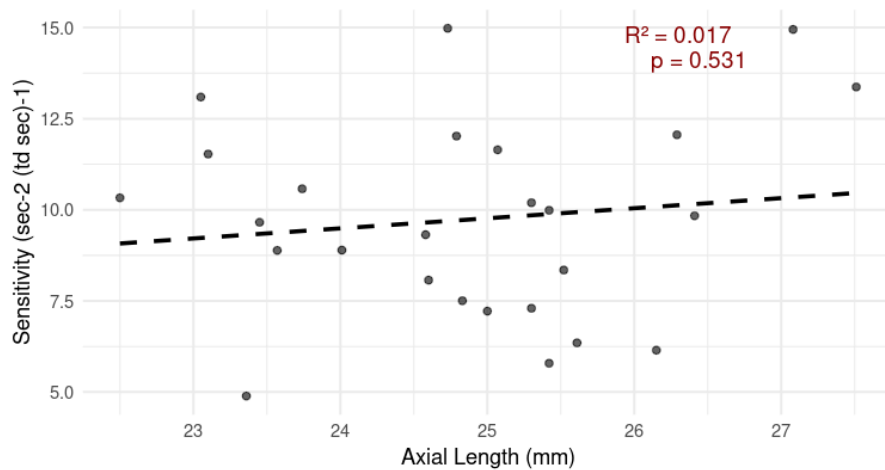


Figure 4.9 - Scatter plot between axial length (AXL, mm) and cone sensitivity (sec⁻²(td sec)⁻¹) of the 29 subjects from the cone ERG experiments with a line of best fit (dashed black line).

Figure 4.10 displays a boxplot of Rmax by the median split of AXL. The median AXL of the 29 subjects was 25.070 mm (Welch Two Sample t-test). The mean Rmax in the longer AXL group was -46.045 uV, and the mean Rmax in the shorter AXL group was -45.939 uV, with a p-value for the difference of 0.985.

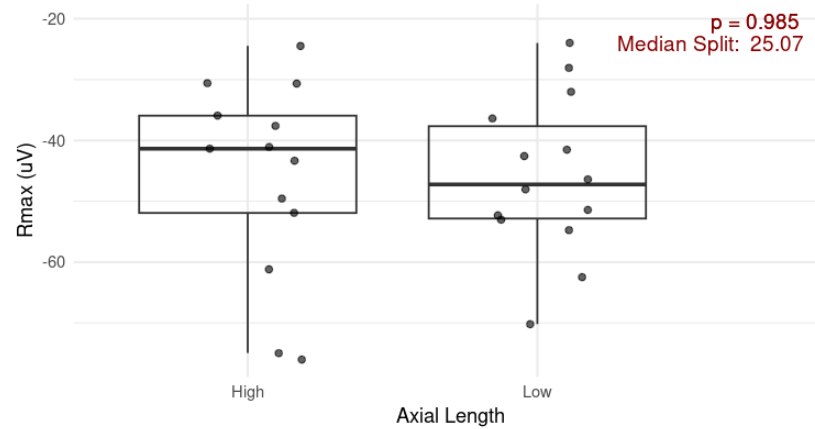


Figure 4.10 - Boxplot of cone Rmax in subjects with longer axial length (AXL) (≥ 25.070 mm), and those with shorter AXL (< 25.070 mm), based on the split median analysis.

Figure 4.11 displays a boxplot of the cone sensitivity by the median split of AXL. The median AXL of the 29 subjects was 24.915 mm (Welch Two Sample t-test). The mean Sensitivity in the longer AXL group was $9.477 \text{ sec}^{-2} (\text{td sec})^{-1}$, and the mean Sensitivity in the shorter AXL group was $9.981 \text{ sec}^{-2} (\text{td sec})^{-1}$, with a p-value for the difference of 0.646.

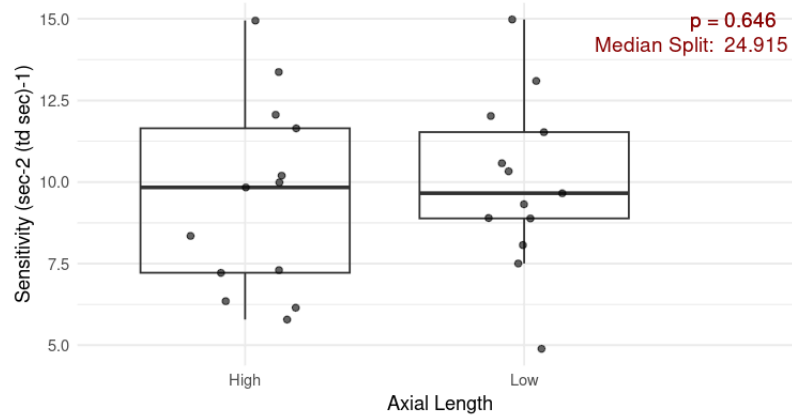


Figure 4.11 - Boxplot of cone sensitivity in subjects with longer axial length (AXL) (≥ 24.915 mm), and those with shorter AXL (< 24.915 mm), based on the split median analysis.

4.4. Electrophysiology: Rod Paired Flash ERGs

Data from 19 subjects were analyzed for the rod paired-flash ERGs. Numerous iterations of the rod-paired flash methodology was developed during the course of this study. The data analyzed is from the version of the method that was finalized midway which led to the reduced sample size that is seen with the rod-paired flash ERGs.

Their mean age was 23.94 ± 1.70 years (mean \pm sd) and the average AXL of the subjects was 25.00 ± 1.21 mm. Figure 4.12 provides an example of the derived rod response to the test flash, with the dashed black line representing the line of best fit for the recovery of the rod photoreceptors. The slope of the line represents the rate of recovery of the subject's rods and that information would be correlated with AXL. The line of best fit was plotted from the interstimulus interval where the rod photoreceptors began to recover, which for many subjects was at the 175ms interstimulus interval. Individual results for each of these 19 subjects can be found in the Appendix.

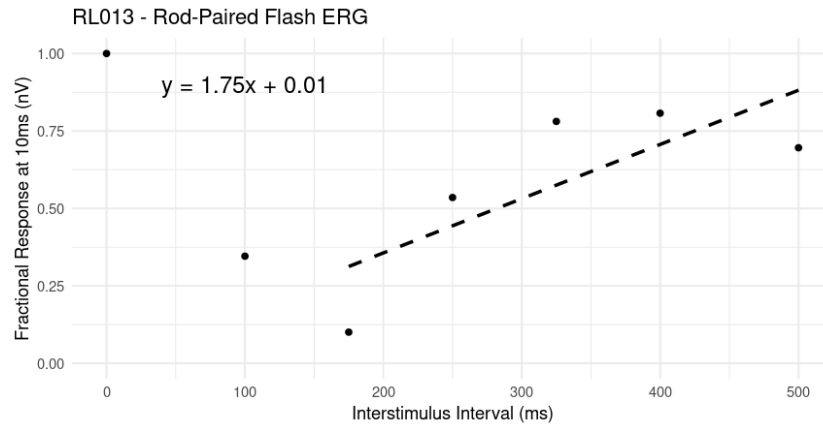


Figure 4.12 - Scatterplot of the derived rod response to a test flash from subject RL013. The dashed purple line is the line of best fit for the recovery of the rod photoreceptors. The slope in the line of best fit represents the rate of recovery of the rod photoreceptors.

The average rate of recovery in rods was 1.835 ± 0.515 nV/ms with a range of 0.949 to 2.952 nV/ms. Figure 4.13 below shows the correlation between the AXL and the rate of recovery of rods.

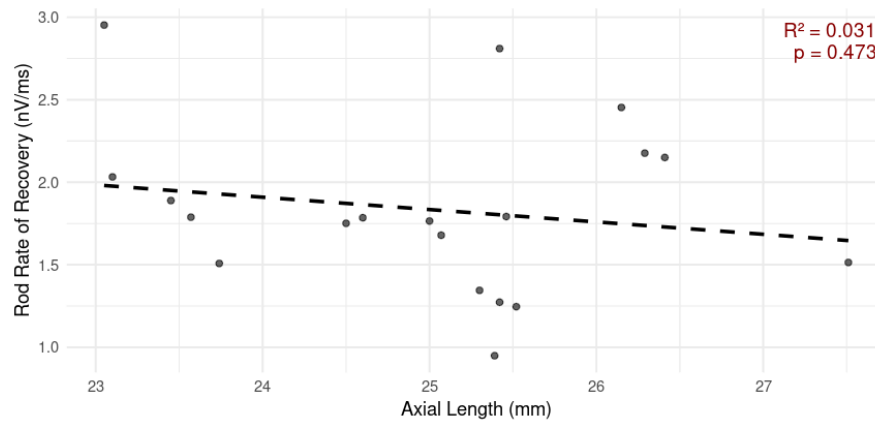


Figure 4.13 - Scatter plot between axial length (AXL) and rod rate of recovery of the 19 subjects from the rod paired-flash ERG experiments with a line of best fit.

Figure 4.14 displays a boxplot of the rod rate of recovery by the median split of AXL. The median AXL of these 29 subjects was 25.300 mm (Welch Two Sample t-test). The mean rod rate of recovery in the high AXL group was 1.818 nV/ms, and the mean rod rate of recovery in the low AXL group was 1.849 nV/ms, with a p-value for the difference of 0.901.

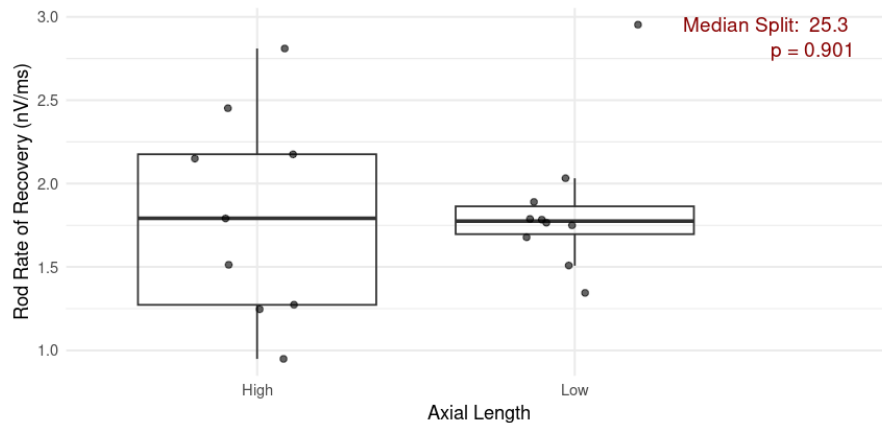


Figure 4.14 - Boxplot of rod rate of recovery in subjects with large axial length (AXL) (≥ 25.300 mm), and those with low AXL (< 25.300 mm), based on the split median analysis.

4.5. Electrophysiology: Cone Paired Flash

Data from 27 subjects were analyzed for the cone paired-flash ERGs. Their mean age was 24.42 ± 1.86 years (mean \pm sd) and the average AXL of the subjects was 24.91 ± 1.24 mm. Figure 4.15 provides an example of the data, with the dashed grey line representing the line of best fit for the phototransduction and the dashed black line representing the line of best fit for the recovery of the cone photoreceptors, respectively. The respective slopes of each line represent the rate of phototransduction or recovery of the subject's cone photoreceptors and that information would be compared to the AXL. Individual results for each of these 27 subjects can be found in the Appendix.

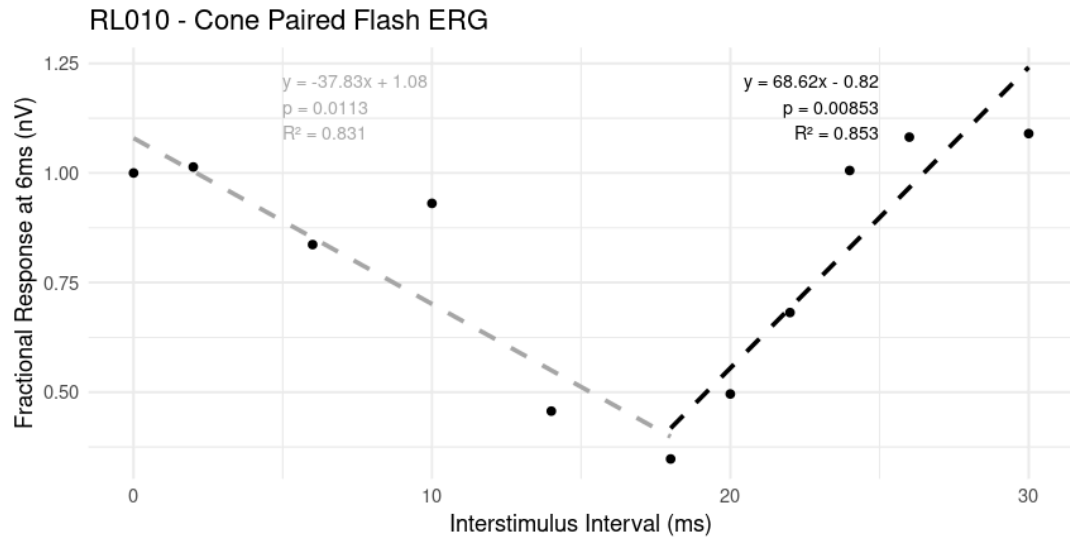


Figure 4.15 - Scatterplot of the derived cone response to a test flash from subject RL010. The grey line is the line of best fit for the phototransduction of the cone photoreceptors and the black line is the line of best fit for the recovery of the cone photoreceptors.

Figures 4.16 and 4.17 show the correlation between the cone phototransduction and AXL and the rate of cone recovery as a function of AXL. The average rate of cone phototransduction was -29.310 ± 7.275 nV/ms, with a range of -49.660 to -18.840 nV/ms, and the average rate of cone recovery was 62.794 ± 19.925 nV/ms, with a range of 28.140 to 121.500 nV/ms.

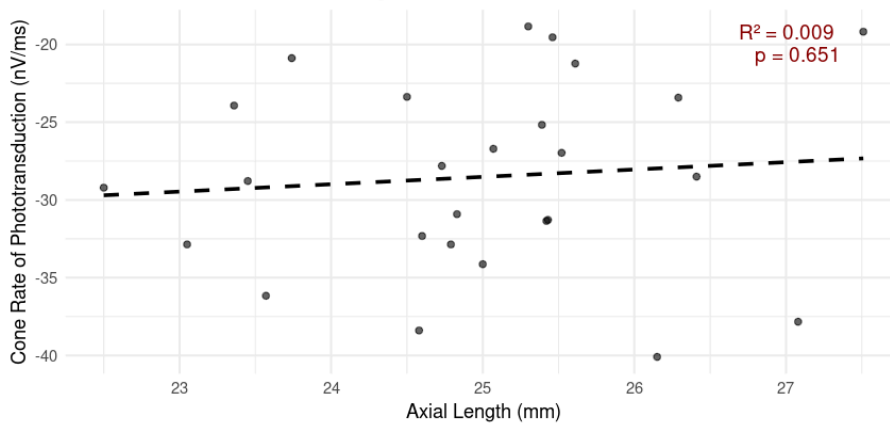


Figure 4.16 - Scatter plot between AXL and cone rate of phototransduction of the 27 subjects from the cone paired-flash ERG experiments with a line of best fit (dashed black line).

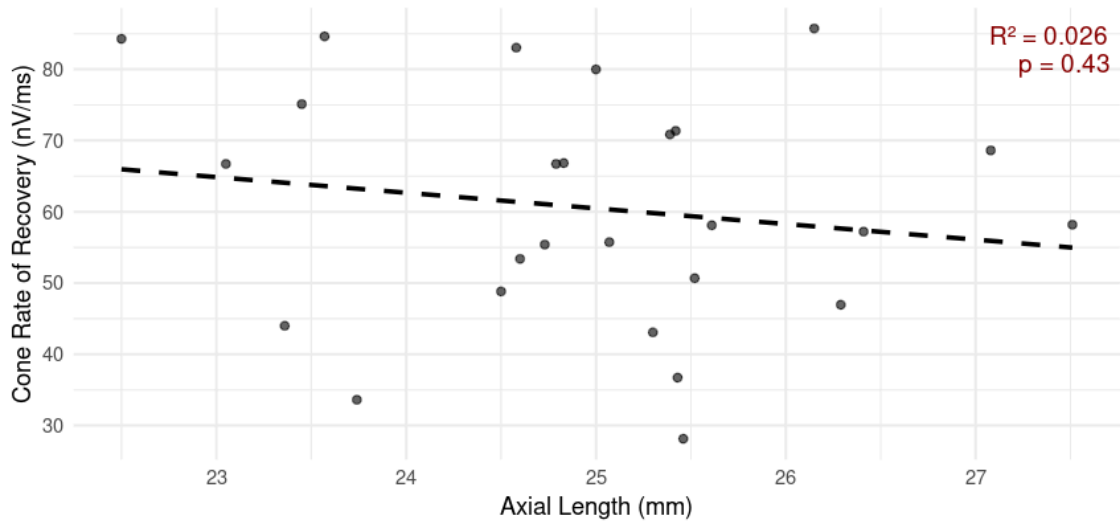


Figure 4.17 - Scatter plot between AXL and cone rate of recovery of the 27 subjects from the cone paired-flash ERG experiments with a line of best fit (dashed black line).

Figure 4.18 displays a boxplot of the cone rate of phototransduction by the median split of AXL. The median AXL of the 27 subjects was 25.035 mm (Welch Two Sample t-test). The mean cone rate of phototransduction in the longer AXL group was -26.931 nV/ms, and the mean cone rate of phototransduction in the shorter AXL group was -30.124 nV/ms, with a difference p-value of 0.192.

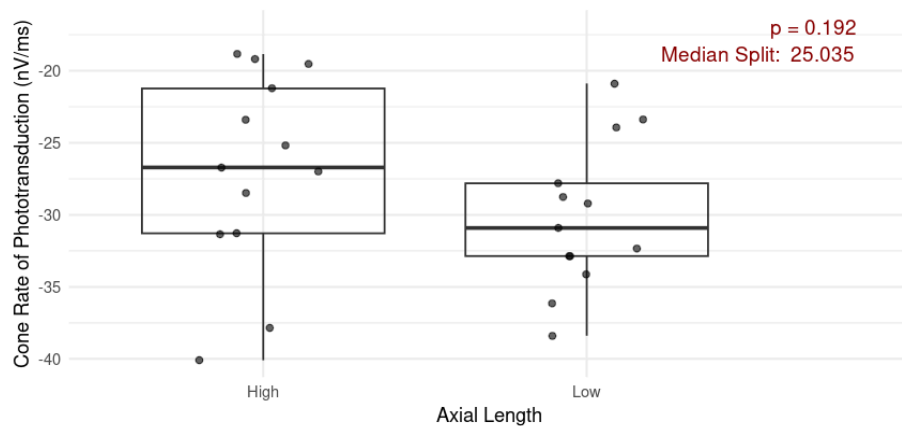


Figure 4.18 - Boxplot of cone rate of phototransduction in subjects with longer axial length (AXL) (≥ 25.035 mm), and those with low AXL (< 25.035 mm), based on the split median analysis.

Figure 4.19 displays a boxplot of the cone rate of recovery by the median split of AXL. The median AXL of the 29 subjects was 25.035mm (Welch Two Sample t-test). The mean cone rate of phototransduction in the longer AXL group was 56.261 nV/ms, and the mean cone rate of phototransduction in the shorter AXL group was 64.812 nV/ms, with a difference p-value of 0.190.

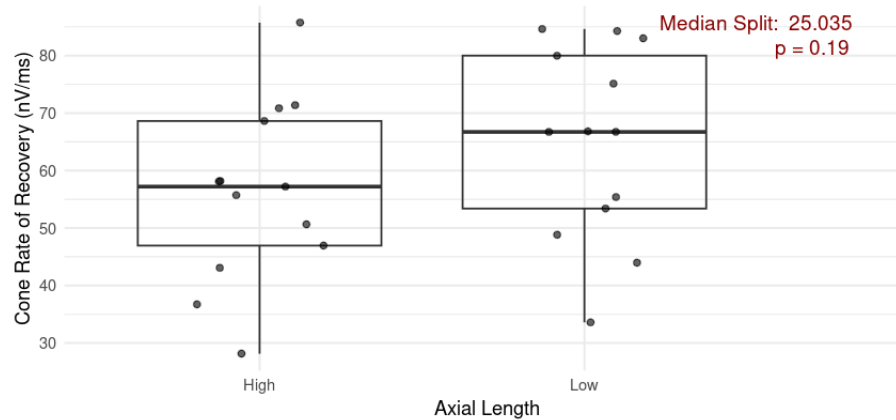


Figure 4.19 - Boxplot of cone rate of recovery in subjects with longer axial length (AXL) (≥ 25.035 mm), and those with low AXL (< 25.035 mm), based on the split median analysis.

4.6. Psychophysics: Cones

Data from 24 subjects were analyzed for the cone psychophysics. Their mean age was 24.54 ± 1.72 years (mean \pm sd) and the average AXL of the subjects was 24.85 ± 1.21 mm. Figure 4.20 provides an example of the data in subject RL007 as it depicts the total area of the curve of the subject's recovery of contrast sensitivity through the course of the experiment. Individual results for each of these 24 subjects can be found in the Appendix.

The data was then modeled as a negative exponential growth model with a rate and asymptote parameter. Equation 3 provides an example of the model utilized in RStudio for this analysis:

$$(3) y = \alpha * (1 - \exp(-k * t))$$

In this equation, alpha represents the upper asymptote, k represents the growth rate, while y is the contrast sensitivity CS and t the interstimulus interval. In the context of this experiment, the upper asymptote would indicate the maximum cone CS recovery of the cone photoreceptors while the growth rate indicates how fast the cone photoreceptors reach their maximum recovery.

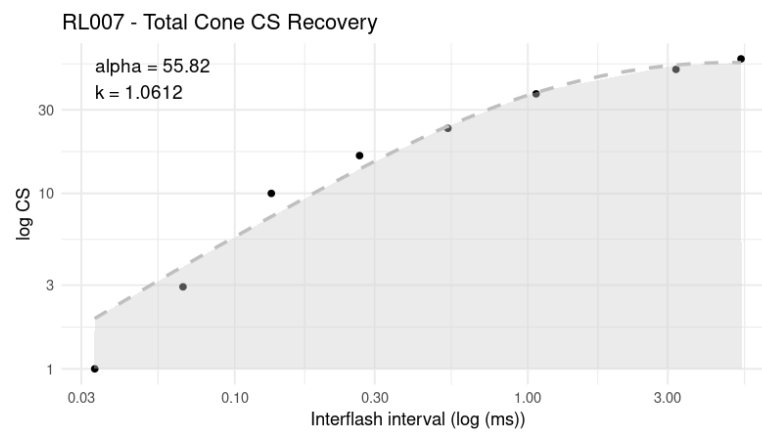


Figure 4.20- Scatter plot with filled area under the curve of the cone contrast sensitivity recovery from subject RL007 in logarithmic scale

The correlations between the AXL and the total cone contrast recovery (area under the curve), the maximum cone CS recovery, and the growth rate of cones are displayed in Figures 4.21, 4.22, and 4.23, respectively.

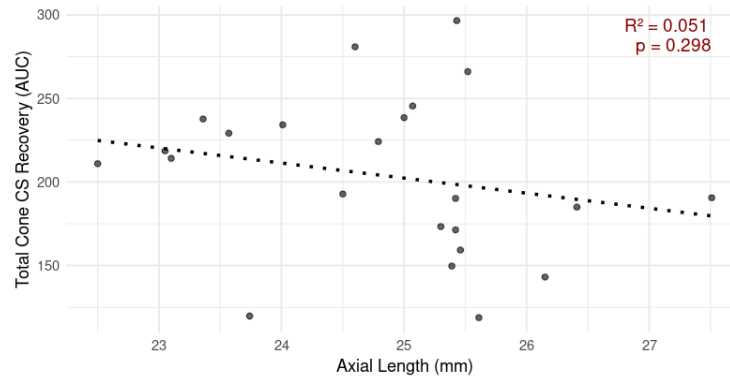


Figure 4.21 - Scatter plot between AXL and total cone contrast sensitivity recovery of the 24 subjects from the cone psychophysics experiment with a line of best fit.

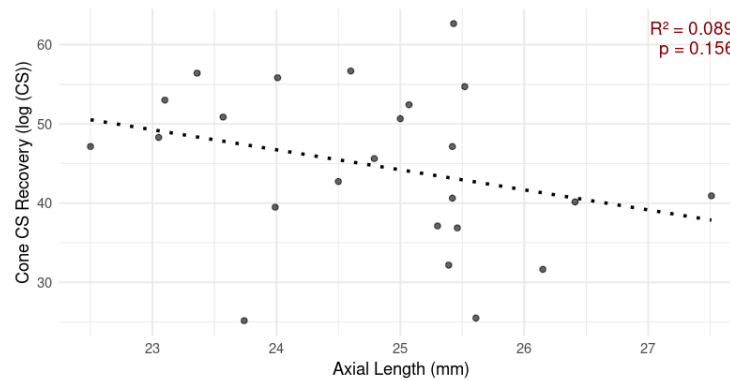


Figure 4.22 - Scatter plot between AXL and maximum cone contrast sensitivity recovery of the 24 subjects from the cone psychophysics experiment with a line of best fit.

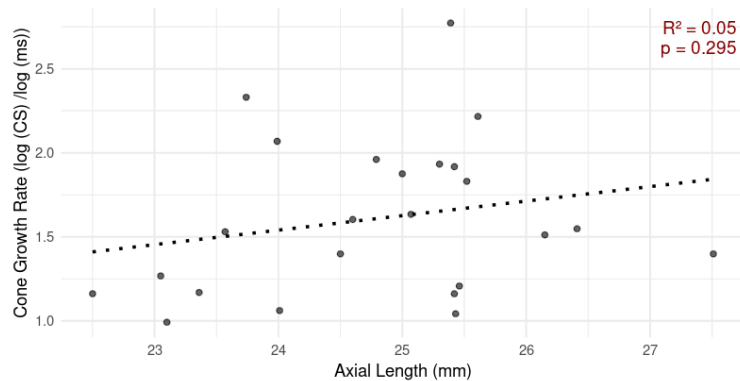


Figure 4.23 - Scatter plot between AXL and cone growth rate of the 24 subjects from the cone psychophysics experiment with a line of best fit.

Figure 4.24 shows a boxplot of the median split analysis on the total cone contrast sensitivity recovery. The median AXL of the 24 subjects was 25.070 mm (Welch Two Sample t-test). The mean rate of contrast sensitivity recovery in the longer AXL group was 185.780 units and the mean rate of contrast sensitivity recovery in the shorter AXL group was 220.521 units, with a p-value for the difference of 0.088.

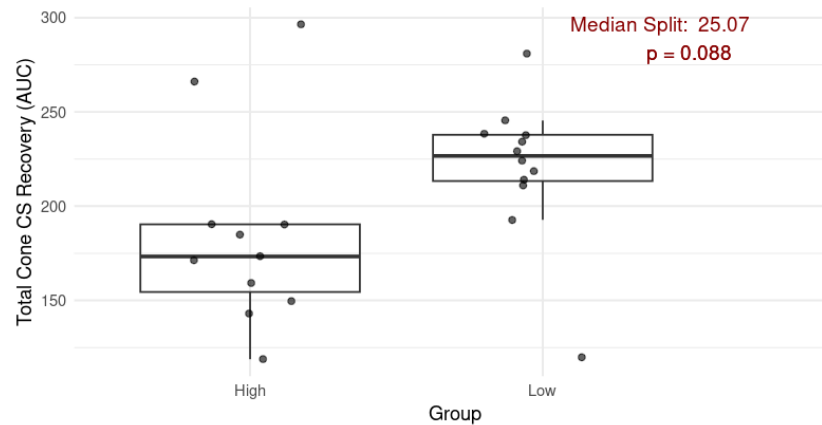


Figure 4.24 - Boxplot of total cone rate of contrast sensitivity recovery in subjects with longer axial length (AXL) (≥ 25.070 mm), and those with shorter AXL (< 25.070 mm), based on the split median analysis.

Similarly, Figure 4.25 shows a boxplot of the median split analysis on the cone maximum contrast sensitivity. The median AXL of the 24 subjects was 25.035 mm (Welch Two Sample t-test). The mean rate of contrast sensitivity recovery in the longer AXL group was 41.824 log CS and the mean rate of contrast sensitivity recovery in the shorter AXL group was 47.654 log CS, with a p-value for the difference of 0.161.

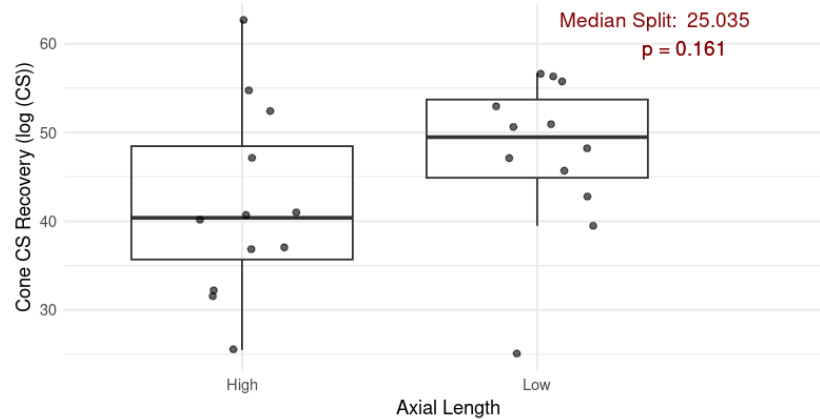


Figure 4.25 - Boxplot of cone maximum contrast sensitivity recovery in subjects with longer axial length (AXL) (≥ 25.035 mm), and those with shorter AXL (< 25.035 mm), based on the split median analysis.

Lastly, Figure 4.26 shows a boxplot of the median split analysis on the cone growth rate. The median AXL of the 25 subjects was 25.035 mm (Welch Two Sample t-test). The mean rate of contrast sensitivity recovery in the longer AXL group was 1.681 log CS / log (ms) and the mean rate of contrast sensitivity recovery in the shorter AXL group was 1.535 log CS / log (ms), with a p-value for the difference of 0.449.

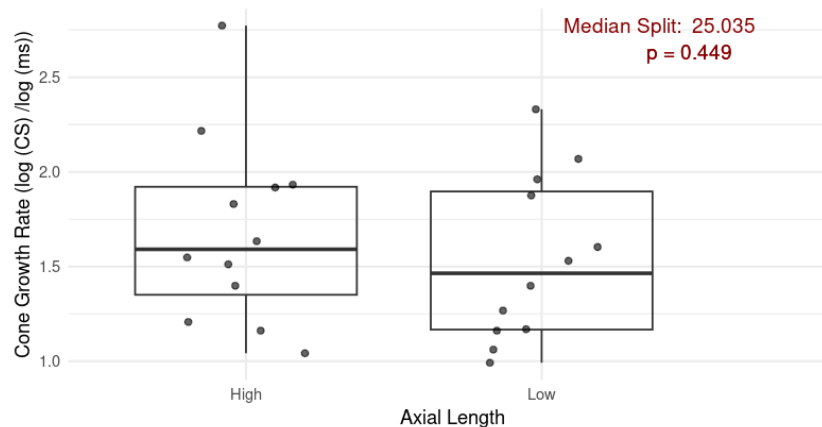


Figure 4.26 - Boxplot of cone growth rate in subjects with longer axial length (AXL) (≥ 25.035 mm), and those with shorter AXL (< 25.035 mm), based on the split median analysis.

5. Discussion

5.1. Summary

This study assessed the effect of AXL on the function of photoreceptors through electrophysiological and psychophysical experiments. Single flash ERGs were utilized to determine the rod-isolating and cone responses. Equation 1 was fitted into those responses to determine the maximum, saturating amplitude (R_{max}) and sensitivity of the photoreceptors. Additionally, paired flash ERGs were utilized to determine the rate of phototransduction in cones and the rate of recovery in rods and cones. Lastly, a psychophysical experiment was performed to determine the total contrast sensitivity recovery, maximum contrast sensitivity recovery, and growth rate of contrast sensitivity recovery in cones.

For each of these experiments, the respective parameters were correlated with AXL. Additionally, a split median analysis was performed to determine if there was a significant difference in the results between subjects with shorter and longer AXL. A total of 36 subjects were recruited in this study, although data from all 36 subjects was not available due to modifications made to some of the experiments during the course of the study. Table 5.1 provides a summary of the experiments performed and the subjects participating in each.

Table 5.1 - Summary of the correlation and split median analyses of the electrophysiology and psychophysics experiments from section four. Rmax = Saturating Amplitude (uV), Sensitivity = Photoreceptor Sensitivity ($\text{sec}^{-2} (\text{td} \cdot \text{sec})^{-1}$), Rod Rec = Rod Rate of Recovery (nV/ms), Cone PT = Cone Rate of Phototransduction (nV/ms), Cone Rec = Cone Rate of Recovery (nV/ms), Cone AUC = Total Cone CS Recovery (AUC), Cone CS Max = Maximum Cone CS Recovery (log (CS)), Cone CS Rate = Cone CS Growth Rate (log (CS) / log (ms)), Axial Length = AXL (mm), * = near statistical significance, ** = statistical significance.

Experiment	Sample Size (n)	Correlation with AXL (mm)	Split Median AXL (mm)	Difference and significance between shorter and longer AXL
Rod-Isolating ERG	34	Rmax: <ul style="list-style-type: none"> • $p = 0.033^{**}$ • $R^2 = 0.134$ Sensitivity: <ul style="list-style-type: none"> • $p = 0.795$ • $R^2 = 0.002$ 	24.935	Rmax: <ul style="list-style-type: none"> • Difference = 23.556 • $p = 0.167$ Sensitivity: <ul style="list-style-type: none"> • Difference = 0.673 • $p = 0.656$
Cone ERG	29	Rmax: <ul style="list-style-type: none"> • $p = 0.513$ • $R^2 = 0.017$ Sensitivity: <ul style="list-style-type: none"> • $p = 0.531$ • $R^2 = 0.017$ 	25.070 24.915	Rmax: <ul style="list-style-type: none"> • Difference = 0.106 • $p = 0.985$ Sensitivity: <ul style="list-style-type: none"> • Difference = 0.504 • $p = 0.646$
Rod Paired-flash ERG	19	Rod Rec: <ul style="list-style-type: none"> • $p = 0.473$ • $R^2 = 0.031$ 	25.300	Rod Rec: <ul style="list-style-type: none"> • Difference = 0.031 • $p = 0.901$
Cone Paired-flash ERG	27	Cone PT: <ul style="list-style-type: none"> • $p = 0.651$ • $R^2 = 0.009$ Cone Rec: <ul style="list-style-type: none"> • $p = 0.430$ • $R^2 = 0.026$ 	25.035	Cone PT: <ul style="list-style-type: none"> • Difference = 3.193 • $p = 0.192$ Cone Rec: <ul style="list-style-type: none"> • Difference = 8.551 • $p = 0.190$
Cone Psychophysics	24	Cone AUC: <ul style="list-style-type: none"> • $p = 0.298$ • $R^2 = 0.051$ Cone CS Max: <ul style="list-style-type: none"> • $p = 0.156$ • $R^2 = 0.089$ Cone CS rate: <ul style="list-style-type: none"> • $p = 0.295$ • $R^2 = 0.050$ 	25.070 25.035 25.035	Cone AUC: <ul style="list-style-type: none"> • Difference = 34.724 • $p = 0.088^*$ Cone CS Max: <ul style="list-style-type: none"> • Difference = 5.830 • $p = 0.161$ Cone CS Rec: <ul style="list-style-type: none"> • Difference = 0.146 • $p = 0.449$

5.2. Electrophysiology

The results of the study showed significant correlations between the rod Rmax and AXL, as subjects with a longer AXL (more myopic) showed a lower Rmax. Similar results have been shown in prior studies from Ishikawa et al. (1990), Kader et al. (2012), and Wang et al. (2013), all of which were described in detail in section 1.4. As the eye becomes elongated in myopia, it is postulated that the photoreceptors become stretched and need to cover larger retinal areas (Park et al., 2013, Flores-Moreno et al., 2013), which leads to a decrease in the density of the photoreceptors that is thought to affect also their structure (Park et al., 2013).

Different variations of the stretched retina hypothesis were presented by Chen et al. (1992) and Westall et al., (2001). The former argued that the increased spacing of the photoreceptors leads to a decrease in their density and sensitivity, thereby greater intensities of light are required to reach a constant saturating amplitude. The latter, on the other hand, postulated that the function of the photoreceptors are affected by the stretched retina and that is observed by a decrease in the saturating amplitude of the photoreceptors. While the Rod Rmax data shows evidence to support the theory that is put forth by Westall et al. (2001), these findings are not observed in the cone photoreceptors in this study. Furthermore, significant differences are not observed in the Rmax, sensitivity, rate of phototransduction, and rate of recovery of rods and cones between subjects with shorter and longer AXLS, based on the results from the split median analysis. This likely is due to the decreased sample size in this study compared to prior research and this limitation is expanded on in section 5.6.

5.3. Cones and Psychophysics

A near significant finding in this study was in the cone psychophysics experiment where subjects with longer axial lengths are shown to have a total lower recovery of their contrast sensitivity (AUC) compared to those with shorter axial lengths ($p = 0.088$). Although these findings are not quite statistically significant, they are similar to recent research involving myopia and contrast sensitivity. Wang et al. (2024) found that high myopic patients displayed significantly lower contrast sensitivity functions compared to emmetropic and low myopic patients. This was attributed to lower cone density, larger spacing of cones, and lower cone regularity in their high myopic patients. Similarly, Ye et al. (2025) found that children with high myopia showed lower contrast sensitivity as well.

5.4. Variance Analysis

While significant differences were not observed in the split median analysis on any of the experiments, the boxplots of the split median analysis of AXL versus rod sensitivity (Figure 4.6) and AXL versus rod rate of recovery (Figure 4.14) show a qualitative difference in the variability of the data points upon first glance. This prompted a variance analysis of the data to determine if there were meaningful differences in the distribution of the parameters in subjects with shorter versus longer AXL. Table 5.2 provides a summary of the variance analysis.

Interestingly, from this analysis, there is a significant difference in variance of the rod rate of recovery ($p < 0.001$), and a near significant difference in variance of the rod sensitivity ($p = 0.057$). In both experiments, subjects with longer AXL had a less uniform distribution of rod sensitivity and rod rates of recovery compared to subjects with shorter AXL. These differences can be attributed back to the stretched retina hypothesis as rod density has been shown to be lower for myopes (Wells-Gray et al., 2016).

Table 5.2 - Summary of the variance analyses of the electrophysiology and psychophysics experiments that were described in section four. Rmax = Saturating Amplitude (uV), Sensitivity = Photoreceptor Sensitivity ($\text{sec}^{-2} (\text{td} \cdot \text{sec})^{-1}$), Rod Rec = Rod Rate of Recovery (nV/ms), Cone PT = Cone Rate of Phototransduction (nV/ms), Cone Rec = Cone Rate of Recovery (nV/ms), Cone AUC = Total Cone CS Recovery (AUC), Cone CS Max = Maximum Cone CS Recovery (log (CS)), Cone CS Rate = Cone CS Growth Rate (log (CS) / log (ms)), Axial Length = AXL (mm), * = near statistical significance, ** = statistical significance.

Experiment	Sample Size (n)	Split Median AXL (mm)	Ratio of variance and significance of variance between shorter and longer AXL
Rod-Isolating ERG	34	24.935	Rmax: <ul style="list-style-type: none"> Ratio = 1.780 p = 0.260 Sensitivity: <ul style="list-style-type: none"> Ratio = 0.364 p = 0.056
Cone ERG	29	25.070 24.915	Rmax: <ul style="list-style-type: none"> Ratio = 0.898 p = 0.851 Sensitivity: <ul style="list-style-type: none"> Ratio = 0.554 p = 0.337
Rod Paired-flash ERG	19	25.300	Rod Rec: <ul style="list-style-type: none"> Ratio = 0.034 p < 0.001**
Cone Paired-flash ERG	27	25.035	Cone PT: <ul style="list-style-type: none"> Ratio = 0.568 p = 0.340 Cone Rec: <ul style="list-style-type: none"> Ratio = 1.136 p = 0.829
Cone Psychophysics	24	25.070 25.035 25.035	Cone AUC: <ul style="list-style-type: none"> Ratio = 0.379 p = 0.288 Cone CS Max: <ul style="list-style-type: none"> Ratio = 2.588 p = 0.130 Cone CS rate: <ul style="list-style-type: none"> Ratio = 2.588 p = 0.130

Moreover, the foveal region is thought to stretch more than retinal periphery, leading to cone photoreceptors being present in regions where rods normally would be found. Xu et al. (2022) observed such a finding and showed that myopia increased contrast sensitivity in superior and inferior visual field locations at 6 deg parafoveal and 12 deg perifoveal regions of the retina due to the increased cone density in these non-foveal regions. However, the rate of this elongation and the degree of impact that a higher AXL has on the photoreceptors is still unclear and this can be evidenced by the high variance in some of the data sets between the two groups of subjects in this study. Prior studies involving OCT (Ng et al., 2016), sinusoidal gratings (Chui et al., 2005), multifocal ERGs (Ismael et al., 2017), have all shown the effects of high myopia and longer AXL on the stretched retina but the changes are thought to be non-uniform since the natural course of high myopia itself is variable.

5.5. Linear Mixed Effect Modeling

A unique element to this study is that it uses both electrophysiology and psychophysics in analyzing the effects of AXL on photoreceptors. The recovery of cone photoreceptors was assessed through both paired-flash ERGs and psychophysics, therefore a linear mixed effect modeling analysis was conducted on those two methods. Equation 4 provides an example of the model utilized in RStudio for this analysis:

$$(4) \text{ Cone Recovery} \sim \text{AXL} * \text{Method} + (1 | \text{Subject})$$

In this equation, the cone rate of recovery is a function of two predictor variables: the AXL of the eye and the method (psychophysics vs. paired-flash ERGs). This analysis is

performed with data from all the subjects and accounts for random effects between subjects. This same equation was utilized when assessing other parameters of the photoreceptors (Rmax, sensitivity) with the other methods in this study (single flash and paired flash ERGs). Table 5.3 summarizes the results.

Table 5.3 - Summary of the linear mixed-effect modeling analysis of the paired-flash ERGs and psychophysics in assessing various parameters of the photoreceptors. * = near statistical significance, ** = statistical significance.

Parameter	Methods Compared	p-value
Cone Rate of Recovery	Cone psychophysics vs. cone Paired-flash ERGs	p = 0.701
Cone Maximum Recovery	Cone psychophysics vs. cone single flash ERG	p = 0.005**
Photoreceptor Rmax	Rod single flash ERG vs. cone single flash ERG	p = 0.006 **
Photoreceptor Sensitivity	Rod single flash ERG vs. cone single flash ERG	p = 0.164
Photoreceptor Rate of Recovery	Rod paired flash ERG vs. cone paired flash ERG	p = 0.070*

The results from the linear mixed modeling show a significant difference in measuring the cone maximum recovery with psychophysics as opposed to the paired-flash ERGs (p = 0.005). In this case, a higher amount of cone recovery is observed with psychophysics as opposed to ERGs. This observance between the two methods could be due to the nature of ERGs and psychophysical experiments. The former provides objective data and involves the biochemical changes that are happening at the molecular level for photoreceptors (Fu, 2018) while the latter relies on higher order cortical processes as well as the biochemical changes of the photoreceptors (Hadjikhani & Tootell, 2000).

There is also a significant difference and a near significant difference in measuring the saturating amplitude ($p = 0.006$) and rate of recovery ($p = 0.070$) in the rod ERGs versus the cone ERG methods. In this study, rods have consistently shown larger saturating amplitudes in their a-waves compared to that of cones in the single flash ERGs. Additionally, rods have also shown a lower rate of recovery compared to that of cones in the paired-flash ERGs. This is likely due to the scotopic and photopic nature of the two protocols. Even though the cone single flash ERG method uses a shorter wavelength, blue light background to saturate the rod contribution in photopic conditions, the cone a-wave in the ERG signal is still compromised by post-receptoral contribution from oscillatory potentials and OFF bipolar cells (Jiang & Mahroo, 2022). These intrusions can affect the saturating amplitude of cones and are likely why there is a difference between the R_{max} between rods and cones. The near significant difference in the recovery rates of rods and cones is likely due to the biochemical differences between rods and cones described in section 1.3. The higher rates of PDE inactivation and cGMP activity in cones compared to that in rods are both factors that contribute to the faster recovery of cone photoreceptors (Kawamura & Tachibanaki, 2012).

5.6. Limitations and Future Directions

The main limitation of this study was the sample size. A power analysis that was conducted prior to the start of the project determined that a sample size of $n = 64$ was required to obtain a medium effect size of 0.50, with an alpha level of 0.05, and a power of 0.80. Due to time constraints related to the long time needed to finalize the study protocols, only 36 participants were recruited and completed all four visits of the study. Furthermore, not all of the participants

had their data analyzed for the electrophysiology and psychophysics experiments. This led to the study to be underpowered. Table 5.4 displays a post-hoc power analysis.

Another limitation of the study involved the lack of psychophysical experiments to assess rod photoreceptors. This is particularly difficult to achieve given the dark-adaptive nature of experiments involving rods and the limitations that arise with the luminance of computer monitors. Additionally, the rod rate of phototransduction could not be sufficiently analyzed in the rod-paired flash experiments as there were only a few data points for the phototransduction portion of the paired-flash recovery curve. This would have provided an insufficient analysis of the rate of rod phototransduction if a line of best fit was plotted on the rod-paired flash recovery.

Table 5.4 - Summary of the post-hoc power analysis for the ERG and psychophysics experiments.

Experiment	Sample Size (n)	Effect Size (post-hoc)	Achieved power (post-hoc)
Rod-Isolating ERG	34	Rmax: $r = 0.366$ Sensitivity: $r = 0.103$	Rmax: power = 0.580 Sensitivity: power = 0.086
Cone ERG	29	Rmax: $r = 0.132$ Sensitivity: $r = 0.129$	Rmax: power = 0.101 Sensitivity: power = 0.096
Rod Paired-flash ERG	19	Rod Rec: $r = 0.175$	Rod Rec: power = 0.111
Cone Paired-flash ERG	27	Cone PT: $r = 0.093$ Cone Rec: 0.162	Cone PT: power = 0.073 Cone Rec: power = 0.124
Cone Psychophysics	24	Cone AUC: $r = 0.254$ Cone CS Max: $r = 0.299$ Cone CS rate: $r = 0.223$	Cone AUC: power = 0.227 Cone CS Max: power = 0.301 Cone CS rate: power = 0.1845

Given those limitations, future directions for this study can involve more comprehensive assessment of rod function through psychophysics and the additional data points in the

rod-paired flash ERGs to determine the rod rate of phototransduction. Moreover, radial scans with the Heidelberg Spectralis OCT were obtained from Visit #3 of this experiment. This data could be used to quantify photoreceptor layer thickness and compare it with the function of photoreceptors in ERGs and psychophysics but also correlate it with AXL. Lastly, given the broader scope of this project, the data of the photoreceptors in this study could be compared with the data of ganglion cells, amacrine cells, bipolar cells, and horizontal cells from the other three studies to fully analyze the effects of AXL on the retinal layers.

6. Conclusions

The purpose of this thesis was to utilize both electrophysiological and psychophysical experiments to assess the effect of AXL on the function of photoreceptors. Single flash ERGs were utilized to assess the saturating amplitude and sensitivity of rods and cones while paired-flash ERGs were utilized to assess the rate of phototransduction of cones as well as the rate of recovery of rods and cones. Lastly, a psychophysical experiment was performed to assess the rate of contrast sensitivity recovery in cones. In each of these experiments, a split median analysis was conducted to determine if there was a significant difference in the parameters in subjects with shorter AXL versus those with longer AXL.

There was a significant correlation between the rod saturating amplitude and AXL. Other notable findings are seen in the variance analysis and the linear mixed effect modeling. There is a higher variance in the rod rate of recovery between subjects with shorter and longer AXL as subjects with longer AXL (more myopic) had a less uniform distribution of their rate of recovery compared to that of subjects with shorter AXL (less myopic). This highlights the difficulty in analyzing photoreceptors in myopic subjects because there is no concise relationship between the stretched retina and its function. The method utilized to assess rods and cones are also shown to have an effect on the measured parameters. There was a higher maximum recovery in cones when measured through psychophysics as opposed to ERGs, the rod single flash ERGs produce larger saturating amplitudes of the a-wave compared to cone single flash ERGs, and the rod paired flash ERGs produce lower recovery rates compared to cone paired flash ERGs.. These findings suggest considerations that must be taken into account regarding the methods that are used to analyze photoreceptors.

7. Bibliography

- Anderson, R. S. (2006). The psychophysics of glaucoma: Improving the structure/function relationship. *Progress in Retinal and Eye Research*, 25(1), 79–97. <https://doi.org/10.1016/j.preteyeres.2005.06.001>
- Asanad, S., & Karanjia, R. (2023). Full-Field Electroretinogram. Retrieved from PubMed website: <https://www.ncbi.nlm.nih.gov/books/NBK557483/>
- Bhatt, Y., Hunt, D. M., & Carvalho, L. S. (2023). The origins of the full-field flash electroretinogram b-wave. *Frontiers in Molecular Neuroscience*, 16, 1153934. <https://doi.org/10.3389/fnmol.2023.1153934>
- Blach, R. K., Jay, B., & Kolb, H. (1966). Electrical activity of the eye in high myopia. *British Journal of Ophthalmology*, 50(11), 629–641. <https://doi.org/10.1136/bjo.50.11.629>
- Brainard, D. H. “The Psychophysics Toolbox.” *Spatial Vision*, vol. 10, no. 4, 1997, pp. 433–436, pubmed.ncbi.nlm.nih.gov/9176952/.
- Brigell, M., Jeffrey, B. G., Mahroo, O. A., & Tzekov, R. (2020). ISCEV extended protocol for derivation and analysis of the strong flash rod-isolated ERG a-wave. *Documenta Ophthalmologica*, 140(1), 5–12. <https://doi.org/10.1007/s10633-019-09740-4>
- Brouzas, D. (1995). Psychophysical tests in X-linked retinitis pigmentosa carrier status. *Survey of Ophthalmology*, 39, S76–S84. [https://doi.org/10.1016/s0039-6257\(05\)80076-1](https://doi.org/10.1016/s0039-6257(05)80076-1)
- Chen, J.-F., Elsner, A. E., Burns, S. A., Hansen, R. M., Lou, P. L., Kwong, K. K., & Fulton, A. B. (1992). The effect of eye shape on retinal responses. *Clinical Vision Sciences*, 7(6), 521–530.
- Chen, P. C., Woung, L. C., & Yang, C. F. (2000). Modulation transfer function and critical flicker frequency in high-myopia patients. *Journal of the Formosan Medical Association = Taiwan Yi Zhi*, 99(1), 45–48. Retrieved from <https://pubmed.ncbi.nlm.nih.gov/10743346/>
- Chen, X. D., & Gardner, T. W. (2021). A critical review: Psychophysical assessments of diabetic retinopathy. *Survey of Ophthalmology*, 66(2), 213–230. <https://doi.org/10.1016/j.survophthal.2020.08.003>
- Cho, B.-J., Shin, J. Y., & Yu, H. G. (2016). Complications of Pathologic Myopia. *Eye & Contact Lens: Science & Clinical Practice*, 42(1), 9–15. <https://doi.org/10.1097/icl.0000000000000223>

- Chui, T. Y. P., Yap, M. K. H., Chan, H. H. L., & Thibos, L. N. (2005). Retinal stretching limits peripheral visual acuity in myopia. *Vision Research*, 45(5), 593–605. <https://doi.org/10.1016/j.visres.2004.09.016>
- Dolgin, E. (2015). The myopia boom. *Nature*, 519(7543), 276–278. <https://doi.org/10.1038/519276a>
- Eckmiller, M. S. (1997). Morphogenesis and renewal of cone outer segments. *Progress in Retinal and Eye Research*, 16(3), 401–441. [https://doi.org/10.1016/s1350-9462\(96\)00026-2](https://doi.org/10.1016/s1350-9462(96)00026-2)
- Flitcroft, D. I., He, M., Jonas, J. B., Jong, M., Naidoo, K., Ohno-Matsui, K., Rahi, J., Resnikoff, S., Vitale, S., Yannuzzi, L. (2019). IMI – Defining and Classifying Myopia: A Proposed Set of Standards for Clinical and Epidemiologic Studies. *Investigative Ophthalmology & Visual Science*, 60(3), M20. <https://doi.org/10.1167/iovs.18-25957>
- Flores-Moreno, I., Ruiz-Medrano, J., Duker, J. S., & Ruiz-Moreno, J. M. (2013). The relationship between retinal and choroidal thickness and visual acuity in highly myopic eyes. *British Journal of Ophthalmology*, 97(8), 1010–1013. <https://doi.org/10.1136/bjophthalmol-2012-302836>
- Friedburg, C., Allen, C. P., Mason, P. J., & Lamb, T. D. (2004). Contribution of cone photoreceptors and post-receptoral mechanisms to the human photopic electroretinogram. *The Journal of Physiology*, 556(3), 819–834. <https://doi.org/10.1113/jphysiol.2004.061523>
- Fu, Y. (2018). Phototransduction in Rods and Cones (H. Kolb, E. Fernandez, & R. Nelson, Eds.). PubMed; University of Utah Health Sciences Center. <https://www.ncbi.nlm.nih.gov/books/NBK52768/>
- Gupta, S. K., Chakraborty, R., & Verkicharla, P. K. (2021). Electroretinogram responses in myopia: a review. *Documenta Ophthalmologica*, 145(2), 77–95. <https://doi.org/10.1007/s10633-021-09857-5>
- Hadjikhani, N., & Tootell, R. B. (2000). Projection of rods and cones within human visual cortex. *Human Brain Mapping*, 9(1), 55. [https://doi.org/10.1002/\(SICI\)1097-0193\(2000\)9:1%3C55::AID-HBM6%3E3.0.CO;2-U](https://doi.org/10.1002/(SICI)1097-0193(2000)9:1%3C55::AID-HBM6%3E3.0.CO;2-U)
- Harris, M. E., Moskowitz, A., Fulton, A. B., & Hansen, R. M. (2011). Long-term effects of retinopathy of prematurity (ROP) on rod and rod-driven function. *Documenta*

- Ophthalmologica. Advances in Ophthalmology*, 122(1), 19–27.
<https://doi.org/10.1007/s10633-010-9251-0>
- Holden, B. A., Fricke, T. R., Wilson, D. A., Jong, M., Naidoo, K. S., Sankaridurg, P., ... Resnikoff, S. (2016). Global Prevalence of Myopia and High Myopia and Temporal Trends from 2000 through 2050. *Ophthalmology*, 123(5), 1036–1042.
<https://doi.org/10.1016/j.opthta.2016.01.006>
- Hood, D. C., & Birch, D. G. (2006). 35: Measuring the Health of the Human Photoreceptors with the Leading Edge of the a-Wave. In J. R. Heckenlively & G. B. Arden (Eds.), *Principles and Practice of Clinical Electrophysiology of Vision* (Second Edition). The MIT Press.
- Hood, D. C., & Birch, D. G. (1994). Rod phototransduction in retinitis pigmentosa: estimation and interpretation of parameters derived from the rod a-wave. *Investigative Ophthalmology & Visual Science*, 35(7), 2948–2961. Retrieved from <https://pubmed.ncbi.nlm.nih.gov/8206712/>
- Hunter, J. J., Merigan, W. H., & Schallek, J. B. (2019). Imaging Retinal Activity in the Living Eye. *Annual Review of Vision Science*, 5(1), 15–45.
<https://doi.org/10.1146/annurev-vision-091517-034239>
- Ismael, Z. F., El-Shazly, A. A. E.-F., Farweez, Y. A., & Osman, M. M. M. (2017). Relationship between functional and structural retinal changes in myopic eyes. *Clinical and Experimental Optometry*, 100(6), 695–703. <https://doi.org/10.1111/cxo.12527>
- Ishikawa M, Miyake Y, Shiroyama N. [Focal macular electroretinogram in high myopia]. *Nippon Ganka Gakkai Zasshi*. 1990 Nov;94(11):1040-7. Japanese. PMID: 2075867.
- Jaworski, A., Gentle, A., Zele, A. J., Vingrys, A. J., & McBrien, N. A. (2006). Altered Visual Sensitivity in Axial High Myopia: A Local Postreceptoral Phenomenon? *Investigative Ophthalmology & Visual Science*, 47(8), 3695. <https://doi.org/10.1167/iovs.05-1569>
- Jiang, X., & Mahroo, O. A. (2022). Human retinal dark adaptation tracked *in vivo* with the electroretinogram: insights into processes underlying recovery of cone- and rod-mediated vision. *The Journal of Physiology*, 600(21), 4603–4621.
<https://doi.org/10.1113/jp283105>

- Jonnal, R. S., Rha, J., Zhang, Y., Cense, B., Gao, W., & Miller, D. T. (2007). In vivo functional imaging of human cone photoreceptors. *Optics Express*, 15(24), 16141. <https://doi.org/10.1364/oe.15.016141>
- Kader, M. A. (2012). Electrophysiological study of myopia. *Saudi Journal of Ophthalmology*, 26(1), 91–99. <https://doi.org/10.1016/j.sjopt.2011.08.002>
- Kawamura, S., & Tachibanaki, S. (2012). Explaining the functional differences of rods versus cones. *Wiley Interdisciplinary Reviews: Membrane Transport and Signaling*, 1(5), 675–683. <https://doi.org/10.1002/wmts.8>
- Lamb, T. D. (2022). Photoreceptor physiology and evolution: cellular and molecular basis of rod and cone phototransduction. *The Journal of Physiology*. <https://doi.org/10.1113/jp282058>
- Liang, H., D.P. Crewther, S. Gillard Crewther, & Barila, A. M. (1995). A role for photoreceptor outer segments in the induction of deprivation myopia. *Vision Research*, 35(9), 1217–1225. [https://doi.org/10.1016/0042-6989\(94\)00241-d](https://doi.org/10.1016/0042-6989(94)00241-d)
- Mäntyjärvi, M., & Tuppurainen, K. (1995). Colour vision and dark adaptation in high myopia without central retinal degeneration. *British Journal of Ophthalmology*, 79(2), 105–108. <https://doi.org/10.1136/bjo.79.2.105>
- Molday, R. S., & Moritz, O. L. (2015). Photoreceptors at a glance. *Journal of Cell Science*, 128(22), 4039–4045. <https://doi.org/10.1242/jcs.175687>
- Mustafi, D., Engel, A. H., & Palczewski, K. (2009). Structure of cone photoreceptors. *Progress in Retinal and Eye Research*, 28(4), 289–302. <https://doi.org/10.1016/j.preteyeres.2009.05.003><https://doi.org/10.1016/j.preteyeres.2009.05.003>
- Ng, D. S. C., Cheung, C. Y. L., Luk, F. O., Mohamed, S., Brelen, M. E., Yam, J. C. S., ... Lai, T. Y. Y. (2016). Advances of optical coherence tomography in myopia and pathologic myopia. *Eye*, 30(7), 901–916. <https://doi.org/10.1038/eye.2016.47>
- Nusinowitz, S, (2006). 50. Effects of High Myopia on the Electroretinogram. In J. R. Heckenlively & G. B. Arden (Eds.), *Principles and Practice of Clinical Electrophysiology of Vision* (Second Edition). The MIT Press.
- Park, S. P., Chung, J. K., Greenstein, V., Tsang, S. H., & Chang, S. (2013). A study of factors affecting the human cone photoreceptor density measured by adaptive optics scanning

- laser ophthalmoscope. *Experimental Eye Research*, 108, 1–9.
<https://doi.org/10.1016/j.exer.2012.12.011>
- Pepperberg, D. R., Birch, D. G., & Hood, D. C. (1997). Photoresponses of human rods in vivo derived from paired-flash electroretinograms. *Visual Neuroscience*, 14(1), 73–82.
<https://doi.org/10.1017/s0952523800008774>
- Pepperberg, D. R., Birch, D. G., & Hood, D. C. (2000). Electroretinographic determination of human Rod flash response in vivo. *Methods in Enzymology*, 202–223.
[https://doi.org/10.1016/s0076-6879\(00\)16725-4](https://doi.org/10.1016/s0076-6879(00)16725-4)
- Pugh, E. N., & Lamb, T. D. (1993). Amplification and kinetics of the activation steps in phototransduction. *Biochimica et Biophysica Acta (BBA) - Bioenergetics*, 1141(2-3), 111–149. [https://doi.org/10.1016/0005-2728\(93\)90038-h](https://doi.org/10.1016/0005-2728(93)90038-h)
- Rehman, I., Mahabadi, N., Motlagh, M., & Ali, T. (2023). Anatomy, Head and Neck, Eye Fovea. PubMed; StatPearls Publishing. <https://www.ncbi.nlm.nih.gov/books/NBK482301/>
- Robson, A. G., Nilsson, J., Li, S., Jalali, S., Fulton, A. B., Tormene, A. P., ... Brodie, S. E. (2018). ISCEV guide to visual electrodiagnostic procedures. *Documenta Ophthalmologica. Advances in Ophthalmology*, 136(1), 1–26.
<https://doi.org/10.1007/s10633-017-9621-y>
- Sachidanandam, R., Ravi, P., & Sen, P. (2017). Effect of axial length on full-field and multifocal electroretinograms. *Clinical and Experimental Optometry*, 100(6), 668–675.
<https://doi.org/10.1111/cxo.12529>
- Saw, S.-M. ., Katz, J., Schein, O. D., Chew, S.-J. ., & Chan, T.-K. . (1996). Epidemiology of Myopia. *Epidemiologic Reviews*, 18(2), 175–187.
<https://doi.org/10.1093/oxfordjournals.epirev.a017924>
- Shapley, R., & Enroth-Cugell, C. (1984). Chapter 9 Visual adaptation and retinal gain controls. *Progress in Retinal Research*, 3, 263–346. [https://doi.org/10.1016/0278-4327\(84\)90011-7](https://doi.org/10.1016/0278-4327(84)90011-7)
- Thorn, F., Corwin, T. R., & Comerford, J. P. (1986). High myopia does not affect contrast sensitivity. *Current Eye Research*, 5(9), 635–640.
<https://doi.org/10.3109/02713688609015130>
- Wang, J., Liu, X., Huang, J., Deng, R., Zhao, S., Chen, Y., Chen, Z., Wang, Y., Rong, Y., Liu, Q., Qu, J., & Mao, X. (2024). Reduced contrast sensitivity function is correlated with

- changes to cone photoreceptors in simple high myopia. *Frontiers in Neuroscience*, 18. <https://doi.org/10.3389/fnins.2024.1274651>
- Wang, P., Xiao, X., Huang, L., Guo, X., & Zhang, Q. (2013). Cone-Rod Dysfunction Is a Sign of Early-Onset High Myopia. *Optometry and Vision Science*, 90(11), 1327–1330. <https://doi.org/10.1097/OPX.0000000000000072>
- Wang, Y., Ye, J., Shen, M., Yao, A., Xue, A., Fan, Y., Huang, S., Wang J., Lu, F., & Shao, Y. (2019). Photoreceptor Degeneration is Correlated With the Deterioration of Macular Retinal Sensitivity in High Myopia. *Investigative Ophthalmology & Visual Science*, 60(8), 2800. <https://doi.org/10.1167/IOVS.18-26085>
- Wells-Gray, E. M., Choi, S. S., Bries, A., & Doble, N. (2016). Variation in rod and cone density from the fovea to the mid-periphery in healthy human retinas using adaptive optics scanning laser ophthalmoscopy. *Eye*, 30(8), 1135–1143. <https://doi.org/10.1038/eye.2016.107>
- Westall, C. A., Dhaliwal, H. S., Panton, C. M., Sigesmund, D., Levin, A. V., Nischal, K. K., & Héon, E. (2001). Values of electroretinogram responses according to axial length. *Documenta Ophthalmologica*, 102(2), 115–130. <https://doi.org/10.1023/a:1017535207481>
- Xu, Z., Zhuang, Y., Chen, Z., Hou, F., Chan, L. Y. L., Feng, L., Ye, Q., He, Y., Zhou, Y., Jia, Y., Yuan, J., Lu, Z.-L., & Li, J. (2022). Assessing the contrast sensitivity function in myopic parafovea: A quick contrast sensitivity functions study. *Frontiers in Neuroscience*, 16. <https://doi.org/10.3389/fnins.2022.971009>
- Ye, Y., Liu, F., Xian, Y., Li, M., Niu, L., Zhou, X., & Zhao, J. (2025). Correlation of contrast sensitivity at low spatial frequencies with myopic shift in Chinese children. *BMC Ophthalmology*, 25(1). <https://doi.org/10.1186/s12886-025-03858-7>
- Young, R. W. (1971). The Renewal of Rod and Cone Outer Segments in the Rhesus Monkey. *Journal of Cell Biology*, 49(2), 303–318. <https://doi.org/10.1083/jcb.49.2.303>

8. Appendix

8.1 Data Collection Forms

8.1.1. De-identifier form

Appendix III: De-identifier form

Study: *Relationship between Axial Length and Retinal Structure and Function*

Assigned Subject ID: _____

Date: ____/____/____

Name: _____

Telephone number: _____

E-mail: _____

Preferred contact method: _____

Are you a NECO student? Yes ☐ No ☐ If so, class of _____

Is it OK to contact you for other studies at Vera-Diaz's Lab? Yes ☐ No ☐

Date of birth: ____/____/____ Gender: Female ☐ Male ☐

Ocular Information: Normal Vision ☐ Eye Disease ☐ _____

Type of Refractive Error: _____

Allergic or sensitive to Tropicamide eye drops? Yes ☐ No ☐

Notes:

8.1.2. Data Form Visit #1

Data form Visit #1. Relationship between Axial Length and Retinal Structure and Function

Subject's ID: _____ Date: ____/____/____ Examiners Initials: _____

1. Before Subject Arrives:

- ☐ One to two days before the scheduled appointment: **remind subject of the appointment** and ask to bring their glasses and contact lenses (if indicated).
- ☐ Book the Shared Research Lab for 1 hour (15 minutes prior to the visit time), Dr. Taylor's Lab for 1.5 hours, and two slots for the Shared Imaging Room (for 15 minutes after the screening and 30 minutes after the psychophysics).
- ☐ Prepare all forms (consent form, de-identifier form, data form, check request form).

2. Vision Screening:

Patient's Ocular and Health History:

Habitual Rx: Glasses ☐ Contact lenses ☐

Date Rx: _____

OD: _____

LogMAR DVA: _____

LogMAR NVA: _____

OS: _____

LogMAR DVA: _____

LogMAR NVA: _____

Cover Test (cc/sc): Distance _____

Near _____

NPC (acc) (cc/sc): _____

EOMs: _____ CFF: _____ Pupils: _____

Dim: _____

Near: _____

Bright: _____

MEM: OD _____ OS _____

Objective Refraction WAM:

Retinoscopy:

OD: _____

OD: _____

OS: _____

OS: _____

Manifest Refraction with Binocular Balance (if needed):

OD: _____

DVA: 20/ _____

NVA: 20/ _____

OS: _____

DVA: 20/ _____

NVA: 20/ _____

3. Slit lamp Examination Anterior Segment and VH angle:

OD: _____

OS: _____

4. IOP: OD _____ OS _____ Time _____

5. Notes on Procedures:

Biometry: _____

Psychophysics (ON pathway): _____

Date and Time Visit #2: _____ Scan this form (Drive). Submit check request.

Examiners' Signature: _____

8.1.3. Data Form Visit #2

Data form Visit #2. Relationship between Axial Length and Retinal Structure and Function

Subject's ID: _____ Date: ____/____/____ Examiners Initials: _____

1. Before Subject Arrives:

- ☐ One to two days before the scheduled appointment: **remind subject of the appointment** and ask to bring their glasses and contact lenses (if indicated).
- ☐ Book Dr. Vera-Diaz Lab for 1.5 hours (starting 15 minutes before the visit time) and Dr. Panorgias' Lab for 2 hours.
- ☐ Prepare all forms (data form, check request form).

2. Patient's Ocular History:

Changes in ocular history or general health history since Visit #1? _____

3. Vision Screening:

Habitual Rx: Glasses ☐ Contact lenses ☐ Date Rx: _____
OD: _____ LogMAR DVA: _____ LogMAR NVA: _____
OS: _____ LogMAR DVA: _____ LogMAR NVA: _____

4. Slit lamp Examination Anterior Segment and VH angle:

OD: _____ OS: _____

5. Notes on Psychophysical Procedures:

CSF Fovea: _____

CSF Periphery: _____

Center-Surround Thresholds Fovea: _____

Center-Surround Thresholds Periphery: _____

6. **Drop Instillation:** Subject eligible? _____ Tropicamide 0.5% OD ☐ Time: _____

7. Notes on ERG Procedures:

Rod-Isolating: _____

Paired-Flash Cones: _____

Paired-Flash Rods: _____

Date and Time Visit #3: _____

Scan this form (Drive). Submit check request.

Examiners' Signature: _____

8.1.4. Data Form Visit #3

Data form Visit #3. Relationship between Axial Length and Retinal Structure and Function

Subject's ID: _____ Date: ____/____/____ Examiners Initials: _____

1. Before Subject Arrives:

- ☐ One to two days before the scheduled appointment: **remind subject of the appointment** and ask to bring their glasses and contact lenses (if indicated).
- ☐ Book Dr. Vera-Diaz Lab for 1.5 hours (starting 15 minutes before the visit time) and Dr. Panorgias' Lab for 2 hours.
- ☐ Prepare all forms (data form, check request form).

2. Patient's Ocular History:

Changes in ocular history or general health history since Visit #2? _____

3. Vision Screening:

Habitual Rx: Glasses ☐ Contact lenses ☐ Date Rx: _____
OD: _____ LogMAR DVA: _____ LogMAR NVA: _____
OS: _____ LogMAR DVA: _____ LogMAR NVA: _____

4. Slit lamp Examination Anterior Segment and VH angle:

OD: _____ OS: _____

5. Notes on Psychophysical Procedures:

Fovea Chromatic Sensitivity: _____

Peripheral Chromatic Sensitivity: _____

Fovea Temporal Sensitivity: _____

Peripheral Temporal Sensitivity: _____

6. Drop Instillation: Subject eligible? _____ Tropicamide 0.5% OD ☐ Time: _____

7. Notes on OCT: _____

8. Notes on ERG Procedures:

Global Flash mfERG: _____

Horizontal Cells: _____

Bipolar Cells: _____

Date and Time Visit #4: _____

Scan this form (Drive). Submit check request.

Examiners' Signature: _____

8.1.5. Data Form Visit #4

Data form Visit #4. Relationship between Axial Length and Retinal Structure and Function

Subject's ID: _____ Date: ____/____/____ Examiner(s): _____

1. Before Subject Arrives:

- ☐ One to two days before the scheduled appointment: remind subject of the appointment and ask to bring their glasses and contact lenses (if indicated).
- ☐ Book Dr. Panorgias' Lab for 1 hour (15 minutes prior to the visit time), Dr. Taylor's Lab for 1.5 hours, and two slots for the Shared Imaging Room (for 15 minutes after the screening and 30 minutes after the psychophysics).
- ☐ Prepare all forms (data form, check request form).

2. Patient's Ocular History:

Changes in ocular history or general health history since Visit #2? _____

3. Vision Screening:

Habitual Rx: Glasses ☐ Contact lenses ☐ Date Rx: _____
OD: _____ LogMAR DVA: _____ LogMAR NVA: _____
OS: _____ LogMAR DVA: _____ LogMAR NVA: _____

4. Slit lamp Examination Anterior Segment and VH angle:

OD: _____ OS: _____

5. Notes on Psychophysical Procedures:

Landolt C with flashes _____

OFF pathway: _____

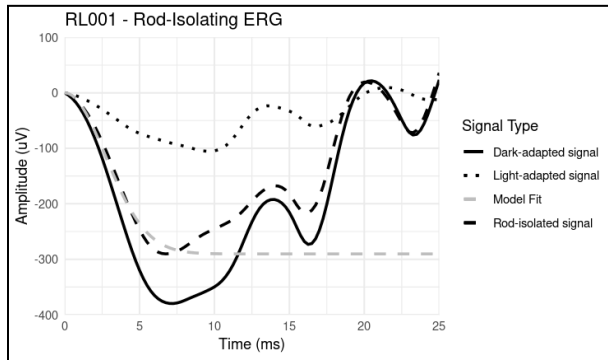
Scan this form (Drive). Submit check request.

Examiners' Signature: _____

8.2 Individual results

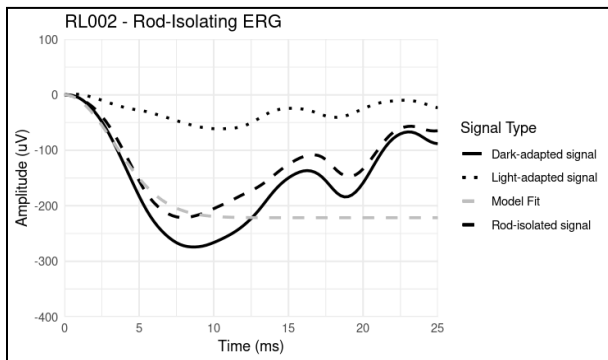
RL001

Rod-Isolating ERG

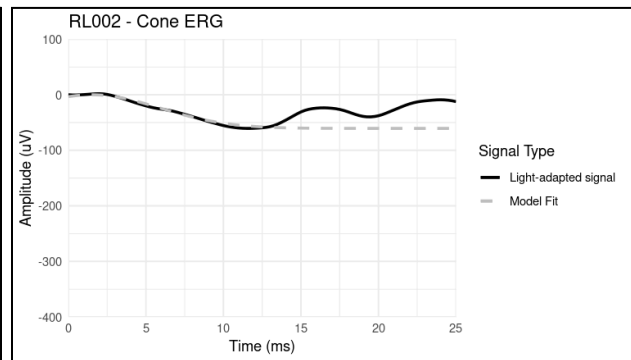


RL002

Rod-Isolating ERG

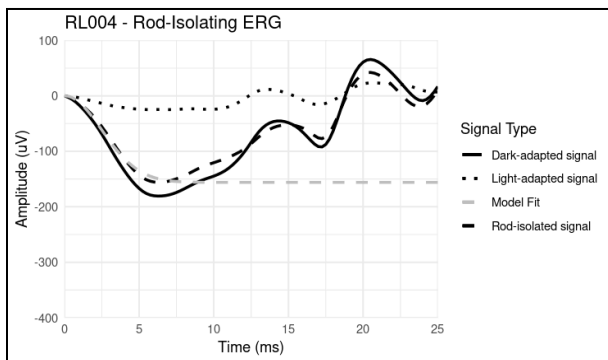


Cone ERG



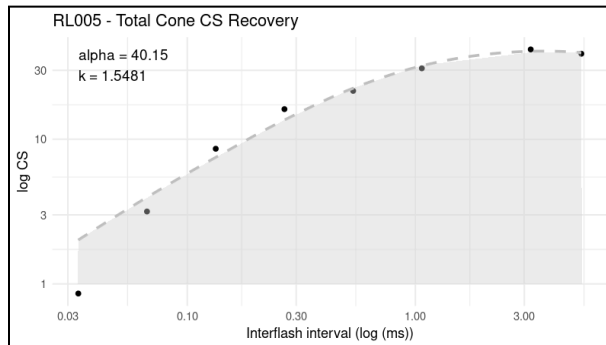
RL004

Rod-Isolating ERG



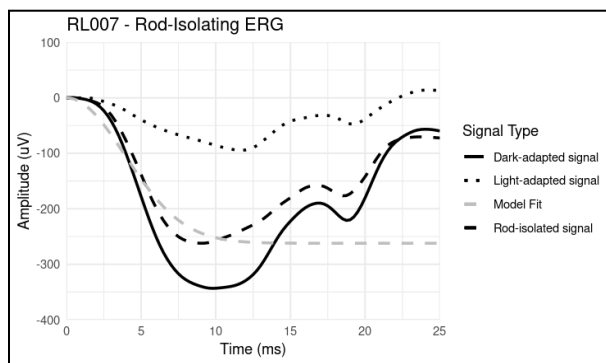
RL005

Cone Psychophysics

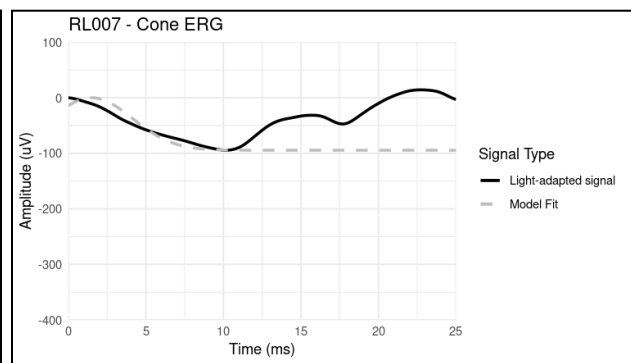


RL007

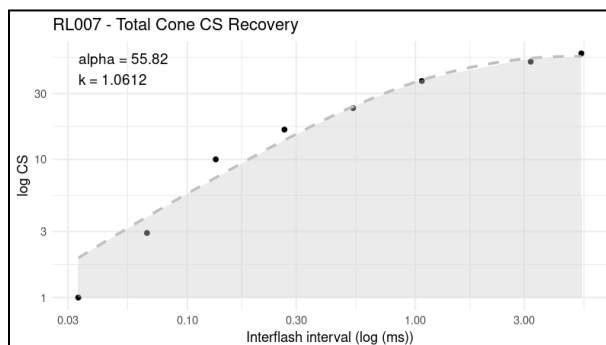
Rod-Isolating ERG



Cone ERG

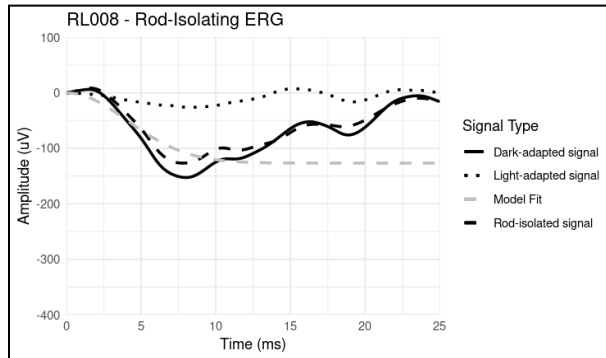


Cone Psychophysics

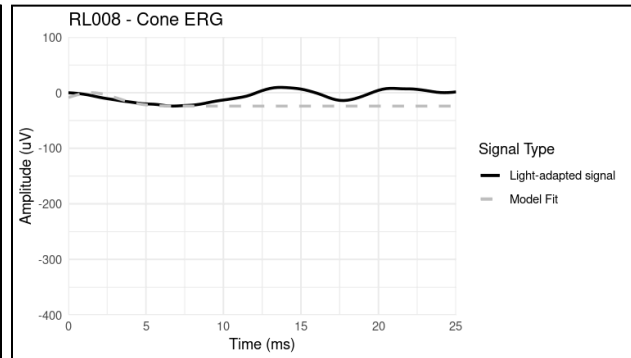


RL008

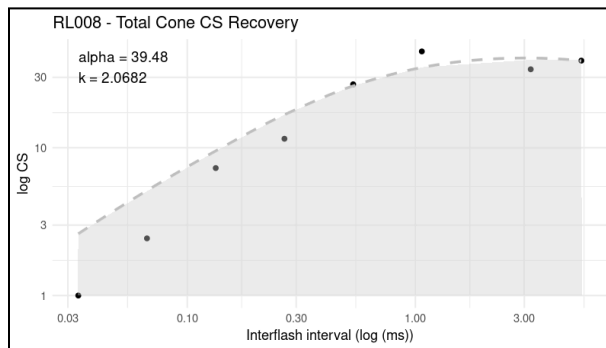
Rod-Isolating ERG



Cone ERG

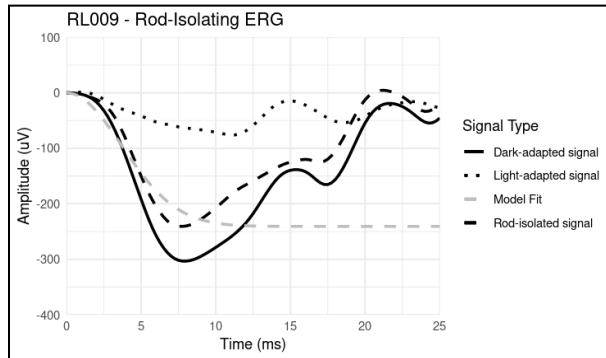


Cone Psychophysics

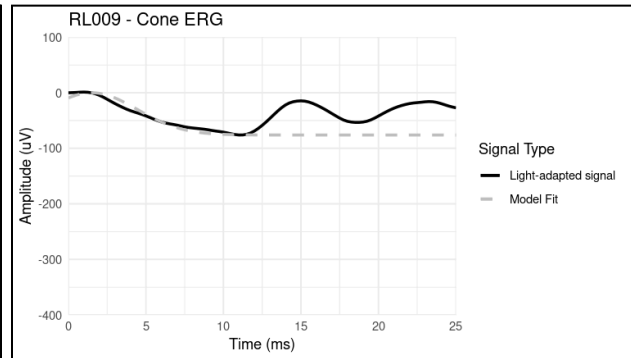


RL009

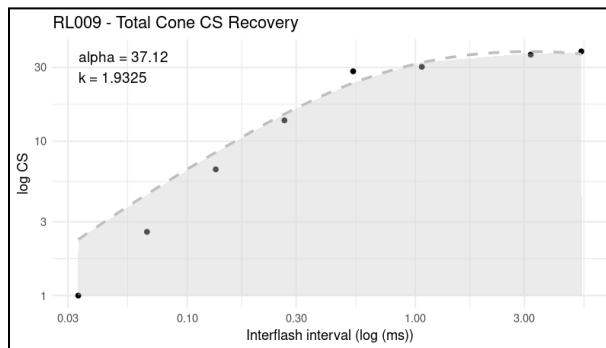
Rod-Isolating ERG



Cone ERG

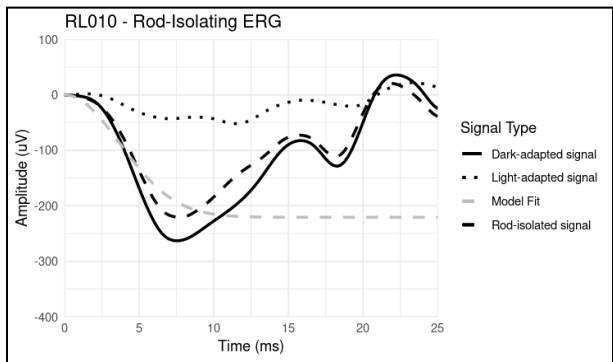


Cone Psychophysics

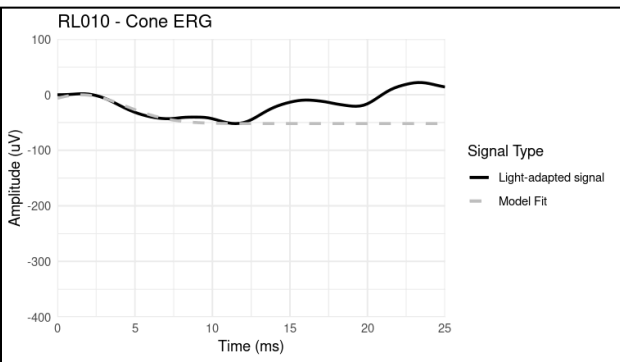


RL010

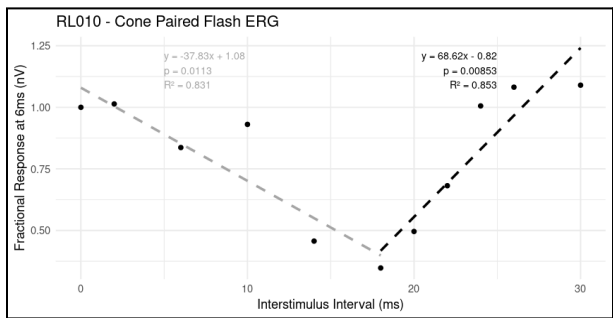
Rod-Isolating ERG



Cone ERG

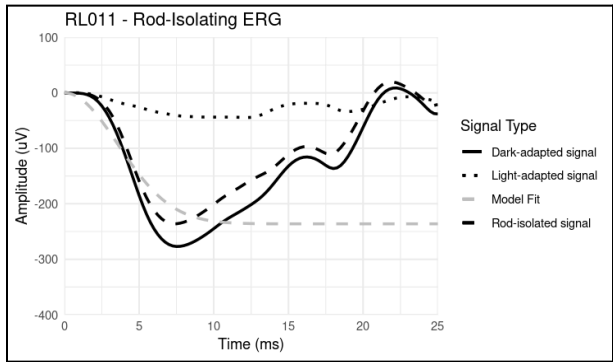


Cone Paired-Flash ERG

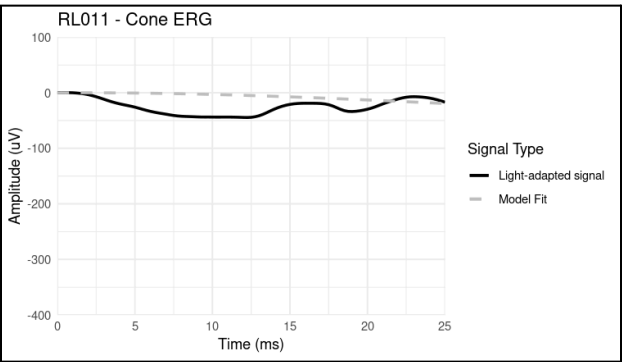


RL011

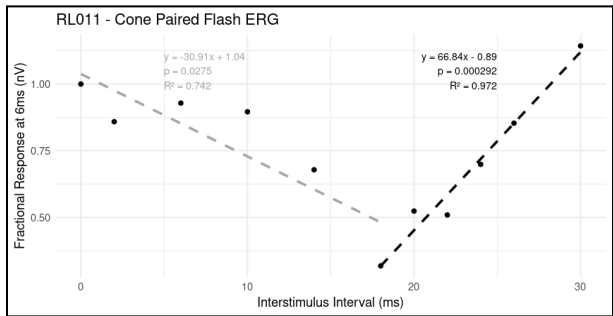
Rod-Isolating ERG



Cone ERG

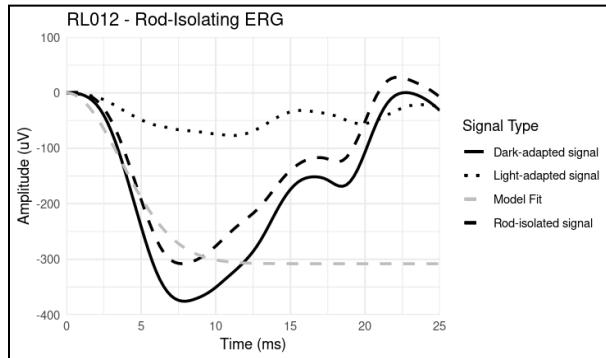


Cone Paired-Flash ERG

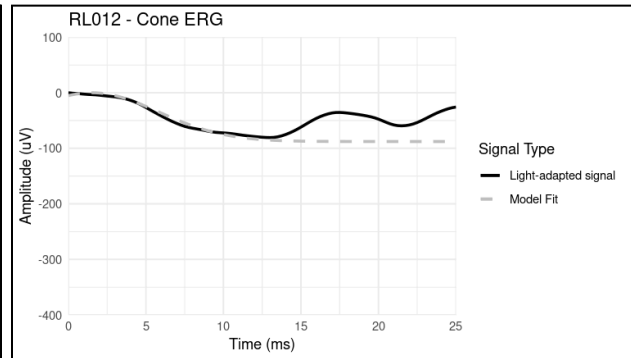


RL012

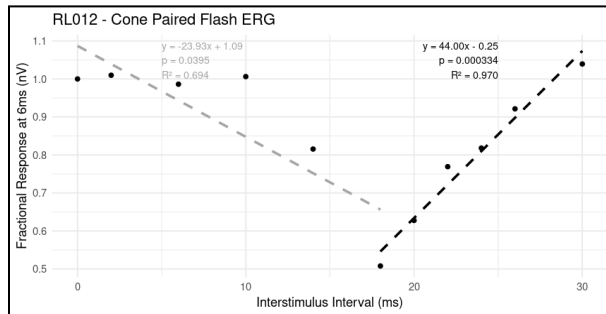
Rod-Isolating ERG



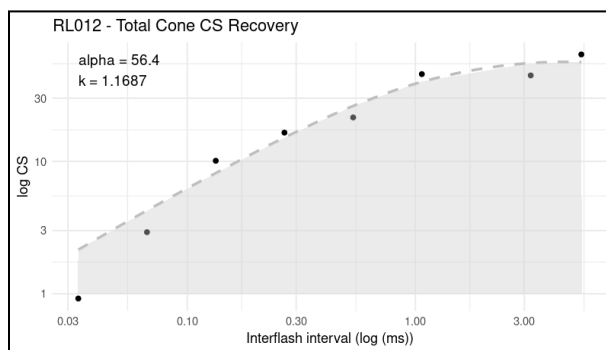
Cone ERG



Cone Paired-Flash ERG

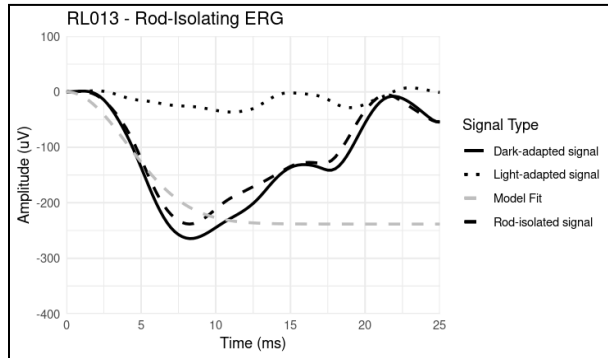


Cone Psychophysics

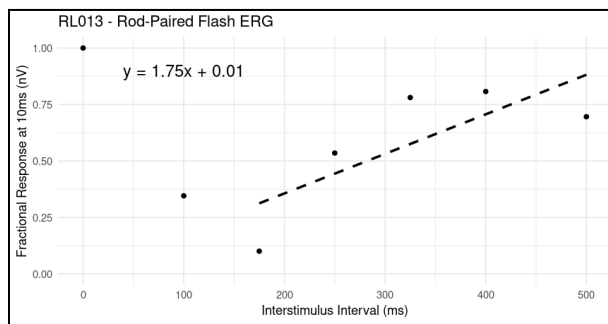


RL013

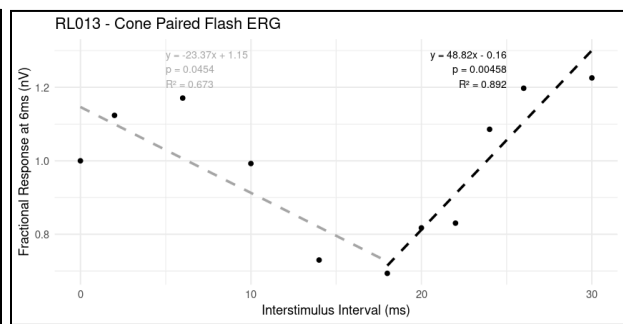
Rod-Isolating ERG



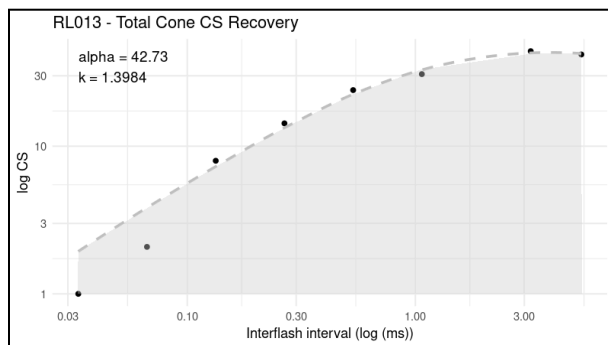
Rod-Paired Flash ERG



Cone-Paired Flash ERG

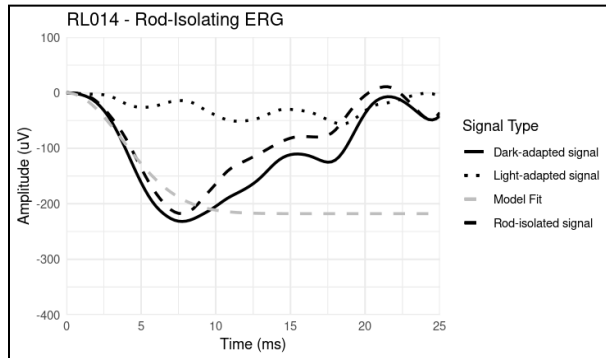


Cone Psychophysics

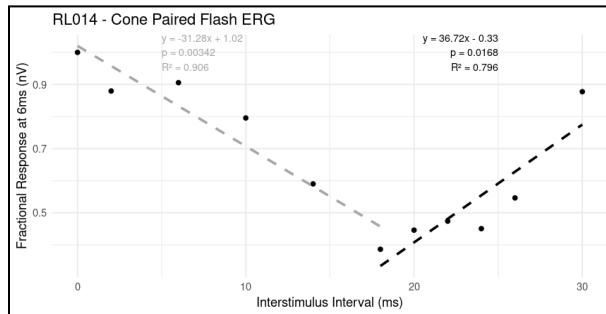


RL014

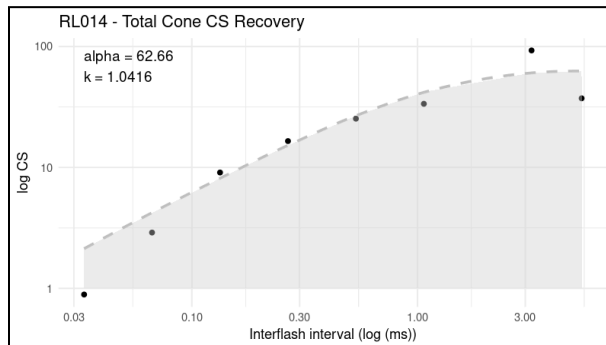
Rod-Isolating ERG



Cone Paired-Flash ERG

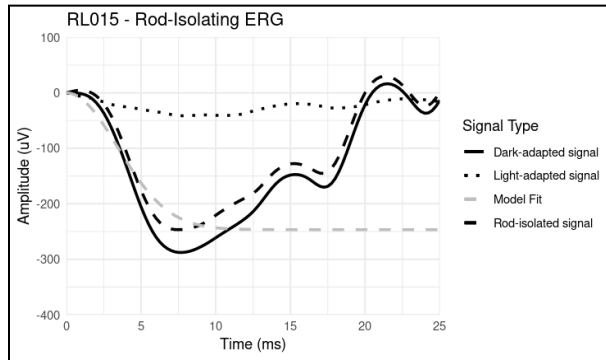


Cone Psychophysics

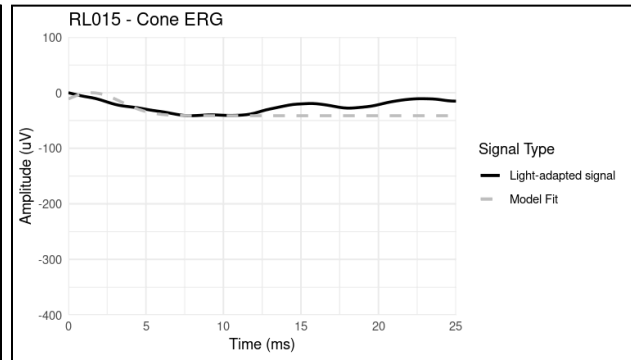


RL015

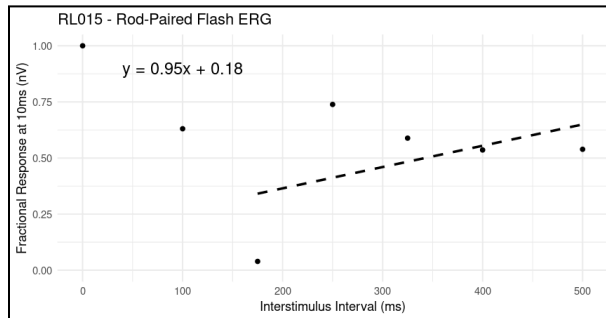
Rod-Isolating ERG



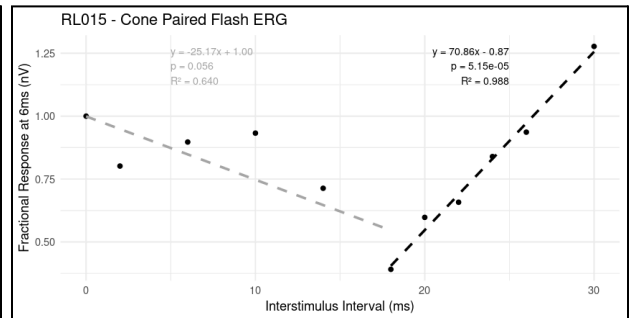
Cone ERG



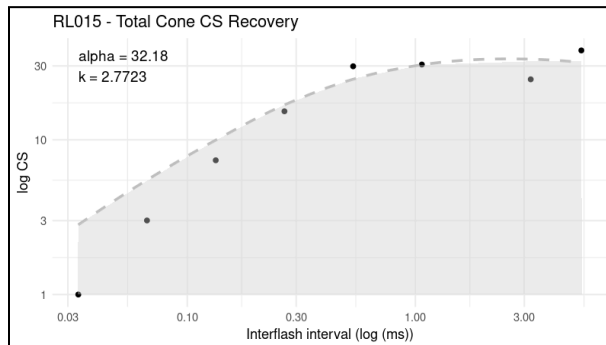
Rod Paired-Flash ERG



Cone Paired-Flash ERG

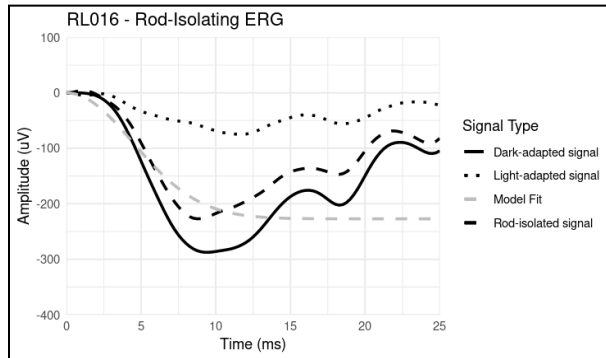


Cone Psychophysics

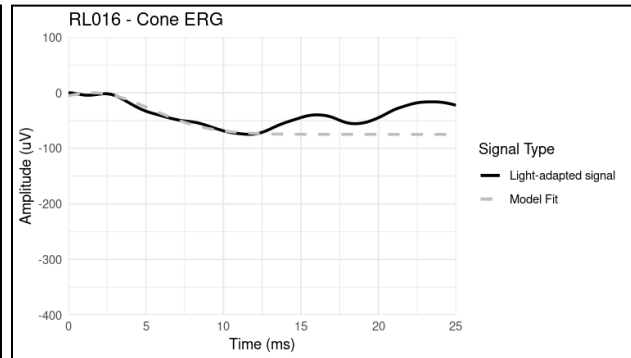


RL016

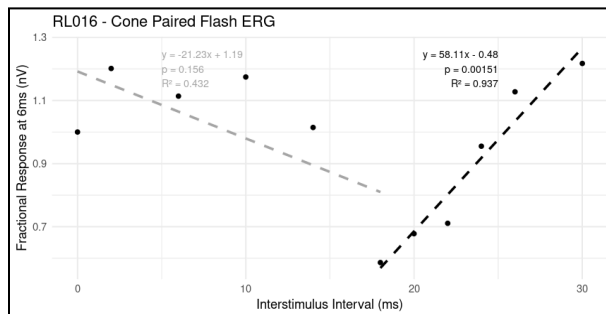
Rod-Isolating ERG



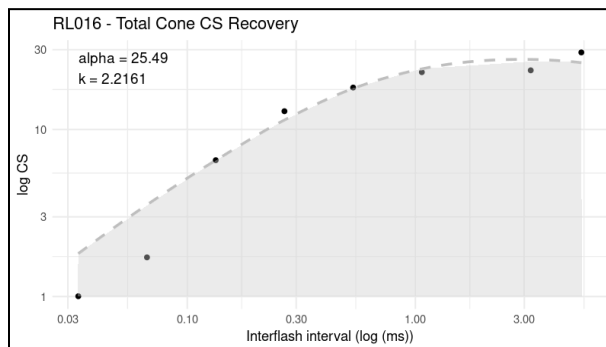
Cone ERG



Cone Paired-Flash ERG

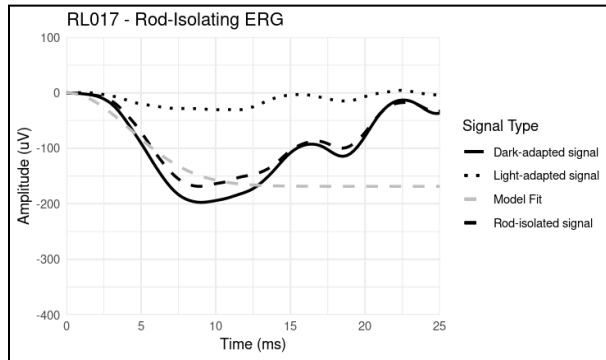


Cone Psychophysics

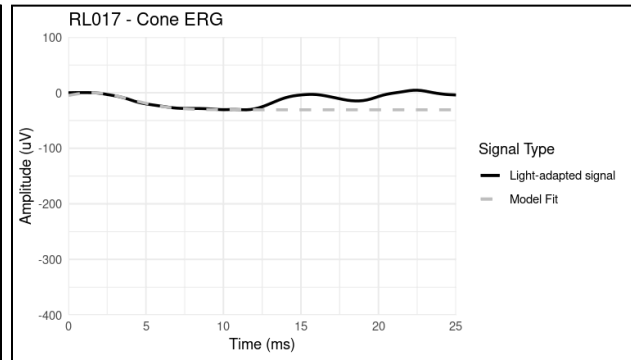


RL017

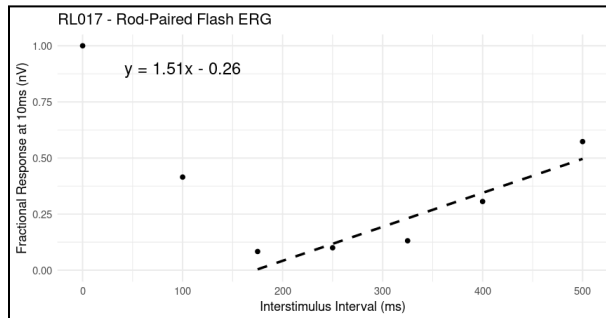
Rod-Isolating ERG



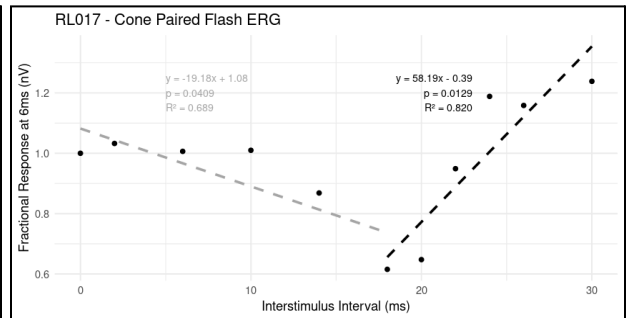
Cone ERG



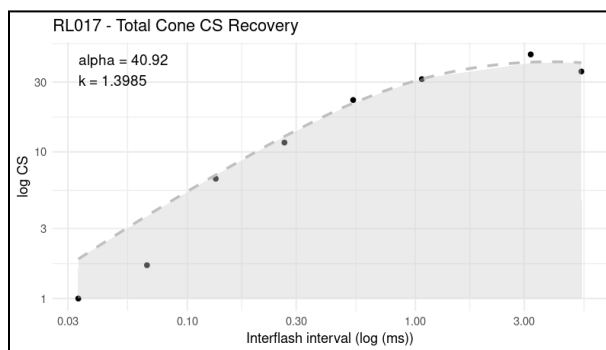
Rod Paired-Flash ERG



Cone Paired-Flash ERG

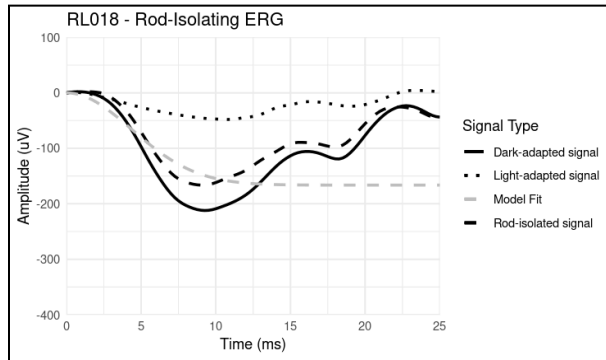


Cone Psychophysics

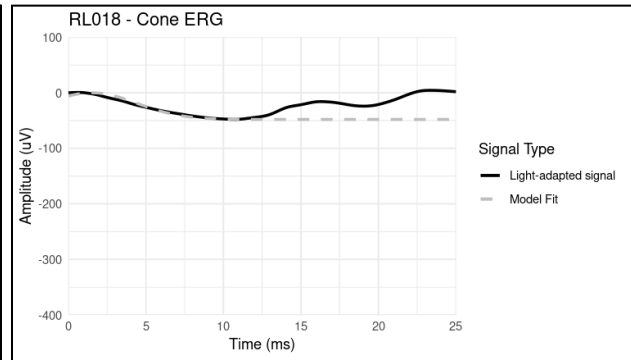


RL018

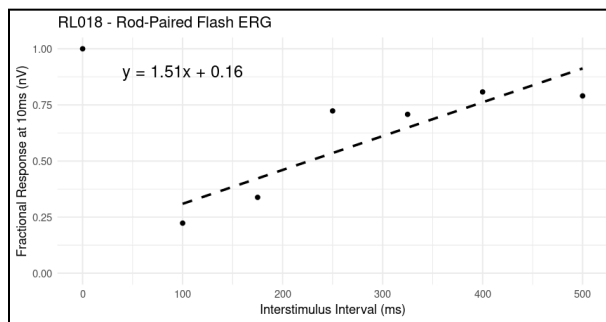
Rod-Isolating ERG



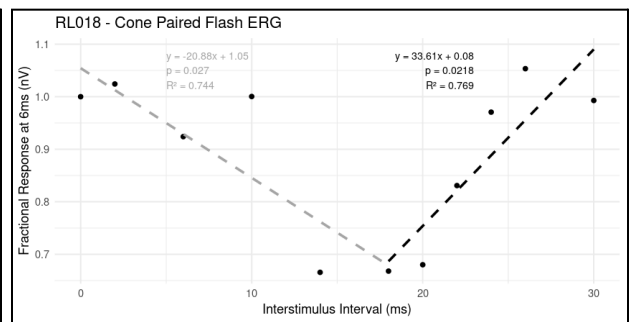
Cone ERG



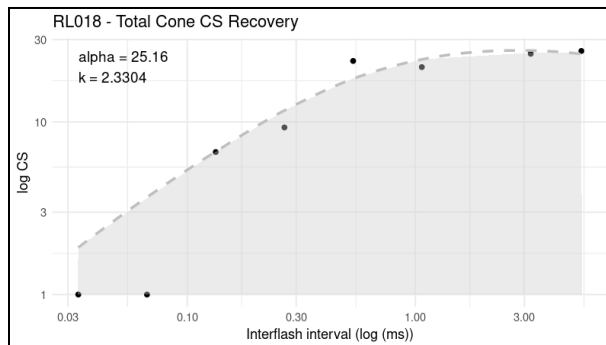
Rod Paired-Flash ERG



Cone Paired-Flash ERG

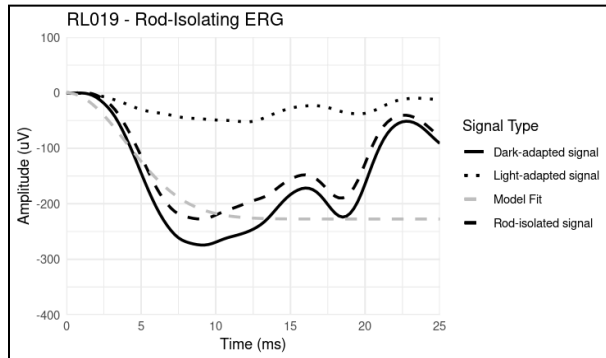


Cone Psychophysics

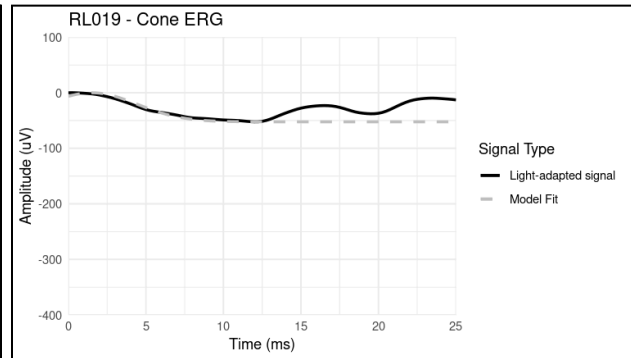


RL019

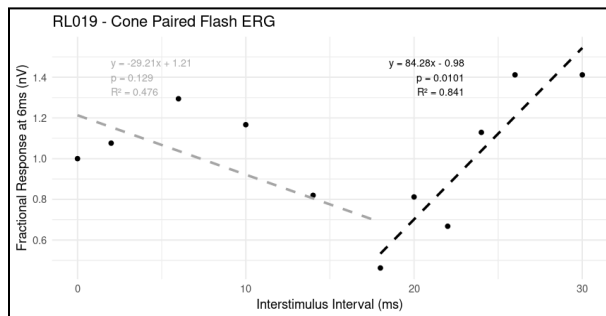
Rod-Isolating ERG



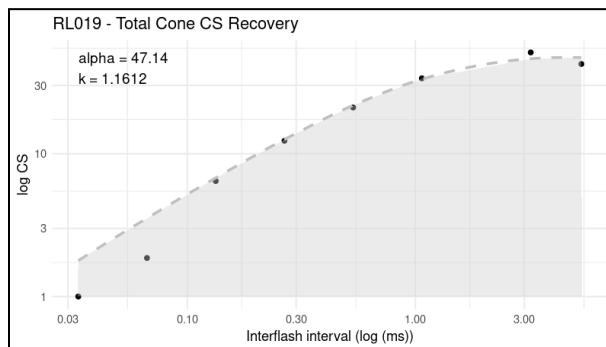
Cone ERG



Cone Paired-Flash ERG

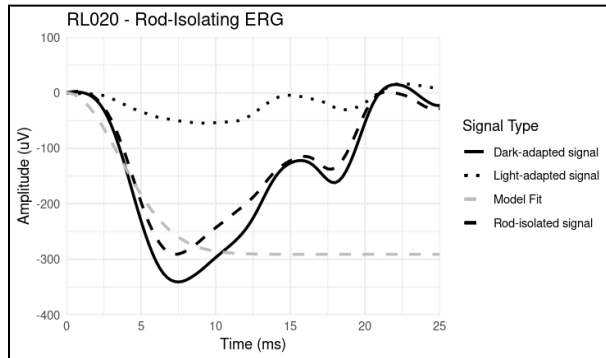


Cone Psychophysics

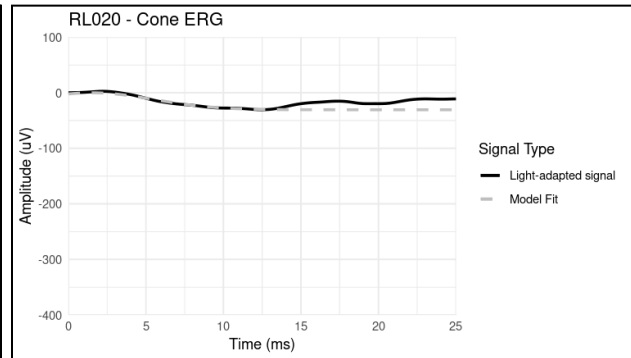


RL020

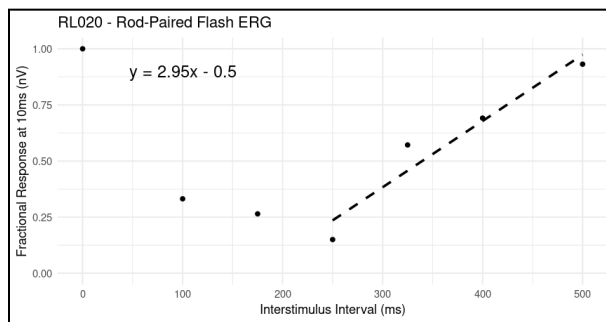
Rod-Isolating ERG



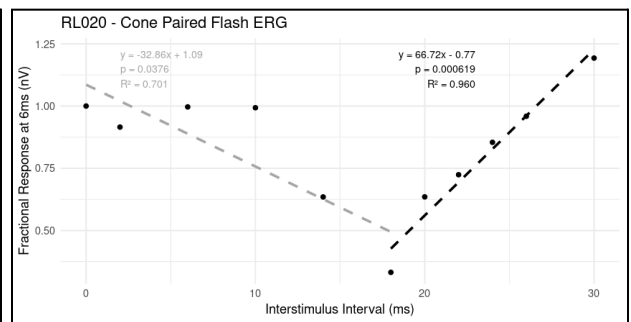
Cone ERG



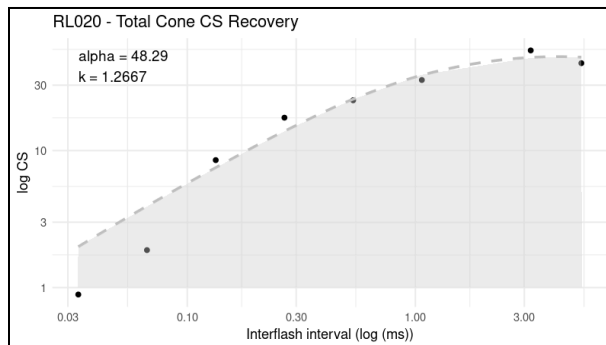
Rod Paired-Flash ERG



Cone Paired-Flash ERG

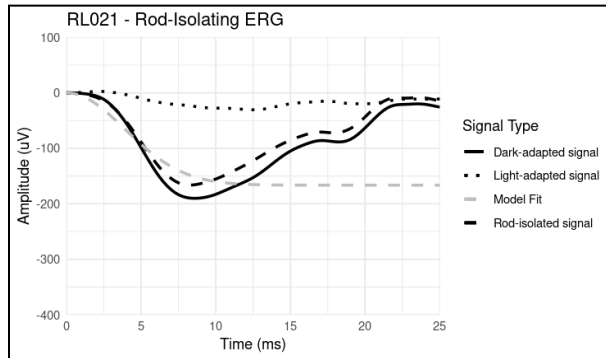


Cone Psychophysics

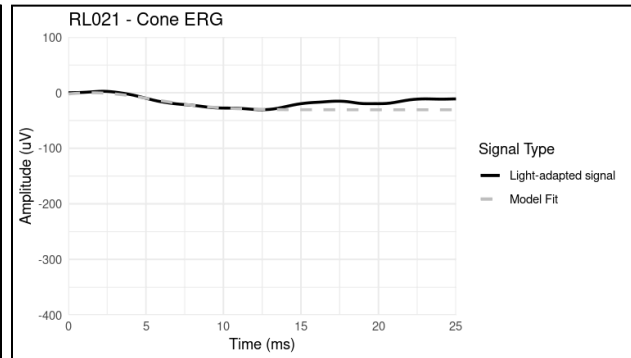


RL021

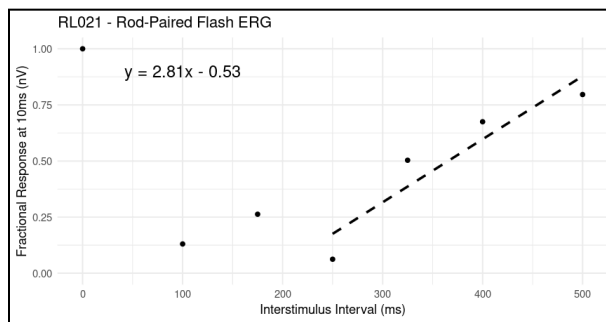
Rod-Isolating ERG



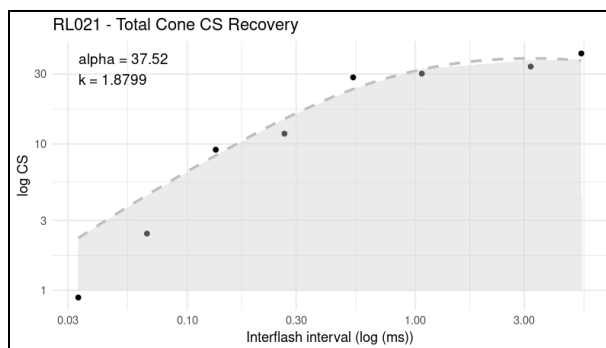
Cone ERG



Rod Paired-Flash ERG

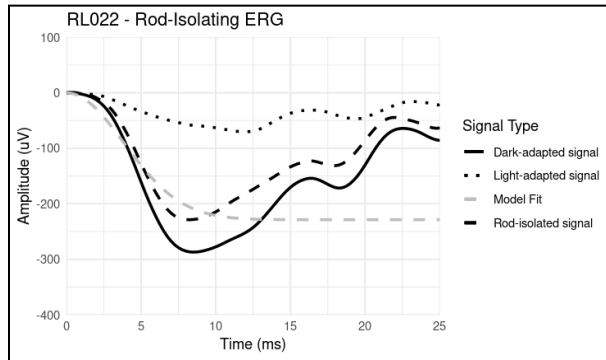


Cone Psychophysics

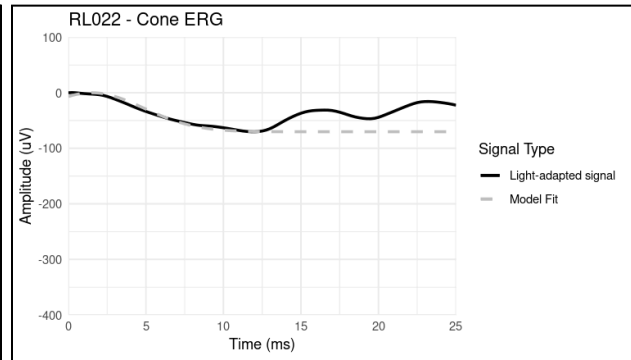


RL022

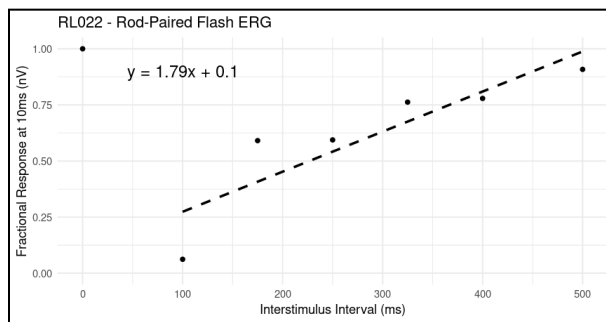
Rod-Isolating ERG



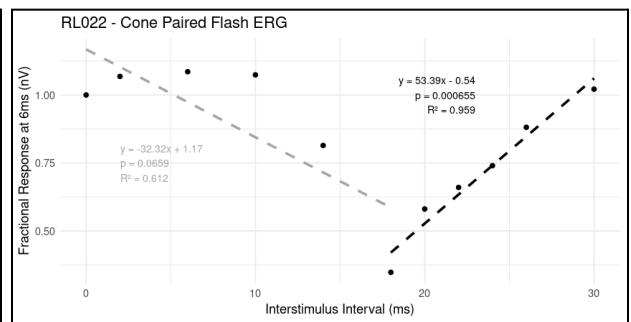
Cone ERG



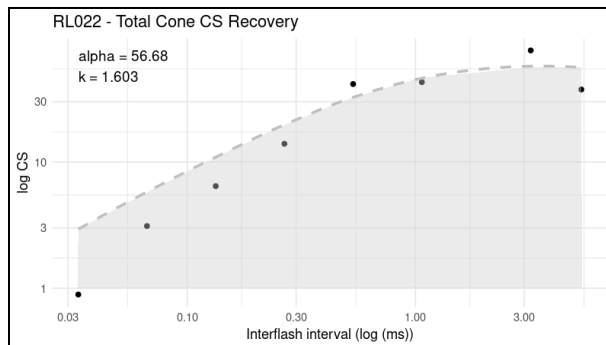
Rod Paired-Flash ERG



Cone Paired-Flash ERG

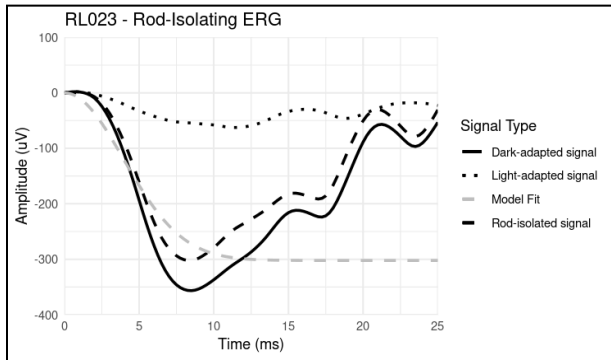


Cone Psychophysics

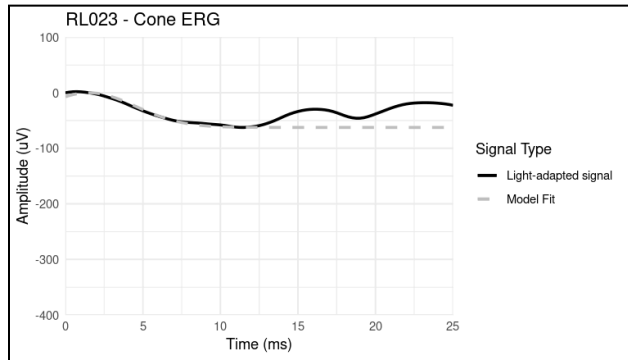


RL023

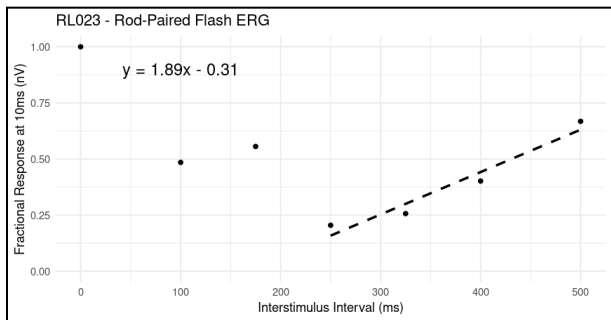
Rod-Isolating ERG



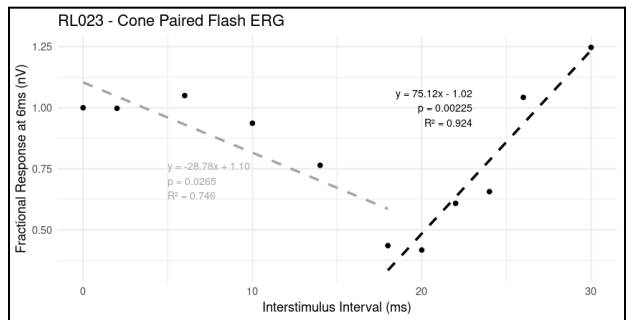
Cone ERG



Rod Paired-Flash ERG

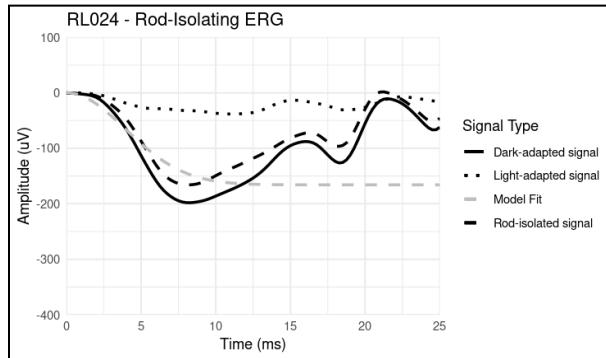


Cone Paired-Flash ERG

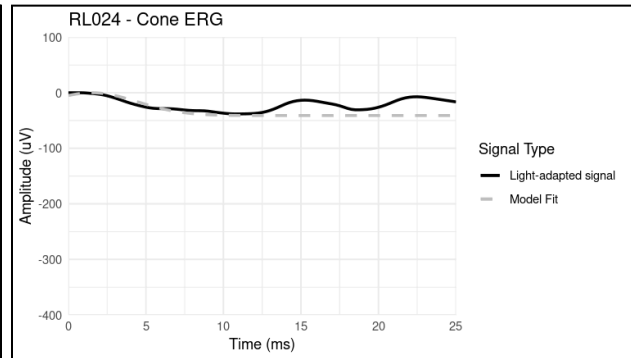


RL024

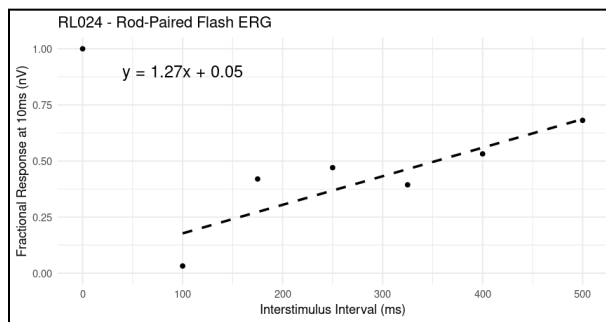
Rod-Isolating ERG



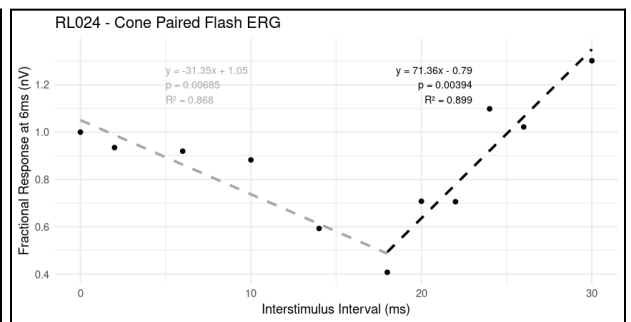
Cone ERG



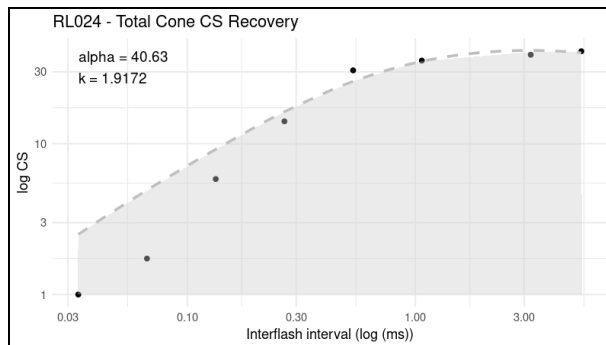
Rod Paired-Flash ERG



Cone Paired-Flash ERG

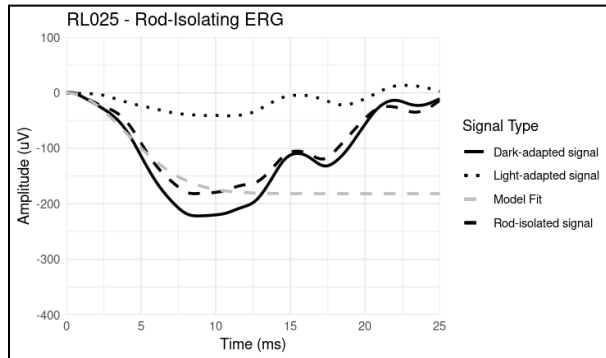


Cone Psychophysics

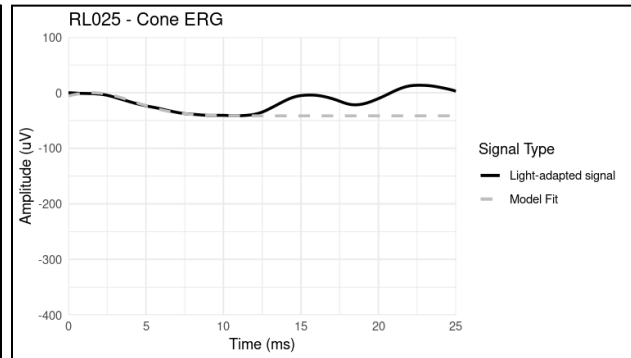


RL025

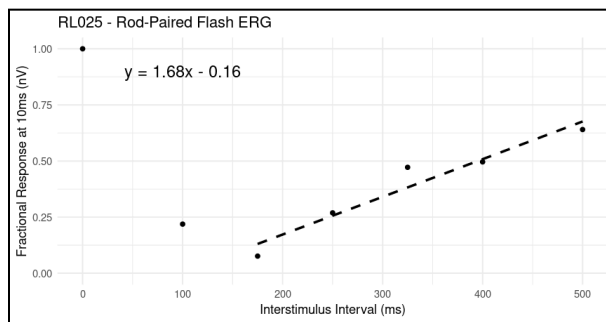
Rod-Isolating ERG



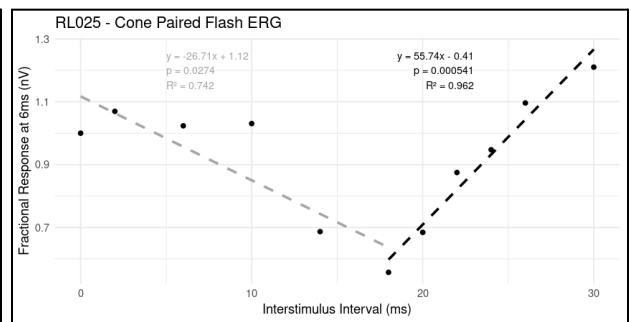
Cone ERG



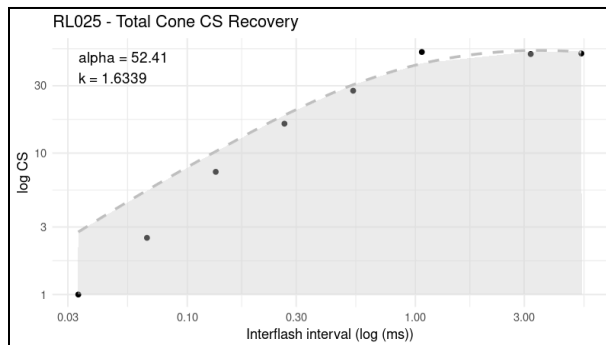
Rod Paired-Flash ERG



Cone Paired-Flash ERG

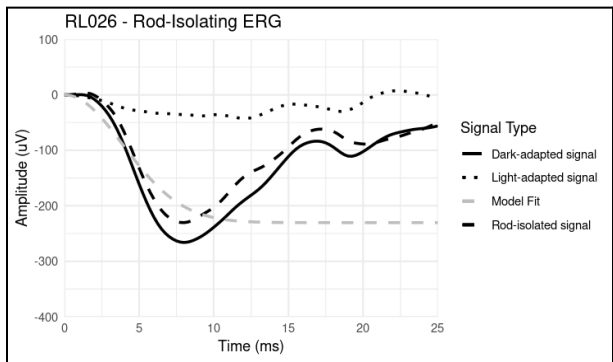


Cone Psychophysics

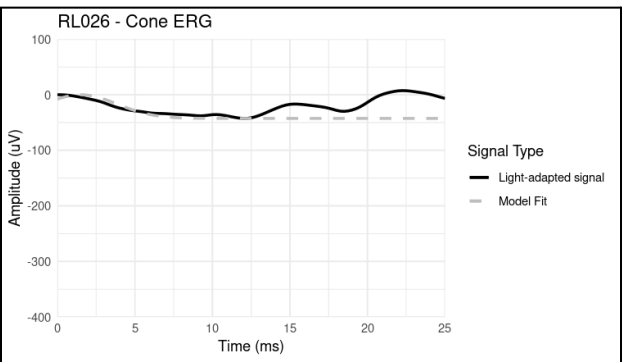


RL026

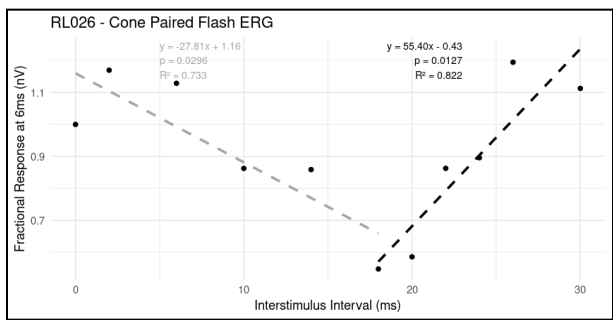
Rod-Isolating ERG



Cone ERG

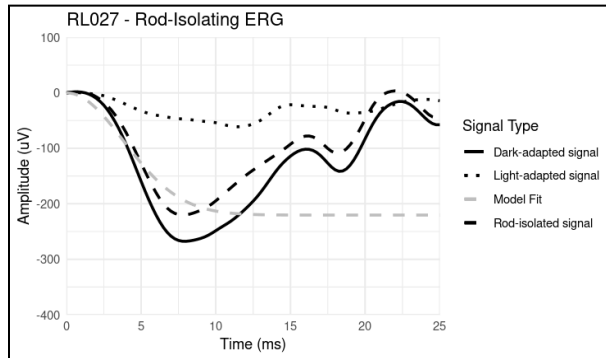


Cone Paired-Flash ERG

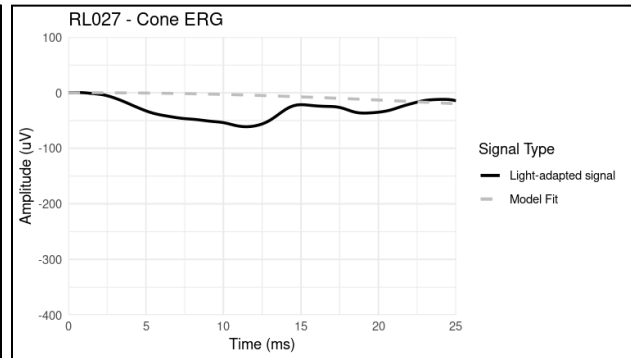


RL027

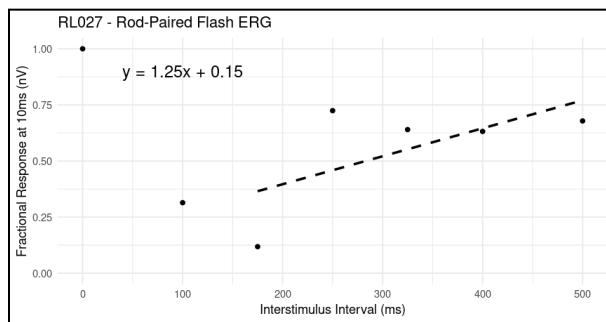
Rod-Isolating ERG



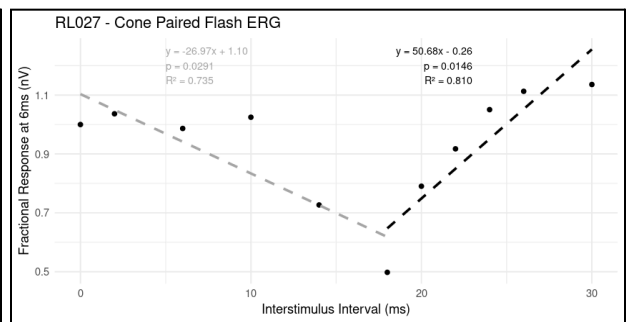
Cone ERG



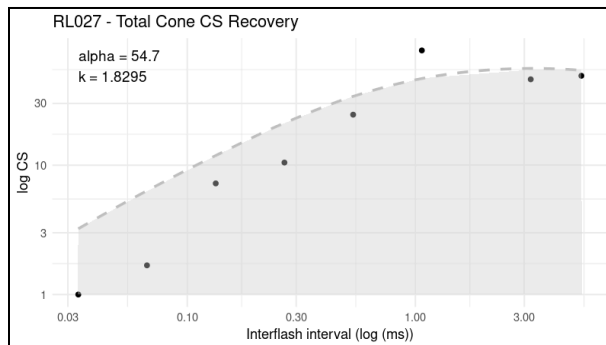
Rod Paired-Flash ERG



Cone Paired-Flash ERG

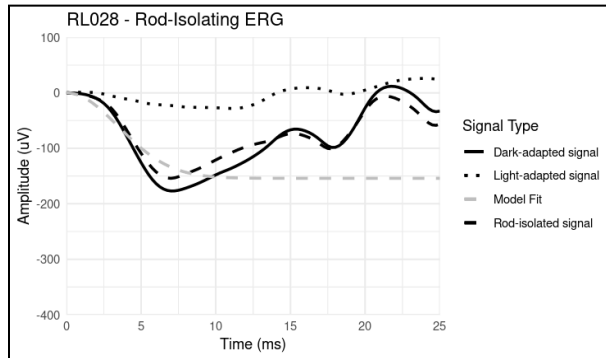


Cone Psychophysics

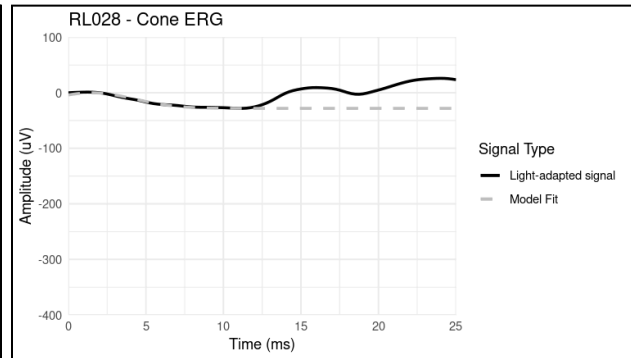


RL028

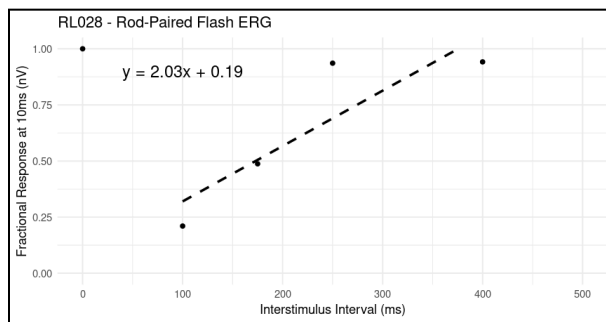
Rod-Isolating ERG



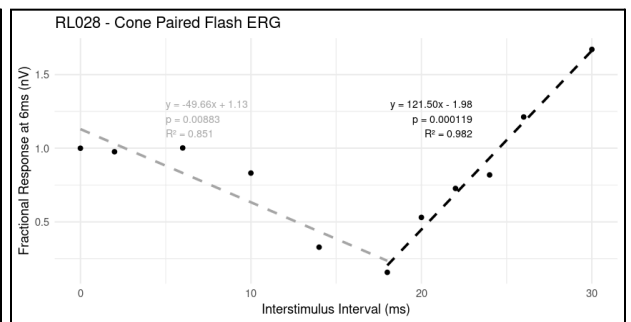
Cone ERG



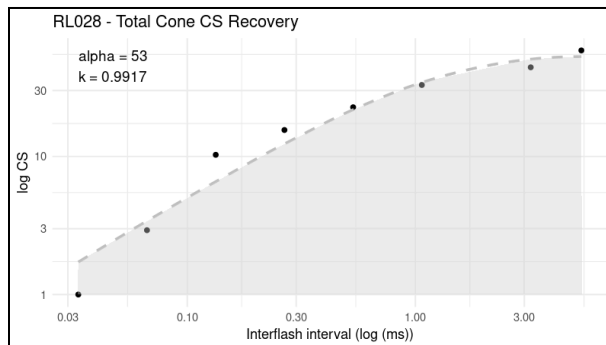
Rod Paired-Flash ERG



Cone Paired-Flash ERG

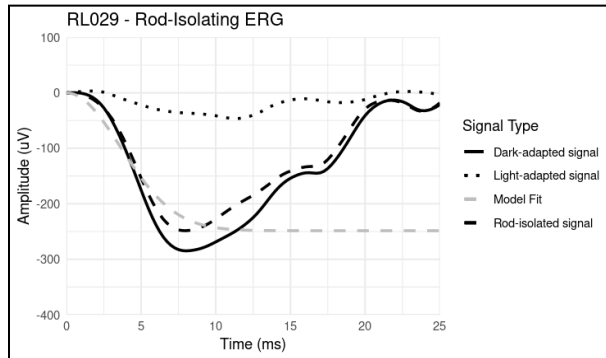


Cone Psychophysics

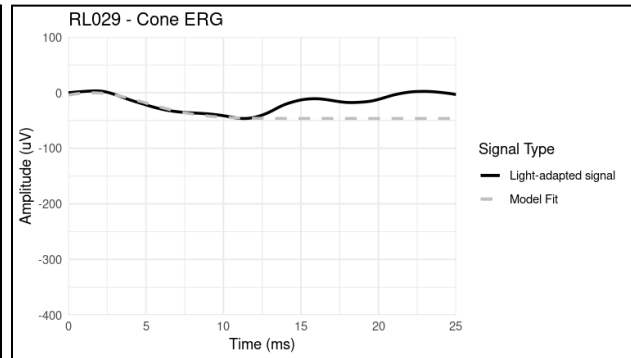


RL029

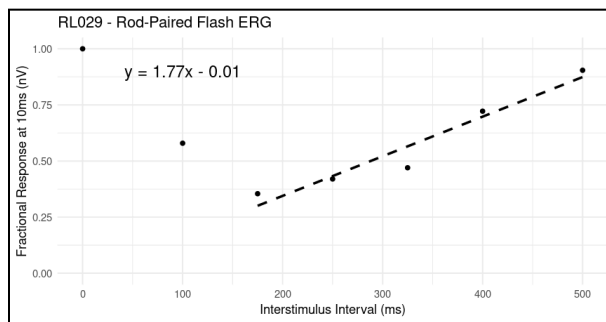
Rod-Isolating ERG



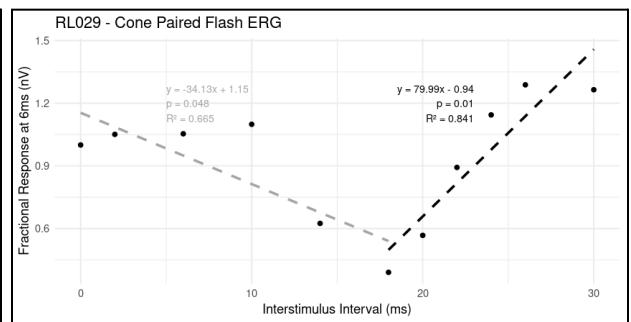
Cone ERG



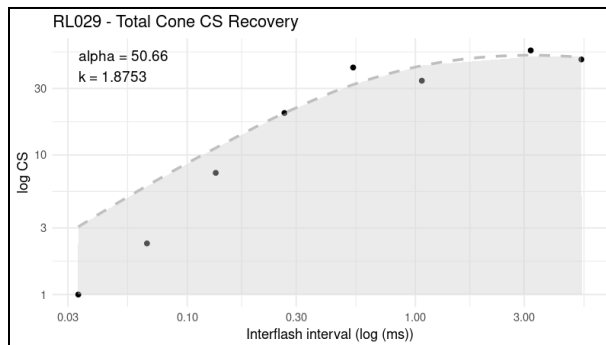
Rod Paired-Flash ERG



Cone Paired-Flash ERG

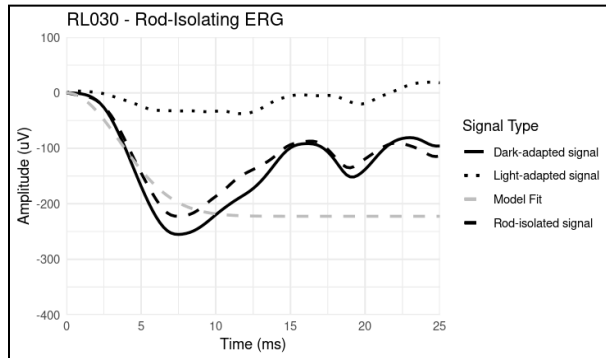


Cone Psychophysics

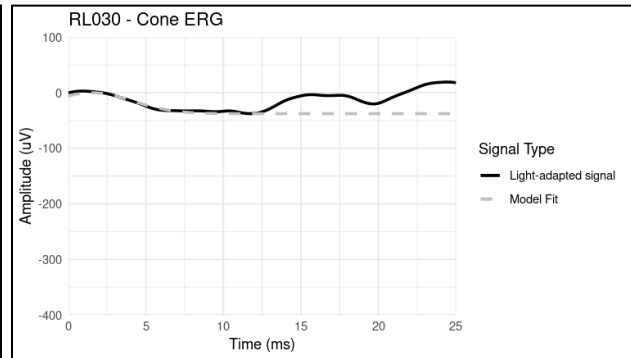


RL030

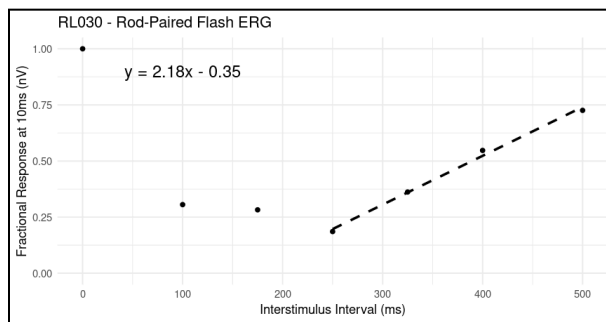
Rod-Isolating ERG



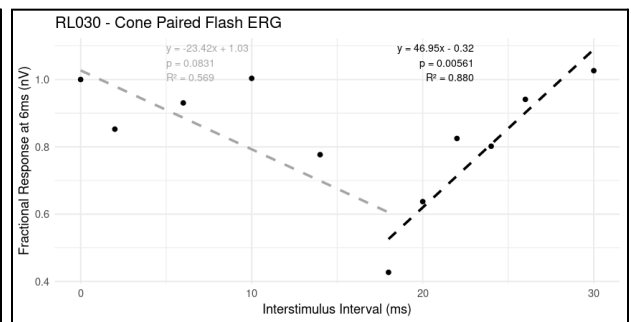
Cone ERG



Rod Paired-Flash ERG

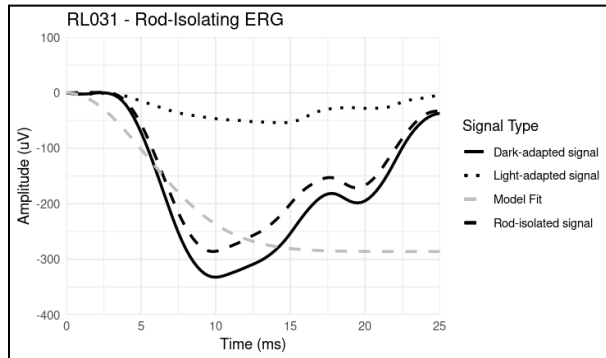


Cone Paired-Flash ERG

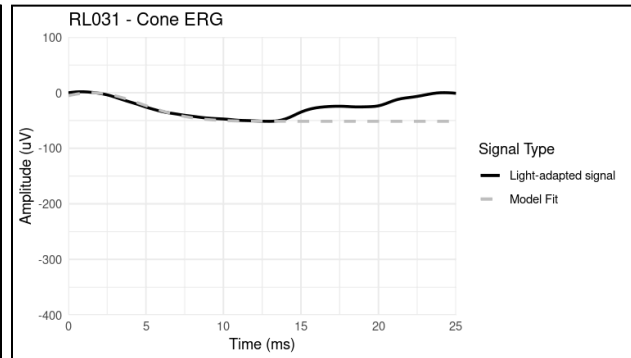


RL031

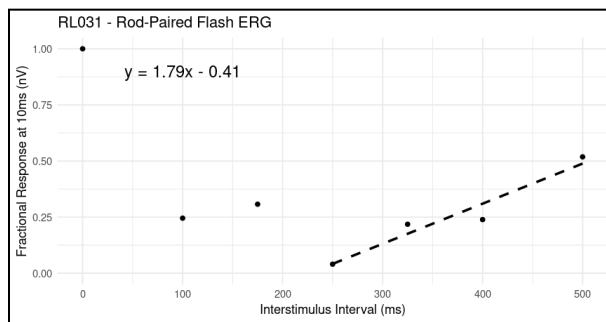
Rod-Isolating ERG



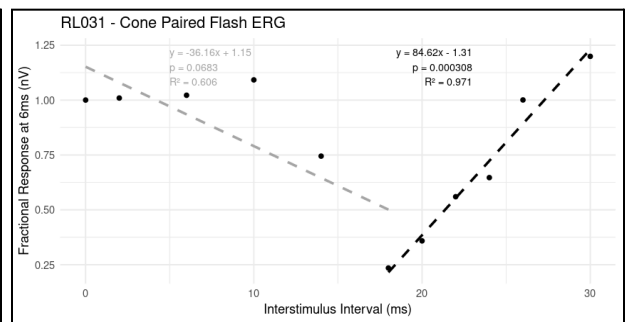
Cone ERG



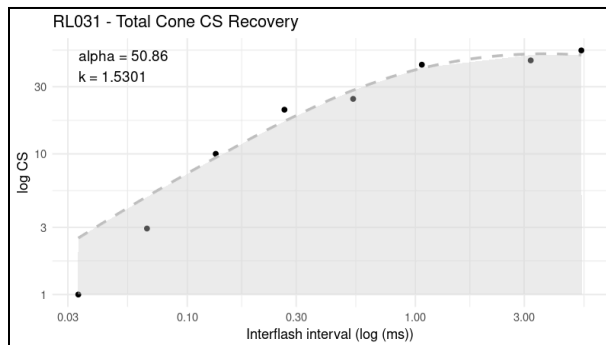
Rod Paired-Flash ERG



Cone Paired-Flash ERG

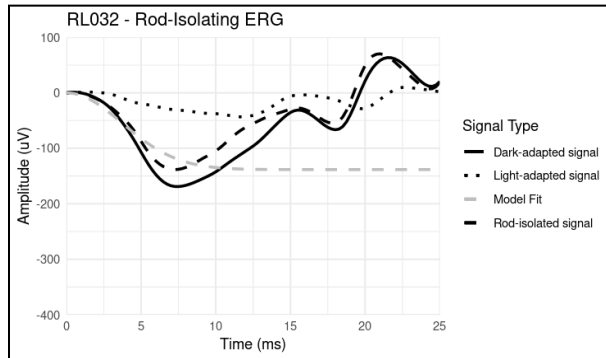


Cone Psychophysics

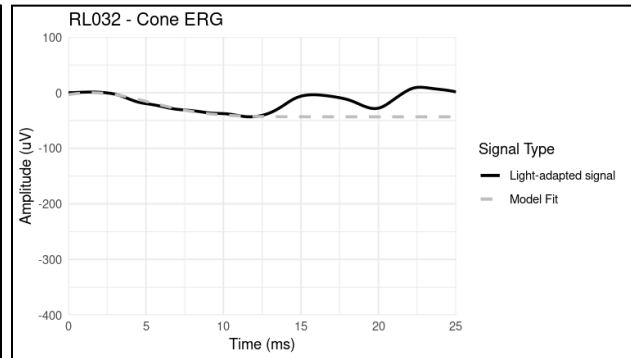


RL032

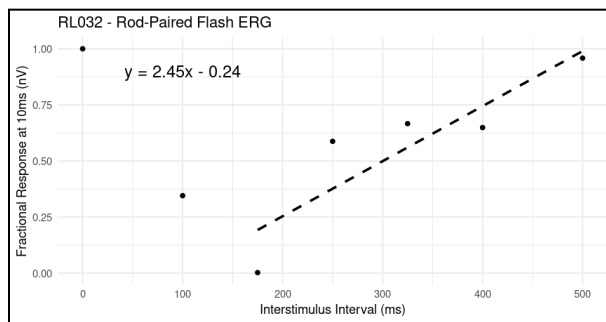
Rod-Isolating ERG



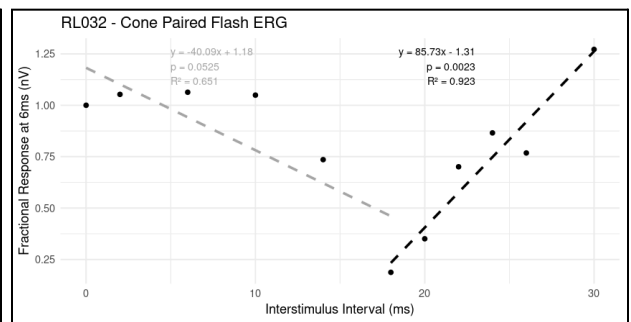
Cone ERG



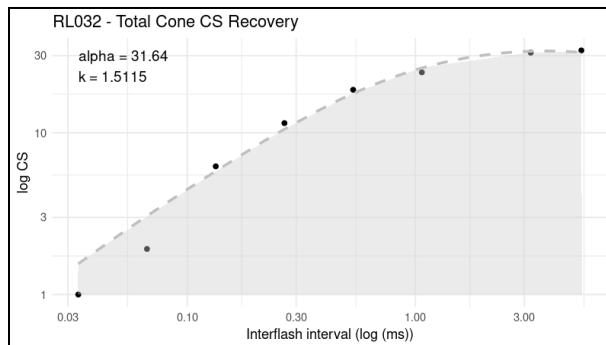
Rod Paired-Flash ERG



Cone Paired-Flash ERG

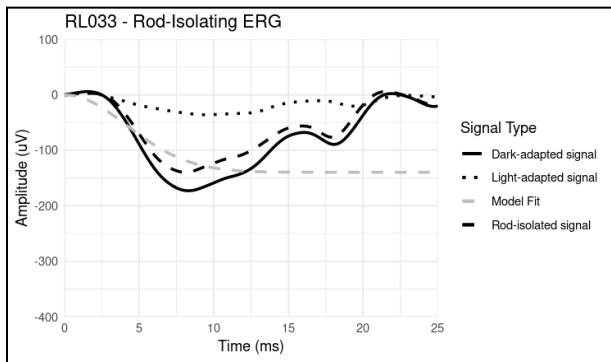


Cone Psychophysics

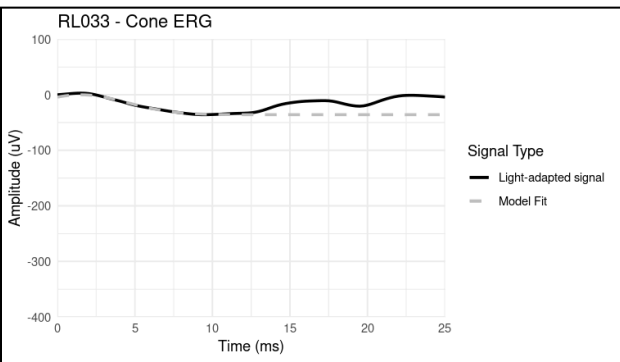


RL033

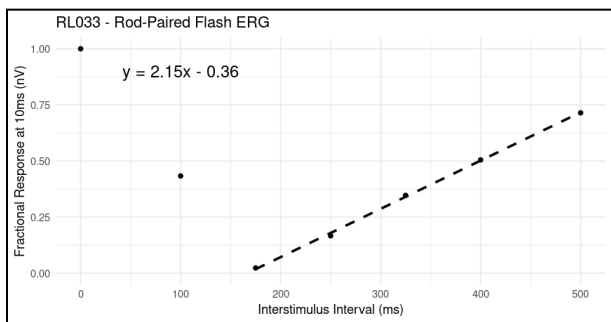
Rod-Isolating ERG



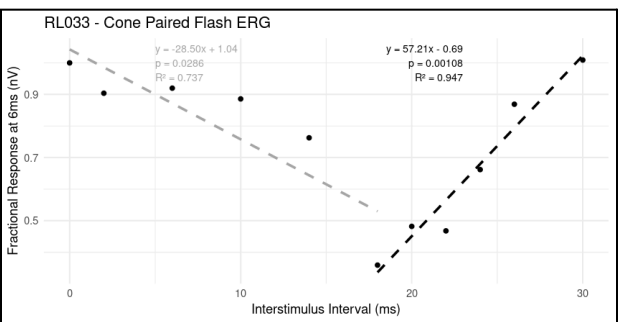
Cone ERG



Rod Paired-Flash ERG

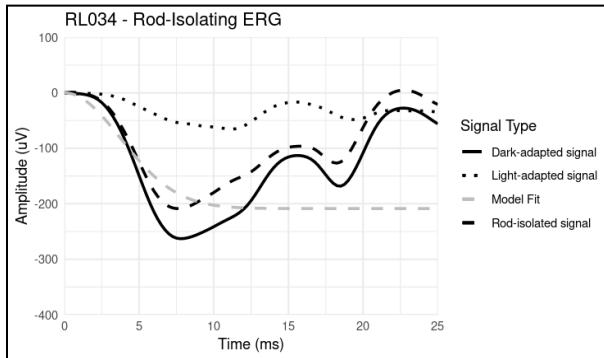


Cone Paired-Flash ERG

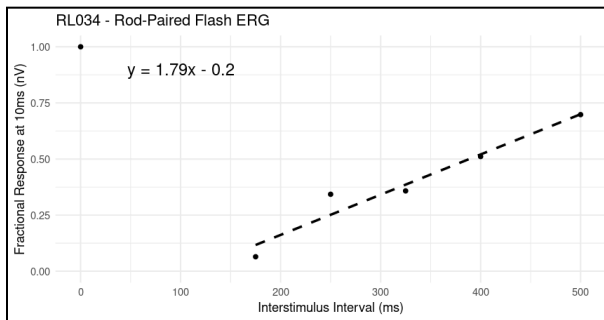


RL034

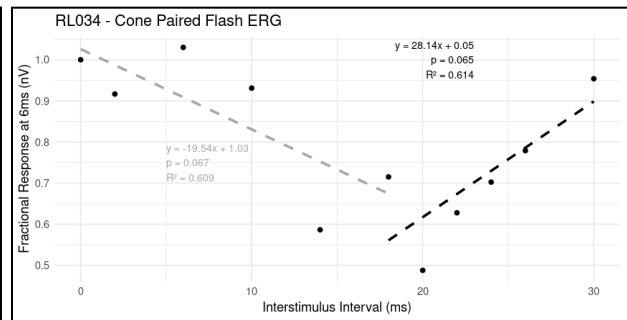
Rod-Isolating ERG



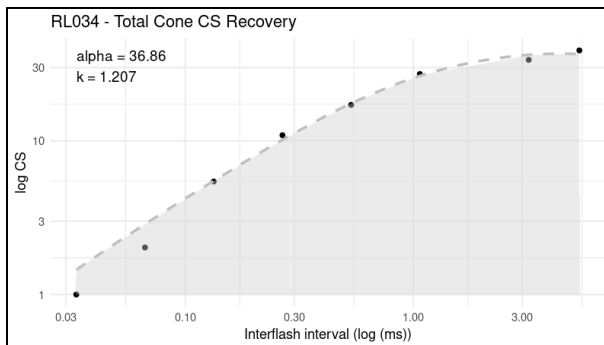
Rod Paired-Flash ERG



Cone Paired-Flash ERG

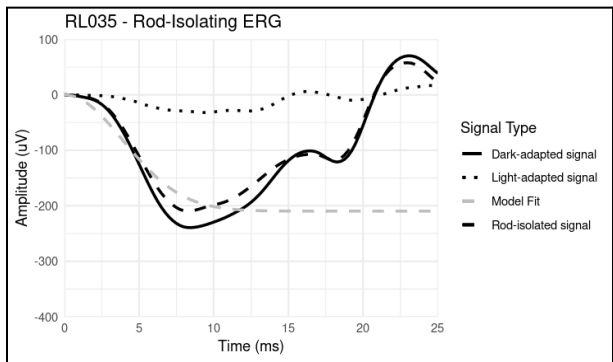


Cone Psychophysics

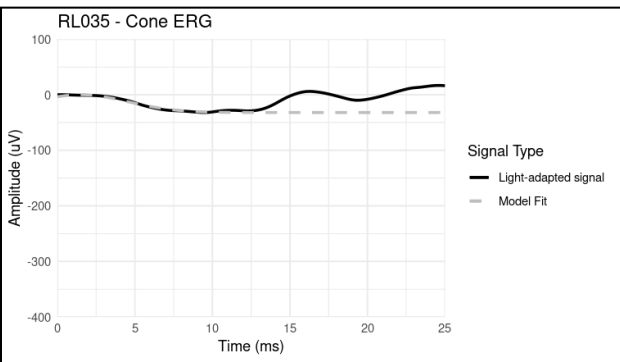


RL035

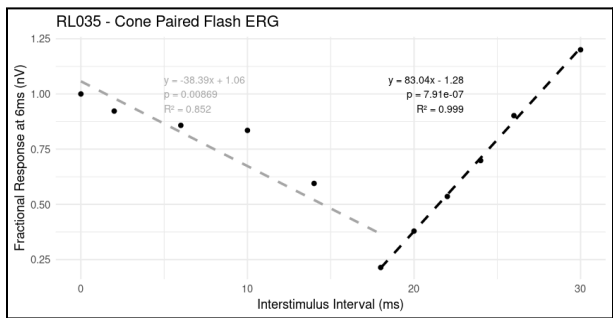
Rod-Isolating ERG



Cone ERG

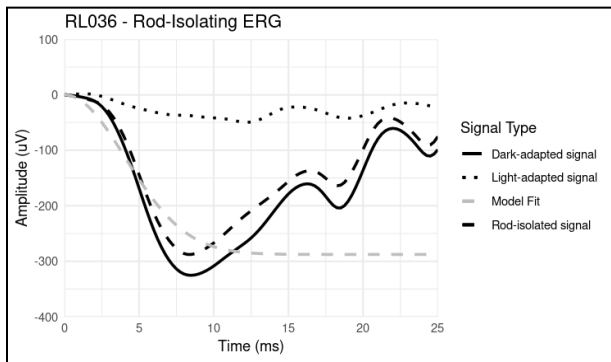


Cone Paired-Flash ERG

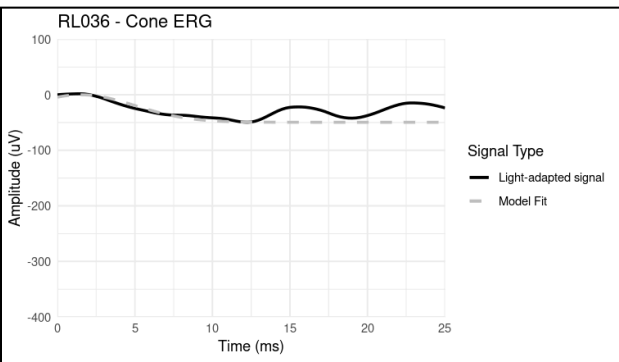


RL036

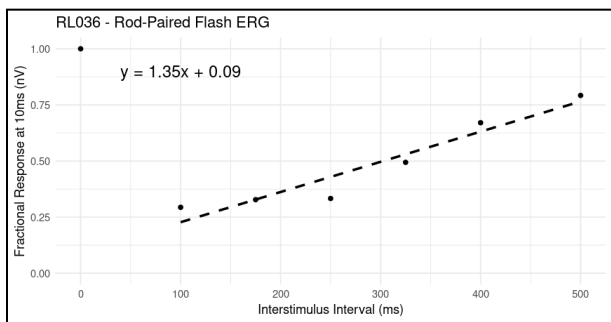
Rod-Isolating ERG



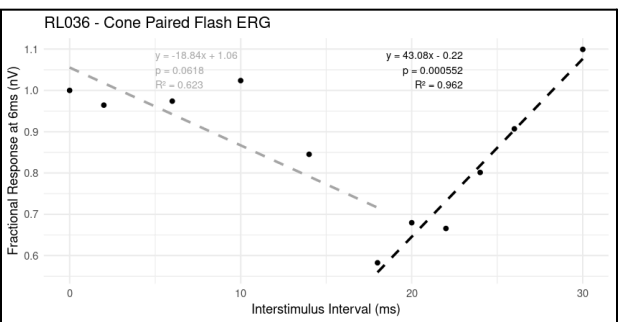
Cone ERG



Rod Paired-Flash ERG

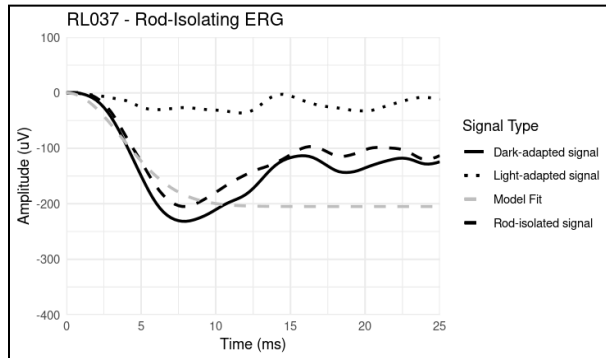


Cone Paired-Flash ERG

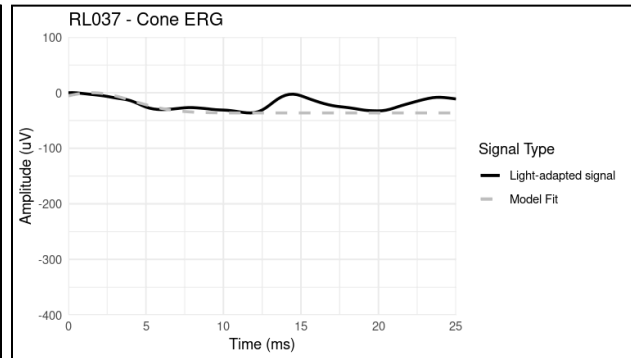


RL037

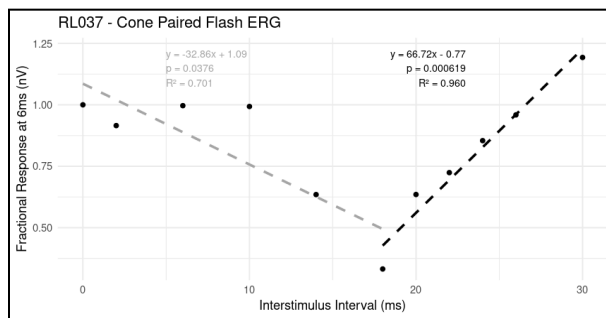
Rod-Isolating ERG



Cone ERG



Cone Paired-Flash ERG



Cone Psychophysics

